# Role of the herpesvirus telomeric repeats and the protein U94 in human herpesvirus 6 integration

Dissertation zur Erlangung des akademischen Grades des

Doktors der Naturwissenschaften (Dr. rer. nat.)

eingereicht im Fachbereich Biologie, Chemie, Pharmazie

der Freien Universität Berlin

vorgelegt von

**Nina Claudia Wallaschek**

aus Würzburg, Deutschland

Berlin 2015

Diese Promotionsarbeit wurde im Zeitraum von Juni 2011 bis November 2015 am Institut für Virologie der Freien Universität Berlin unter der Leitung von Professor Dr. Nikolaus Osterrieder angefertigt.

1. Gutachter: Prof. Dr. Nikolaus Osterrieder
2. Gutachter: Prof. Dr. Petra Knaus

Disputation am 17.02.2016

*‘I’m still confused, but on a higher level.’*

Enrico Fermi (1901-1954)

# 1 Table of contents

# 2 List of figures and tables

# 3 Abbreviations

| | |
|---|---|
| AAV-2 | Adeno-associated virus 2 |
| ALT | Alternative lengthening of telomeres |
| Amp | Ampicillin |
| BAC | Bacterial artificial chromosome |
| bp | Base pairs |
| BSA | Bovine serum albumin |
| Cam | Chloramphenicol |
| CBMC | Cord blood mononuclear cell |
| CRISPR | Clustered regularly interspaced short palindromic repeats |
| d | Day |
| Da | Dalton |
| $ddH_2O$ | Double distilled water |
| DDR | DNA damage response |
| DMSO | Dimethylsulfoxide |
| DNA | Deoxyribonucleic acid |
| dpi | Days post infection |
| DR | Direct repeat |
| DSB | Double strand break |
| dsDNA | Double-stranded deoxyribonucleic acid |
| E | Early |
| *E. coli* | Escherichia coli |
| EDTA | Ethylendiamine tetraacetic acid |
| EBV | Epstein-Barr virus |
| EtOH | Ethanol |
| FBS | Fetal bovine serum |
| FCS | Fetal calf serum |
| FISH | Fluorescence *in situ* hybridization |
| for | Forward |
| gH/gL/gQ1/gQ2 | Glycoprotein H, L, Q1 and Q2 complex |
| gRNA | Guide RNA |
| GFP | Green fluorescent protein |
| h | Hour |
| HCMV | Human Cytomegalovirus |
| HDAC | Histone de-acetylase |
| hDaxx | Human Death domain-associated protein 6 |
| HHV | Human herpesvirus |
| HHV-6 | Human herpesvirus 6 |
| HHV-7 | Human herpesvirus 7 |
| HSV-1 | Herpes simplex virus 1 |
| HR | Homologous recombination |
| IE | Immediate early |
| iHHV-6 | Integrated HHV-6 |
| IL-2 | Interleukin 2 |
| impTMR | Imperfect telomeric repeat |
| int | Intermediate |

| | |
|---|---|
| IR | Internal repeat |
| $IR_L$ | Internal repeat long |
| $IR_S$ | Internal repeat short |
| Kana | Kanamycin |
| Kb | Kilobases |
| Kbp | Kilobase pairs |
| L | Late |
| LB | Luria-Bertrani medium or lysogeny broth |
| LATs | Latency-associated transcripts |
| MDV | Marek's disease virus |
| MEM | Minimum essential Medium Eagle |
| min | Minutes |
| miRNA | Micro ribonucleic acid |
| mTMR | Multiple telomeric repeat |
| ND10 | Nuclear domain 10 |
| o/n | Overnight |
| $OD_{600}$ | Optical density, 600 nm wavelength |
| ORF | Open reading frame |
| PBMC | Peripheral blood mononuclear cells |
| PBS | Phosphate buffer saline |
| PCR | Polymerase chain reaction |
| PHA | Phytohemagglutinin |
| p.i. | Post infection |
| PML | Promyelocytic leukemia |
| pTMR | Perfect telomeric repeat |
| P/S | Penicillin/streptomycin |
| qPCR | Quantitative real Time PCR |
| rev | Reverse |
| rev | Revertant |
| RFLP | Restriction fragment length polymorphism |
| RNA | Ribonucleic acid |
| rpm | Rotations per minute |
| RT | Room temperature |
| SDS | Sodium dodecyl sulfate |
| sec | Seconds |
| SEM | Standard error of the mean |
| shRNA | Small hairpin RNA |
| siRNA | Small interfering RNA |
| Sp100 | Speckled protein of 100 kDa |
| ssDNA | Single-stranded deoxyribonucleic acid |
| sTMR | Short telomeric repeat |
| TAE | Tris-acetate-EDTA buffer |
| TERC | Telomerase RNA component |
| TERRA | Telomeric repeat-containing RNA |
| TERT | Telomerase reverse transcriptase |
| TFR-2 | Telomere repeat binding factor 2 |
| TGN | Trans-Golgi network |
| TMR | Telomeric repeat |
| TPA | Tetradecanoylphorbol acetate |

| | |
|---|---|
| TPE | Telomere position effect |
| TR | Terminal repeat or Telomerase RNA |
| $TR_L$ | Terminal repeat long |
| $TR_S$ | Terminal repeat short |
| TSA | Trichostatin A |
| U | Unique |
| $U_L$ | Unique long |
| $U_S$ | Unique short |
| vTR | Viral telomerase RNA |
| wt | Wild type |

# 4 Prolog

*'The deepest sin against the human mind is to believe things without evidence.'*
Thomas Henry Huxley (1825-1895)

Can herpesviruses be endogenous viral elements (EVEs)?

By definition, EVEs are considered to be DNA sequences (entire genomes or fragments) derived from a virus but present within the germline of a non-viral organism; having their origin in 'accidental' host germline integration. Next, 'endogenization' occurs; a process in which population fixation of these integrated viruses is accomplished, followed by subsequent vertical transmission to offspring as part of the host gene repertoire. Noteworthy, EVEs still have the potential to produce infectious virus (in case of provirus integration) or at least express some proteins or RNA (integration of fragments/partial viral genomes) from their endogenous state [1-3]. EVEs have been identified in animals, plants as well as fungi [2, 4-6].

Thanks to such EVEs, ancestries of some viral families could be dated back almost 100 million years, and hence turned out to be far older than previously assumed from phylogenetic analysis of their exogenous relatives [7]. Once a virus becomes endogenous, its evolution slows down several orders of magnitude to its host's rate. The rather new, emerging discipline of paleovirology deals with these questions and makes extended use of novel innovations in sequencing technology needed for the rapid and affordable sequencing of whole genomes [1]. Besides, EVEs also allow us to gain further insights into the long-lasting 'arms-race' between hosts and viruses that is based on selection and counter-selection [7].

Since integration is an essential part of the retrovirus life-cycle, these viruses were the first EVEs to be characterized and represent the vast majority of these existing viral fossils in vertebrates. Endogenous retroviruses account for roughly 5-8 % of the human genome [3, 7]. Nevertheless, viruses from all known genome types and replication strategies can give rise to EVEs and have been identified in vertebrate genomes, e.g. parvoviruses, circoviruses, filoviruses and bornaviruses [2, 6]. The search for EVEs of large viral genomes like herpesviruses, however, is far more complex and challenging. Herpesviruses were always excluded in former EVE studies, due to their size, their low sequence conservation level, their lack of consistent gene order and proof of host-gene recombination [1]; a wrong decision? In past years, several herpesviruses including EBV (Epstein-Barr virus), MDV (Marek's disease virus) and HHV-6 (human herpesvirus 6) were shown to integrate into host chromosomes [8]. Intriguingly, Aswad and Katzourakis could

recently identify novel *Herpesviridae*-like sequences in the genome of the Philippine tarsier (*Tarsius syrichta*). This represents the first endogenous herpesvirus ever identified, whose ancestral exogenous relative closely resembles HHV-6 [1].

HHV-6 is a remarkable human virus that finally received well-deserved attention in recent years, after the discovery of its germline integration (termed ciHHV-6) [9]. One might speculate, whether ciHHV-6 could be considered an EVE at the onset of the fossilization process [1]?

# 5 Introduction

## 5.1 Herpesvirales

At present, the number of herpesvirus species classified by the International Committee on Taxonomy of Viruses (ICTV) exceeds well over 100. This number still strongly underestimates the abundance of all herpesvirus species, as many viruses became extinct along with their hosts during evolution. Moreover, the presence of these viruses has only been investigated in few animal species, leaving a considerable proportion yet unidentified [10].

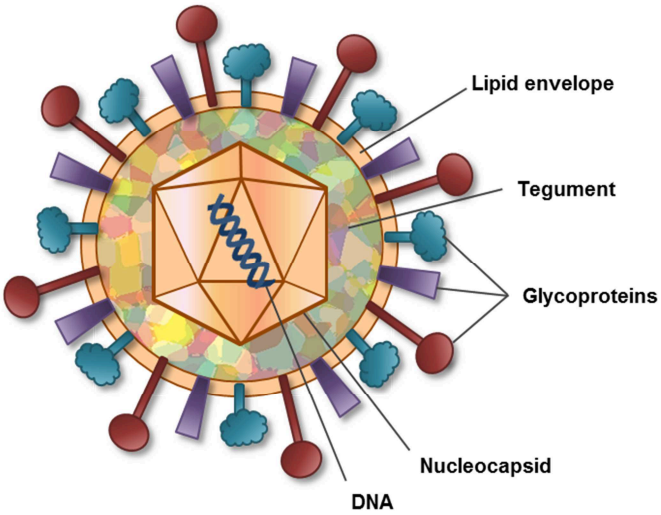


**Figure 1: Schematic representation of a herpesvirus virion.** The nucleocapsid containing the dsDNA genome is embedded into the tegument. The lipid envelope, spiked with virally encoded glycoproteins, surrounds the tegument.

Generally, herpesviruses are among the largest and most complex viruses. Their virions have a diameter ranging from 200-250 nm. The inner core contains the large linear, double-stranded DNA (dsDNA) genome, varying in size from 125-245 kbp, and is packed within an icosahedral capsid. A matrix comprising numerous virus-coded proteins called tegument surrounds the capsid. The outer layer of the virion is the lipid envelope, which contains several viral glycoproteins on its surface (Figure 1) [10, 11].

Due to their dsDNA genome, herpesviruses are categorized as class I of the Baltimore scheme; this classifies all known viruses according to the nature of their genome (RNA or DNA, single-stranded or double-stranded, negative or positive polarity) [12]. Moreover, phylogenetics, the study of evolutionary relationships among groups, makes use of a hierarchical organization into order, family, subfamily, genus and species. Several years ago, the ICTV updated the hitherto existing classification of herpesviruses by introducing a new higher taxon, the order of *Herpesvirales*. This order now comprises the three families of *Malacoherpesviridae*, having invertebrate hosts like oyster and abalones [13, 14], the *Alloherpesviridae*, infecting fish and frogs, as well as the *Herpesviridae* that contain viruses of mammals, birds and reptiles [15, 16]. The *Herpesviridae* are subdivided into three subfamilies based on their biological properties: the *Alphaherpesvirinae*, the

*Betaherpesvirinae*, and the *Gammaherpesvirinae*. Worth mentioning is a proposal from 2014, to recognize a novel subfamily, the *Deltaherpesvirinae*, which would include at least six elephant endotheliotropic herpesviruses (EEHVs) [17].

The hallmark unifying all herpesviruses is their ability to establish lifelong persistent or latent infections in their hosts, while occasional reactivation results in virus replication and spread to naïve individuals. Whereas *Alphaherpesvirinae* display a wider host range, a comparably short reproductive cycle, and primarily use sensory ganglia as their latency reservoir, *Betaherpesvirinae* are rather restricted in their host range, have a long reproductive cycle and can establish latency in differentiating cells such as hematopoietic stem cells. *Gammaherpesvirinae*, however, usually infect T- or B-lymphocytes and maintain their genome in a latent form in lymphoid tissue [11]. To date, there are nine members of human herpesviruses (HHV) identified, representing the *α*, *β* and *γ* subfamilies (Table 1).

**Table 1: Classification of human herpesviruses [11].**

| Abbreviation | Specific name | Subfamily |
|---|---|---|
| **HHV-1** / **HSV-1** | Herpes Simplex Virus 1 | α |
| **HHV-2** / **HSV-2** | Herpes Simplex Virus 2 | α |
| **HHV-3** / **VZV** | Varicella-Zoster Virus | α |
| **HHV-4** / **EBV** | Epstein-Barr Virus | γ |
| **HHV-5** / **CMV** | Cytomegalovirus | β |
| **HHV-6A** | Human Herpesvirus 6A | β |
| **HHV-6B** | Human Herpesvirus 6B | β |
| **HHV-7** | Human Herpesvirus 7 | β |
| **HHV-8** / **KSHV** | Kaposi's Sarcoma-associated Herpesvirus | γ |

Herpesviruses are extremely well adapted to their specific hosts due to millions of years of co-evolution. Therefore, most herpesviruses only display low pathogenicity; usually primary infections are asymptomatic in the immunocompetent host. This balanced equilibrium between virus and host is fundamental to achieve persistence in the host population over an evolutionary time scale - the virus *per se* is rarely keen on killing or seriously harming its host [10].

## 5.2 Human herpesvirus 6

### 5.2.1 History and general facts

The discovery of human B-lymphotropic virus in patients with lymphoproliferative disorders and AIDS by Salahuddin *et al.* in 1986 typified the first member of the genus *Roseoloviruses* (next to HHV-7), within the *Betaherpesvirinae* subfamily. Later, the

nomenclature was adopted to human herpesvirus 6 (HHV-6) [18]. Based on major differences regarding their genetic, immunological, epidemiological and biological characteristics, all existing isolates were distributed into two distinct variants, HHV-6A or 6B [19, 20]. Due to these major discrepancies, the International Committee on Taxonomy of Viruses (ICTV) finally classified HHV-6A and HHV-6B as two separate virus species in 2012 (Figure 2) [21].

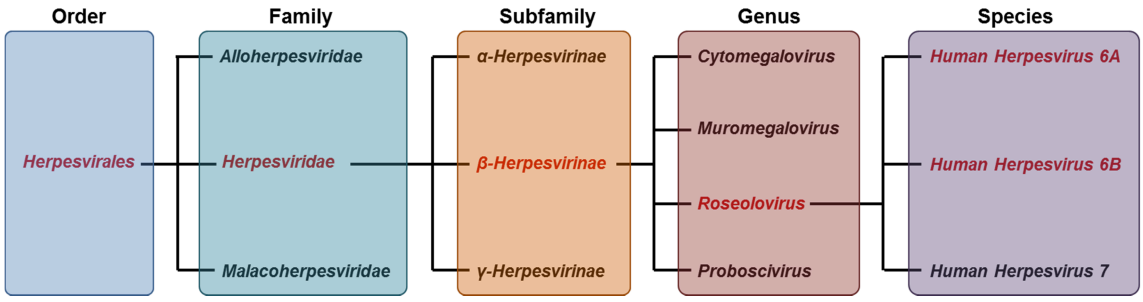


**Figure 2: Classification of human herpesvirus 6 in the hierarchy.**

With a seroprevalence above 90 % in the human population, HHV-6 has to be termed ubiquitous. Newborns usually have maternal antibodies to HHV-6, which typically fade by four to six months of age. In addition, congenital HHV-6 infections can occur in ~1 % of births, which has also been described for HCMV (human cytomegalovirus) [22]. HHV-6 is thought to be transmitted via the saliva and primary infection occurs in early childhood until the age of 3 [23-25]. Physicians primarily diagnose infections based on presented clinical symptoms at examination [26]. Mainly HHV-6B is the causative agent of a febrile illness accompanied with a skin rash, predominantly on the trunk, neck and face (also called *roseola infantum*, *exanthema subitum* or sixth disease). This leads to a substantial number of medical care visits [27], but only in rare cases children exhibit severe neurological complications like seizures and encephalitis [28, 29]. HHV-6A on the other hand was only detected in a majority of infants of an HIV-endemic region of sub-Saharan Africa [30]. Generally speaking, HHV-6 can be considered a mere opportunistic pathogen that typically manifests asymptomatic, lifelong persistence in all immunocompetent individuals. To date, no antiviral drug has been officially approved for the treatment of HHV-6 infection. Therefore, anti-CMV drugs such as the nucleoside analog valganciclovir, the nucleotide analog cidofovir or the pyrophosphate analog foscarnet are currently the drug of choice to medicate HHV-6 infections [31].

Nonetheless, severe pathologies are linked to the virus in the context of its reactivation, especially during phases of immunosuppression. HHV-6 is associated with scores of diseases including encephalitis, multiple sclerosis, chronic fatigue syndrome, infections or graft rejection following transplantation (bone marrow, stem cell and solid organ transplantations) and a more rapid AIDS progression [32, 33]. Intriguingly, HHV-6 and HIV

were observed to infect $CD4^+$ T-lymphocytes simultaneously *in vitro*, resulting in a synergistically accelerated cytopathic effect. Besides, infection with HHV-6 upregulates expression of CD4, thereby broadening the spectrum of cells susceptible to HIV infection. Furthermore, HHV-6 was shown to trans-activate the long terminal repeat promoter of HIV [26, 34]. Overall, extensive research is conducted on these, in part controversial, topics. Due to the omnipresence of HHV-6, it is often hard to discriminate if the virus really is the cause or rather if its reactivation is the consequence of the clinical condition of the patient.

### 5.2.2 Animal models

There is an urgent need for relevant and suitable animal models for HHV-6, to gain deeper insights into viral pathogenesis. Furthermore, these models would support the development of novel diagnostic tools as well as the evaluation of antiviral compounds and/or vaccines. So far unfortunately scarce, recently, several mouse and ape models were developed [35, 36]. Some of them can be used to reproduce the neuropathology of the virus (e.g. to further investigate the correlation between HHV-6A and multiple sclerosis). One is the marmoset model [37] and the other one is using CD46 transgenic or humanized mice [38]. To study immunomodulation and immunodeficiency, a pig-tailed macaque model was developed, in which the virus causes typical clinical symptoms of primary infection such as fever and/or rash. This model could be used to determine if HHV-6 indeed facilitates a more rapid AIDS progression [39]. Likewise, chimpanzees were proposed for similar studies [40]. Interestingly, a study from 1989 described the presence of antibodies against HHV-6 in different primate species, suggesting that HHV-6-related viruses exist in monkeys [41]. And sure enough, a HHV-6 homolog was found in drill monkeys (named MndHVbeta) and chimpanzees (named PanHV6) [42, 43]. Moreover, in 2014, Staheli *et al.* discovered homologs of both HHV-6 and HHV-7 in pig-tailed macaques (named MneHV-6 and MneHV-7) [44]. This would allow to study HHV-6 (and -7) infection and disease associations in a natural virus-host infection model.

### 5.2.3 Genome structure

The HHV-6 genome was completely sequenced in 1995 [45]. Its class A genome is ~160 kb in length and is composed of a ~144 kb unique segment (U) that is flanked by ~8 kb direct repeats (DR), left and right (Figure 3).

Variability within HHV-6A and HHV-6B species is considerably low, with 1 % or less across the genome. The overall nucleotide sequence identity between HHV-6A and HHV-6B is 90 % and their genomes are co-linear over their entire length. [32]. The glycoprotein *gp82/105*, the *IE* genes and the region between *U86* to $DR_R$ is most diverse, Therefore, it has been hypothesized that these genes could be relevant or responsible for the observed

biological differences between HHV-6A and HHV-6B [46, 47]. Collectively, 119 ORFs (open reading frames) are predicted [32]; 43 of those, the so-called core genes, forming seven major blocks, are present in all herpesviruses and most probably arose from a common ancestor. The resulting proteins are crucial for efficient virus replication, cleavage and packaging. The more recently acquired non-core genes can be virus-specific and often help the pathogen to fit in a particular niche. These specific genes exhibit functions belonging to four main categories: 1) cellular tropism, 2) control over cellular processes, 3) manipulation or evasion of the host immune system and 4) latency [48]. Amongst those are *Betaherpesvirinae*-specific genes, several that are only found in members of the *Roseoloviruses*, as well as some unique for HHV-6A or -6B.

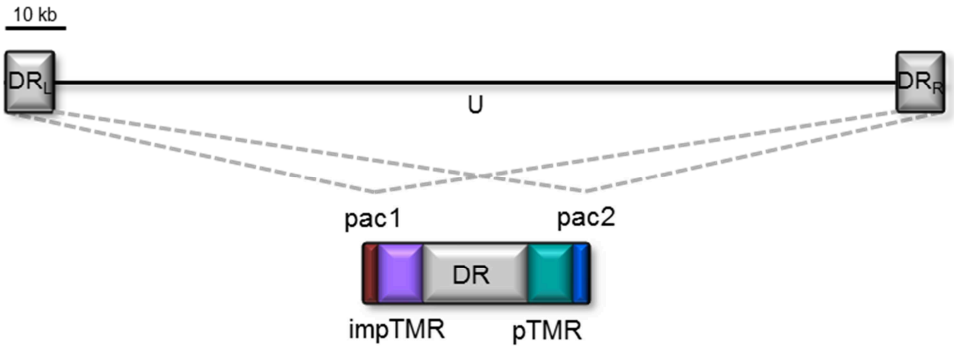


**Figure 3: Schematic representation of the HHV-6 genome with focus on the DR region.** The HHV-6A genome contains a unique region (U), flanked by terminal direct repeats ($DR_L$ and $DR_R$). DR regions are depicted as grey boxes. A focus on the DR region is shown with the telomeric repeats (imperfect TMRs (impTMRs) and perfect TMRs (pTMRs)) and the packaging sites pac1 and pac2.

Coding regions are located on both DNA strands, and splicing occurs in a few viral genes after transcription [32], enabling differential regulation at distinct parts of the virus life-cycle. Non-coding RNAs such as the latency-associated transcripts (LATs) and micro RNAs (miRNAs) are also encoded in the genome. The number of genes, however, seems to be currently underestimated due to alternative splicing, translational frame shifting, internal translation initiation sites and antisense open reading frames [11]. A couple years back, hundreds of previously unidentified open reading frames were found for HCMV using ribosome profiling; especially usage of alternative transcription start sites seems to play a pivotal role in augmenting complexity [49, 50].

### 5.2.4 Immunobiology

The interaction between a virus and its host's immune system is a fascinating and complex process. Upon viral entry, the intruders are confronted with pattern recognition receptors that launch host innate immune responses. These involve cytokines and

chemokines, in turn activating and attracting natural killer cells to destroy infected cells. In addition, the adaptive immune response is triggered by type II interferons and initiates cytotoxic T-cells and neutralizing antibodies. Supplementary, infected cells can induce programmed cell death through apoptosis to remove themselves along with the virus.

To remain hidden from the immune system, up to half of the large genome of herpesviruses can be dedicated to counteract or escape this plethora of host defenses [51]. Herpesviruses have acquired an array of strategies enabling immune evasion or manipulation of the host immune system. Molecular mimicry, expressing homologs of cellular interleukins, chemokines or chemokine receptors is just one of these strategies. Moreover, the presentation of viral antigens via the major histocompatibility complex (MHC) is manipulated by many herpesviruses [52].

*Roseoloviruses* in principal evolved an ideal balance of stimulation and evasion, as healthy infected hosts are capable of lifelong virus transmission [53]. Therefore, it is rather surprising that in case of HHV-6 only few proteins could be explicitly associated with such functions so far (~40 in HCMV). Presumably, there are many others, yet uncharacterized genes that are likewise involved in immune evasion processes [51]. Overall, immunomodulatory functions of HHV-6 gene products involve the inhibition of both innate and adaptive immune responses, as well as the interference with cell death/apoptosis and T-cell signaling [51]. For example, the IE1 protein severely impairs IFN-ß gene induction and IFN-stimulated gene activation, which is crucial to circumvent anti-viral measures and to allow efficient virus replication. U21 downregulates MHC class I by binding and targeting the molecules to endosomal compartments, thus avoiding HHV-6 antigen presentation and immune recognition [31, 51]. Furthermore, it was shown by several laboratories that HHV-6 infection inhibits cell growth, proliferative responses and results in immune suppression, as evidenced by reduced interleukin-2 (IL-2) synthesis; which is likely mediated by the U54 tegument protein [54-56]. In contrast, it was also shown that T-cell activation (IL-2 or mitogen phytohemagglutinin (PHA)) can enhance HHV-6 replication [57, 58]. In addition, U24 expression leads to internalization of the T-cell receptor/CD3 complex at the cell surface, resulting in improper T-cell activation by antigen-presenting cells. As mentioned above, HHV-6 also applies the mechanism of molecular piracy or mimicry. Using this strategy, the chemotactic U83 protein is capable of binding chemokine receptors, whereas two other genes, *U12* and *U51,* are virally encoded chemokine receptors [51].

### 5.2.5 Replication cycle

Activated $CD4^+$ T-lymphocytes are the preferred cell type for infection and efficient HHV-6 replication [59, 60]. Infection causes a strong cytopathic effect with characteristic enlarged

syncytial cells [32]. Nevertheless, a variety of other cell types such as natural killer cells, $CD8^+$ T-cells, macrophages/monocytes, astrocytes, endothelial cells, dendritic cells, fibroblasts, epithelial cells and bone marrow progenitors can be infected, although with limited productive replication [34, 61].

#### 5.2.5.1 Nuclear domains 10 (ND10s)

The genomes of herpesviruses, and other DNA viruses that replicate in the nucleus, localize to subnuclear structures termed nuclear domains 10 (ND10s) or PML nuclear bodies. Viral transcription and DNA replication are commonly detectable in close proximity to these domains. Whether this is a targeted process still remains to be elucidated. Novel ND10 structures were found to form *de novo* at the sites of viral genomes within minutes [62, 63]. ND10s are dynamic, spherical, macromolecular structures with distinct foci between the chromosomes in the nucleus. By definition, ND10s are accumulations of multiple -up to 70- proteins. The size can vary between 0.2 to 1 µm and 2-30 ND10 bodies per cell are observed, depending on cell type and status. The major constitutive components of ND10s are PML (promyelocytic leukemia protein- a TRIM family member), hDaxx (human Death domain-associated protein 6- a transcriptional co-repressor) and Sp100 (speckled protein of 100 kDa- a transcriptional repressor), all of which are subject to post-translational modification by SUMO (small ubiquitin-like modifier). In addition, a plethora of factors can be present at ND10s transiently under particular circumstances. Under physiological conditions, PML is critical for the proper assembly (recruitment of other network proteins) and maintenance of ND10s [63-69]. ND10s undergo major dynamic changes concerning their protein content, suggesting that they are involved in diverse cellular processes such as transcriptional regulation, post-transcriptional protein modification, DNA repair, senescence and apoptosis. Intriguingly, several ND10 components are interferon-inducible and harbor 'IFN-stimulated response elements' (ISRE) or 'IFN-gamma activation sites' (GAS) in their promoters. This is underlined by the fact that number, size and intensity of ND10s increases after interferon stimulation. As a first and intrinsic line of defense, they impede viral replication and initiation of viral *IE* gene expression, forming a repressive chromatin structure via epigenetic processes. Some ND10 components are demonstrably involved in chromatin metabolism and remodeling. Overexpression of exogenous PML restricts infection of a number of RNA and DNA viruses, underlining that the individual ND10 components contribute independently to certain processes [64, 65, 67]. A very elegant study by Glass and Everett in 2013 demonstrated that several ND10 components (PML, hDaxx and Sp100) act in a cooperative manner to regulate herpesvirus replication. Simultaneous depletion by shRNAs against PML, hDaxx and Sp100, using a single lentiviral vector, greatly improved HSV-1 and HCMV replication compared to control shRNAs and individual knockdown of

the proteins. Nevertheless, there are likely additional cellular factors that suppress virus replication [70].

From the virus perspective, it is a corollary to evolve countermeasures against the cellular defense mechanisms. ND10 bodies are usually dispersed, modified or disrupted after herpesvirus infection by various viral strategies and elements/proteins, as early as two hours post infection in the case of HSV-1. This dispersion correlates with the efficiency of viral infection. One prominent example is the HSV-1 ICP0 protein, which is accountable for the proteasome-dependent degradation of sumoylated PML and Sp100. In HCMV, the tegument-delivered pp71 protein facilitates the proteasomal degradation of hDaxx. This leads to the relief of the major immediate early promoter (MIEP) repression and subsequent stimulation of HCMV *IE* (immediate early) gene expression, whereas the IE1 protein abrogates PML sumoylation. Both effects are necessary collaboratively to initiate efficient lytic replication. Besides herpesviruses, also other DNA viruses such as adenoviruses (early protein E4 ORF3), papillomaviruses (minor capsid protein L2) and polyomaviruses (large T-antigen) as well as RNA viruses like rhabdoviruses (Phosphoprotein p of rabies virus), retroviruses (Tax oncoprotein of human T-cell leukemia virus type 1 (HTLV-1)) or orthomyxoviruses (matrix protein M1 as well as the non-structural polypeptides NS1 and NS2 of influenza A virus) can interact with and disarm ND10 domains [63-65, 67].

In case of HHV-6, there is very little data available yet. Proteins from the *IE* locus were shown to affect ND10s. The IE1 protein is covalently modified by SUMO conjugation, localizes rapidly to ND10 bodies and forms a stable interaction throughout lytic infection. Even though the structure of ND10s is preserved, ND10s fuse into few larger entities during the course of infection; a mechanism presumably dependent on additional viral proteins [71, 72]. Besides, the transcriptional trans-activator U19 localizes to ND10s as well, but seems to be negatively regulated by PML or its associated proteins [73].

#### 5.2.5.2 Lytic phase

The first step of the HHV-6 replication cycle is the binding of the virus to a host receptor. For cell attachment, HHV-6A utilizes the CD46 complement regulator receptor. The surface of all nucleated cells is positive for this type I transmembrane glycoprotein, which also serves as the receptor for measles virus, Neisseria gonorrhoeae and group A streptococcus [74, 75]. Recently, CD134, a member of the TNF receptor superfamily, was identified as the specific receptor for HHV-6B [76]. After receptor binding of the virion via the glycoprotein complex gH/gL/gQ1/gQ2 and potential binding of other glycoproteins to yet unidentified cellular receptors, the virus infiltrates the cell via endocytosis (Figure 4A). As a next measure, the viral envelope fuses with the cellular membranes in the

endosomal compartment, releasing the capsid into the cytoplasm (Figure 4B). After transport of the capsid along tubulin microtubules, the DNA enters the nucleus via the nuclear pore complex and the activity of importin-ß (Figure 4C). Once the viral DNA genome is injected into the nucleus it is circularized [75, 77]. In the nucleus, the vital and complex processes of viral transcription, DNA replication and nucleocapsid assembly occur (Figure 4D).

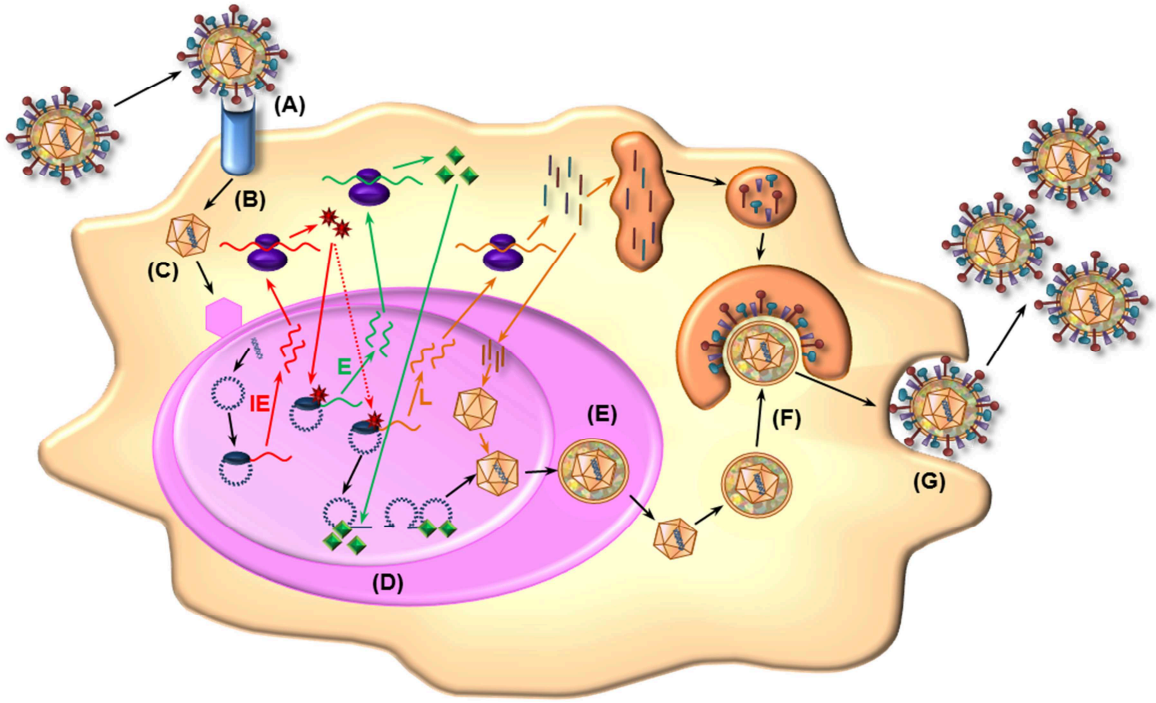


**Figure 4: Schematic representation of the HHV-6 lytic replication cycle. (A)** Virus attachment and entry; **(B)** release of the capsid; **(C)** transport to the nucleus; **(D)** transcription, DNA replication and nucleocapsid assembly; **(E)** nuclear egress: envelopment/de-envelopment process; **(F)** final tegumentation and envelope acquisition at the TGN; **(G)** exocytosis.

The cellular RNA polymerase II facilitates transcription of viral messenger RNAs (mRNAs), with subsequent 5' capping and 3' polyadenylation [77]. A trans-activator brought along in the viral particle initiates the classic regulatory cascade of herpesvirus gene expression observed during productive infection. The immediate-early (*IE*) genes require no prior viral protein synthesis for their own expression, but act as activators for the early (*E*) genes. *E* genes are expressed independently of viral DNA synthesis and function in replication, metabolism and blockade of antigen processing. The late (*L*) genes are expressed last and are dependent on viral DNA synthesis. These L proteins primarily play structural roles for the capsids, tegument and the viral envelope [11, 52]. There are several viral products ensuring expression of viral transcripts at the expense of cellular protein biosynthesis by degrading cellular mRNAs [77]. However, recently it could be

shown for HSV-1 that rather a disruption of transcription termination, resulting in extensive transcription for thousands of nucleotides beyond poly(A) sites and sometimes even into downstream genes, of cellular, but not viral origin, can be held responsible for the observed effect. Thus, hundreds of cellular genes are transcriptionally induced without being further processed and translated [78].

To activate DNA replication, the HHV-6 virus genome harbors discrete sites called origins of lytic replication (oriLyt) located between *U41* and *U42* [11, 77, 79]. Next, a set of 7 virus-encoded proteins that is conserved among herpesviruses is needed for reliable virus replication. A major factor is the DNA polymerase, exhibiting 3'-5' proof-reading exonuclease and RNaseH activity (HHV-6 U38 in combination with a DNA polymerase processivity factor HHV-6 U27). Additionally, a heterotrimeric helicase-primase complex is needed (HHV-6 U43, U74 and U77), a single-strand (ss) binding protein (HHV-6 U41) protecting the ssDNA template during replication, as well as a protein that recognizes the origin of DNA synthesis (HHV-6 U73) [48, 77]. Virus genome replication occurs by 'rolling circle replication', resulting in multiple unit-length virus genomes termed concatemers, linked in a head-to-tail fashion. The concatemers are cleaved at *cis*-acting sequences called pac1 and pac2, present in the terminal *a* sequence of all herpesviruses. Subsequently, unit-length virus genomes are packaged into pre-assembled capsids [48, 77, 80]. The filled capsids exit the nucleus by a sequence of envelopment/de-envelopment steps (Figure 4E). Via budding into the perinuclear cisternae, the capsids are equipped with a temporary envelope (envelopment) devoid of glycoproteins. After stripping of this temporary envelope (de-envelopment), the capsid is released into the cytoplasm, where it acquires the complete tegument. The virus obtains the final re-envelopment along with glycoproteins at the trans-Golgi network (TGN) or post-TGN-derived membranes (Figure 4F). The mature virions exit the cell by exocytosis or cell lysis (Figure 4G) [48, 75]. Completion of one entire HHV-6 replication cycle from infection to release of new virions lasts approximately 72 h [33].

#### 5.2.5.3 Latent phase

Besides the well-defined lytic stage of infection, a hallmark of herpesviruses is the establishment of a persistent infection in the host for life, termed latency, as mentioned above. The viral genome is never fully cleared by the immune system. During the course of latency, the viral genome does not undergo amplification. Despite the absence of the production of infectious virions, the viral genome, however, is maintained in the nucleus of the infected cells. Viral and likely also cellular factors assure suppression of virus gene expression and replication during the establishment and maintenance of the latent phase [77]. Accessory, persistence may include stages of chronic replication with continuous or

intermittent production of infectious progeny [32]. *Betaherpesvirinae* establish latency in various leukocyte subsets [52].

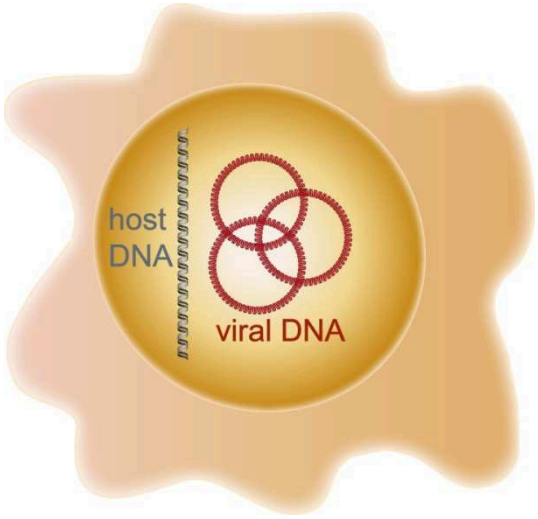


**Figure 5: State of viral DNA during ß-herpesvirus latency.** Viral DNA is present in differentiating cells as episomes in multiple copies, but the association with the host chromosome is yet for most parts unknown.

For successful establishment of latency, the viral genome is typically circularized to form episomes (autonomous covalently closed circles) associated with histones (Figure 5). [52]. Based on CMV studies, regulatory activating and repressive factors such as histone packaging of the DNA or distinct methylation/acetylation marks are suggested to pose the switch between lytic and latent infection [81]. The production of viral proteins must be sustained at a minimal level to avoid inadvertent immune responses. *IE* and other basic genes for productive infection need to be transcriptionally silent in latently infected cells. Heterochromatic modifications of histones like de-methylated H3K4, de-acetylated H3K9 and mono- and di-methylated H3K9, as well as other epigenetic factors seem to be involved in latency; brought about by co-repressor complexes, consisting e.g. of histone de-acetylases (HDACs). Solely genes that are actively expressed during latency show euchromatic histone modifications [81]. ND10s might also be involved in the establishment of latency, as their transcriptional repression must be overcome to initiate lytic replication.

Additional potential protagonists in latency are the miRNAs, small non-coding RNAs of ~17-23 nucleotides, which are capable of targeting mRNAs for degradation or translation repression, resulting in reduced protein levels. Following the discovery of the first viral miRNA in EBV 2004 [82], there are to date more than 200 miRNAs known to be encoded by viruses. Approximately 100 of them are present in human herpesviruses. Viral miRNAs are expressed in latently and/or lytic infected cells. Some miRNAs target viral mRNAs, therefore regulating the switch between lytic replication and latency. Others aim at cellular mRNAs, hence reducing antiviral immune responses (as they are non-immunogenic) or manipulating cell cycle regulation [83, 84]. For HSV-1, several miRNAs are encoded in the LAT locus [84]. Several EBV and KSHV miRNAs are also evidently expressed during latency. Many herpesvirus miRNAs target *IE* genes thereby suppressing lytic replication, a strategy with good prospect to enter and maintain latency [85]. In 2012, the first four

miRNAs were identified for HHV-6B. Those are encoded in the DR regions of the viral genome. They reside in antisense orientation to the *IE* ORFs and are thought to regulate key viral genes [86]. Several months ago, the first HHV-6A miRNA that is encoded in the complementary strand of the *IE* gene *U86* was reported. The miRNA directly targets *U86* and has an influence on the regulation of viral replication [87]. Since only lytic infected cells were analyzed so far, it would be exciting to investigate if these miRNAs are also expressed during latency.

Several studies demonstrated that HHV-6 establishes latency in cells of the monocyte and macrophage lineage. Viral DNA could be readily detected in these cell types after more than one month in culture, devoid of virus replication [88]. In addition, HHV-6 was shown to establish latency in early bone marrow progenitor cells [89], two myeloid cell lines [90], an astrocytoma cell line [91] and an oligodendrocyte cell line [92], rendering those as useful tools for *in vitro* experiments. Four sets of latency-associated transcripts are expressed by HHV-6 in latently infected cells that have structural homology to the HCMV latency transcripts. Even though they are present in the *IE1/IE2* locus, their transcription is only latency associated. The latent start site 1 was found 9.7 kb upstream of the *IE1/IE2* start site and number 2 between exons two and three of *IE1/IE2* [93, 94]. These latency-associated transcripts showed maximal expression during establishment of latency and reactivation both *in vivo* and *in vitro* [95]. Furthermore, the expression of the *U94* gene was shown to be clearly elevated in latently infected cells [96].

In cell culture systems, different chemicals can be applied for reactivation of latent herpesviruses e.g. HDAC inhibitors like trichostatin A (TSA), a protein kinase C activator tetradecanoylphorbol acetate (TPA) or sodium butyrate [52, 81, 88]. *In vivo*, an improper functioning immune system, which fails to surveil viral infection, can tip the balance between viral activity and immune suppression. HHV-6 frequently reactivates in immuno-compromised individuals like AIDS patients, organ recipients or elderly. In addition, phases of physical or psychological stress can lead to reactivation of herpesviruses from latency [52].

## 5.3 HHV-6 integration

The peculiarity of HHV-6 in comparison with all other human herpesviruses is its ability to integrate into the telomeres of latently infected cells [97-101], rather than forming episomes. Already in the 1950s, the integration of viral genetic material into host genomes has been documented; initially in bacteriophages. Other viruses with RNA (such as retroviruses, bornaviruses and flaviviruses) or DNA genomes (like adeno-associated viruses, adenoviruses, papillomaviruses and polyomaviruses) were shown to integrate

into host DNA [102]. For some viruses, integration is a mandatory part of the viral life-cycle (as for retroviruses and adeno-associated viruses), while integration is rather accidental or restricted to certain conditions for other viruses. As a huge benefit, integration ensures automatic replication of the virus genome during host cell proliferation. Another advantage is the stable maintenance of the virus genome in infected cells. Silencing of the integrated virus genome also minimizes detection by the immune system, a prerequisite for long-term persistence in the host. As far as herpesviruses are concerned, EBV has been shown to integrate its entire genome in transformed cells [103, 104], but reactivation of the integrated EBV was never observed. Another herpesvirus that integrates into the telomeres of host chromosomes is MDV. This highly oncogenic avian alphaherpesvirus [105] can efficiently reactivate again to full bloom emanating from the integrated state [106]. In case of HHV-6, sequencing confirmed that a full-length viral genome containing both DRs of HHV-6 (-A and -B) becomes endogenized [107-109], located in the telomeric region of the human chromosome (Figure 6).

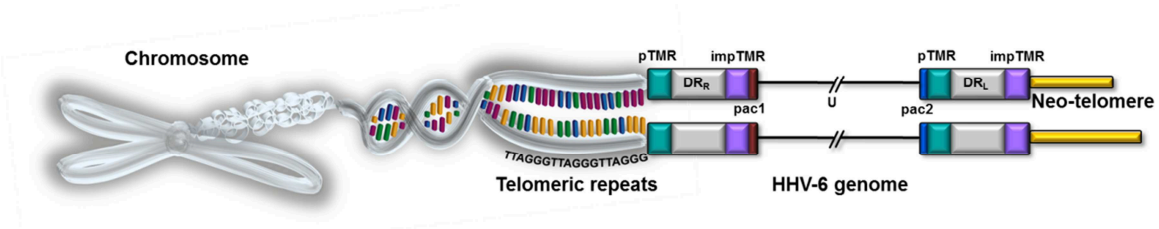


**Figure 6: Telomere integration of HHV-6.** Genome structure of integrated HHV-6, in which HHV-6 $DR_R$ pTMRs are fused with the telomeric repeats of the chromosome and the $DR_L$ impTMRs shape a neo-telomere $(TTAGGG)_n$.

The perfect telomeric repeats (pTMRs) in the $DR_R$ region are adjacent to the end of the chromosome. On the other site of the integrated HHV-6 (iHHV-6) genome, the imperfect telomeric repeats (impTMRs) at the end of the $DR_L$ region get extended to form a neo-telomere [110]. Pac2 at $DR_R$ and pac1 at $DR_L$ are lost in the course of the integration process.

### 5.3.1 Telomere biology

Telomeres can be regarded as the guards of linear chromosome ends, ensuring chromosome stability. The length of telomeres differs between species: ~20bp in protozoans such as *Oxytricha* [111], a few hundred bp in *S. cerevisiae* [112], 10-2000 kbp in chicken [113], 10-150 kbp in mice [114] and 5-15 kbp in humans [115]. In vertebrates, telomeres are composed of repeated arrays of the hexanucleotide TTAGGG. In addition to tissue differences, telomere lengths vary between cells and among chromosomes within the same cell [116-118]. Furthermore, genetic and environmental factors influence telomere length [118].

The G-rich strand at the extreme end of the telomere is longer than the C-rich strand, resulting in a 3‘ end overhang at telomeres of about 100-200 nucleotides that is important for telomere function. A t-loop (telomere loop) is formed, when the TTAGGG G-strand overhang invades the duplex telomere sequence several kilobases upstream of the terminus; this gives rise to the so-called d-loop (displacement loop). This mechanism generates a structure distinct from a broken DNA end (Figure 7) [117-119].

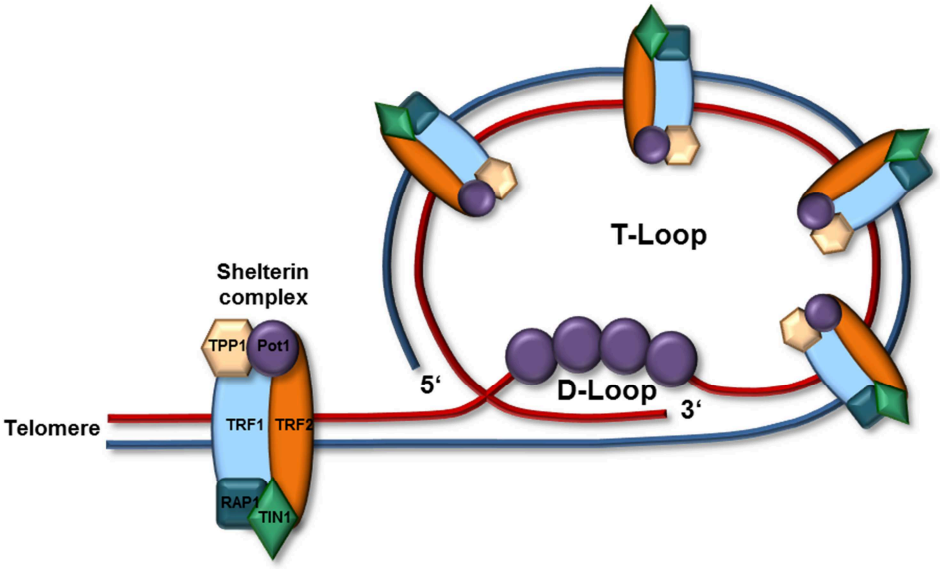


**Figure 7: Schematic representation of telomere T-loop structure with telomere-specific binding proteins.** The ssDNA at the end of the telomere is able to invade and anneal with part of the duplex DNA (thereby forming a displacement (D)-loop) in the same telomere, with the overall result being a telomere (T)-loop. Several proteins bind specifically to telomeric DNA, forming the protective shelterin complex.

In addition, binding of the so-called shelterin complex plays a critical role in the protection of chromosomes. This complex consists of six core proteins: the telomeric DNA repeat binding proteins TRF1 (telomeric repeat binding factor 1) and TRF2 (telomeric repeat binding factor 2), both capable of binding to dsDNA, POT1 (protection of telomeres protein 1), binding ssDNA in the 3‘ G-strand overhang, together with TIN2 (TRF1 interacting protein 2), TPP1 (tripeptidyl peptidase 1) and RAP1 (repressor-activator protein 1), which interconnect the individual components and facilitate complex formation (Figure 7). The shelterin complex assures protection of the telomeres by maintaining telomere structure, repressing DNA repair machinery at telomeres and regulating telomere length [116, 118]. In the absence of shelterin components, excessive telomere shortening and severe telomere uncapping would occur; chromosome ends would be recognized as double-strand breaks (DSBs), resulting in DNA damage responses (DDRs) [116, 117].

Generally, telomere sequences are progressively lost with each round of cell division in somatic cells (50-200bp per division) due to the 'end-replication problem', which outlines the inability of the replication machinery to amplify the terminal sequences of the lagging strand [116, 120]. Therefore, telomeres are sometimes referred to as the 'molecular clock', underlying organismal ageing and regulating the replicative potential of cells [117, 118]. The minimal number of TTAGGG repeats, termed Hayflick limit, is 12.5 repeat units in length [121, 122]. Further shortening results in chromosome fusion and irreversible growth arrest called senescence [123]. Furthermore, it was shown that not the average telomere length, but rather the shortest telomere is crucial for chromosome stability and cell viability [118, 124, 125]. Critically short or dysfunctional telomeres can result in DDRs, end-to-end fusion, genomic instability and chromosomal abnormalities- a predisposition for cancer development. In addition, induced apoptosis, cell cycle arrest and senescence cause major ageing pathologies [116, 117, 120].

Telomere length can be maintained by the ribonucleoprotein complex termed telomerase. The telomerase complex is comprised of a telomerase RNA component (TERC or TR) and the reverse transcriptase catalytic subunit (TERT). This enzyme is able to extend the telomeres by *de novo* synthesis, whereat TERT uses TERC as an associated RNA template. It recognizes the hydroxyl group (OH) at the 3' end of the G-rich strand overhang and in this manner elongates the telomere. Telomerase activity, however, is tightly regulated and basically restricted to germline and stem cells, but is often upregulated in cancer cells [116-118].

Cells lacking telomerase activity can compensate for telomere loss by a mechanism termed alternative lengthening of telomeres (ALT). Approximately 10 % of all human tumors utilize ALT for telomere maintenance, especially those of mesenchymal origin [126-129]. Homologous recombination (HR) is most probably the driving force in $ALT^+$ cells. HR can occur between heterologous chromosomes, sister telomeres or with extra-chromosomal circles [120, 126, 129]. HR in $ALT^+$ cells was first identified by Dunham *et al.* in 2000, showing that a DNA tag introduced into a single telomere was copied to multiple other chromosome ends [130]. The characteristics of $ALT^+$ cells are the incidence of heterogeneous telomere length, the existence of special PML bodies accompanied by telomeric DNA and shelterin proteins (APBs, ALT-associated PML bodies), the presence of extra-chromosomal telomeric DNA, a higher number of DNA damage response foci at telomeres and an elevated frequency of sister-chromatid exchange [118, 126]. Beyond that, $ALT^+$ cells show high level of inter- and intra-telomeric recombination [127], exploiting certain DDR components to counteract telomere shortening [128].

Generally speaking, the telomeric region of a chromosome is mostly inactive or 'silenced'. This heterochromatic structure is depicted by an overrepresentation of repressive histone marks such as trimethylation of histone H3 at lysine K9 (H3K9m3) and H4K20 (H4K20m3) and binding of heterochromatin protein 1 (HP1). Nevertheless, telomeric chromatin is dynamic, allowing for changes of the predominant state [116].

### 5.3.2 Integration during latency vs. the germline

In 1993, a study from Luppi and colleagues provided the first indication for HHV-6 virus integration. They demonstrated by pulsed-field gel electrophoresis (PFGE) that viral sequences were not present in the linear or circular form, but were rather linked to high molecular weight cellular DNA in patients with lymphoproliferative disorders [97]. Substantial evidence for integration, and moreover, the existence of a vertical transmission route for HHV-6 from parents to offspring came several years later from a Japanese family. There, the HHV-6 genome was detected in an integrated state in three subsequent generations in the same chromosome location [131]. So presumably, HHV-6 manages to enter the germline of individuals and is passed on to the next generations. This condition termed chromosomally integrated HHV-6 (ciHHV-6) was substantiated by several groups over the years, demonstrating identical sites of chromosome integration and identifying the exact same virus strain in parents and their affected children [9, 101, 131-135]. ciHHV-6 is present in roughly 1 % of the human population (both HHV-6A and HHV-6B) [134-141] and to date 10 differential integration sites have been confirmed by fluorescence *in situ* hybridization (FISH); all in the telomeric region of the chromosomes: 17p13.3 [98, 100, 101, 142, 143], 18q23 [101, 132], 22q13.3 [9, 99, 101, 134], 9q34.3, 10q26.3, 11p15.5, 19q13.4 [100], 1q44 [9, 131, 144, 145], 18q, 11q, 2p [132].

At first inconceivable, but ciHHV-6 individuals carry the iHHV-6 genome in every nucleated cell of their body [146, 147]. High HHV-6 levels in whole blood quantitative PCR testing, exceeding 5.5 x $10^6$ copies/ml, are strongly suggestive of a ciHHV-6 status of an individual; for reliable diagnosis, though, the existence of HHV-6 DNA in hair follicles can be checked for instance (one copy/hair follicle cell) [136-139, 146, 148]. Clinicians unaware of this condition could expose, especially immunocompromised, patients to considerable risks of toxic antiviral treatment due to a false diagnosis of an active HHV-6 infection [138, 149, 150]. The recently developed digital droplet PCR is now frequently used to identify ciHHV-6 with a high specificity [151].

A question that is still poorly understood is if ciHHV-6 poses a predisposition for certain diseases or if reactivation from its integrated state could possibly harm the patient [8, 141]. Curiously enough, recapitulation of a multitude of conducted studies worldwide determined that ciHHV-6 is 2.3 x more frequent in diseased (various diseases) individuals

compared to healthy ones [141]. Some ciHHV-6 carriers can be persistently infected with exogenous HHV-6 strains, presenting a wide range of neurological symptoms [152]. Besides, ciHHV-6 was recently described to be a risk factor for the development of angina pectoris [153] as well as myocarditis [135]. ciHHV-6 might also pose a risk to transplant patients [154]. The interesting finding that ciHHV-6 associated telomeres are often among the shortest in somatic cells could make them susceptible to deletions, premature senescence or development of other instability problems with unknown outcomes [109]. As of yet, there are already multiple lines of evidence for *in vivo* reactivation of ciHHV-6 [155-160]. Among those, two studies convincingly showed transplacentally acquired HHV-6, derived from the mothers upon reactivation of their ciHHV-6 [148, 161, 162]. Conclusive data was also provided from a patient with X-linked severe combined immunodeficiency (X-SCID). Viral RNA, antigens and signs of lytic infection were detected in PBMCs and bone marrow. The isolated replicating virus was identical (4 viral genes sequenced) to the germline-integrated HHV-6A strain present in the patient and his father. Therefore, *de novo* infection could be ruled out. In addition, antiviral treatment proofed to be effective against the child's symptoms [157].

Despite initial skepticism, the phenomenon of ciHHV-6 is now widely accepted in the scientific field. Intriguingly, Arbuckle *et al.* demonstrated in 2010 and 2013 that HHV-6 integrated likewise after *in vitro* infection of human cell lines (JJHan, HEK293T) just as *in vivo* previously described. No linear viral genomes or free circular episomes could be detected. Besides the FISH technique, they used a direct cloning and sequencing approach to determine the virus-host junction. Integrated HHV-6 was also capable of producing virions *in vitro* upon reactivation; from ciHHV-6 patient PBMCs as well as from infected and integrated cell lines [101, 132]. Other researchers confirmed that integrated copies of HHV-6 are capable to be excised from the chromosome - supposedly through a t-loop excision mechanism - giving rise to a complete viral genome harboring one DR region [108, 109].

HHV-6 integration might therefore not only be a whim of nature that occurs in certain cells such as germ cells, but is an essential step of HHV-6 to establish latency (Figure 8)?

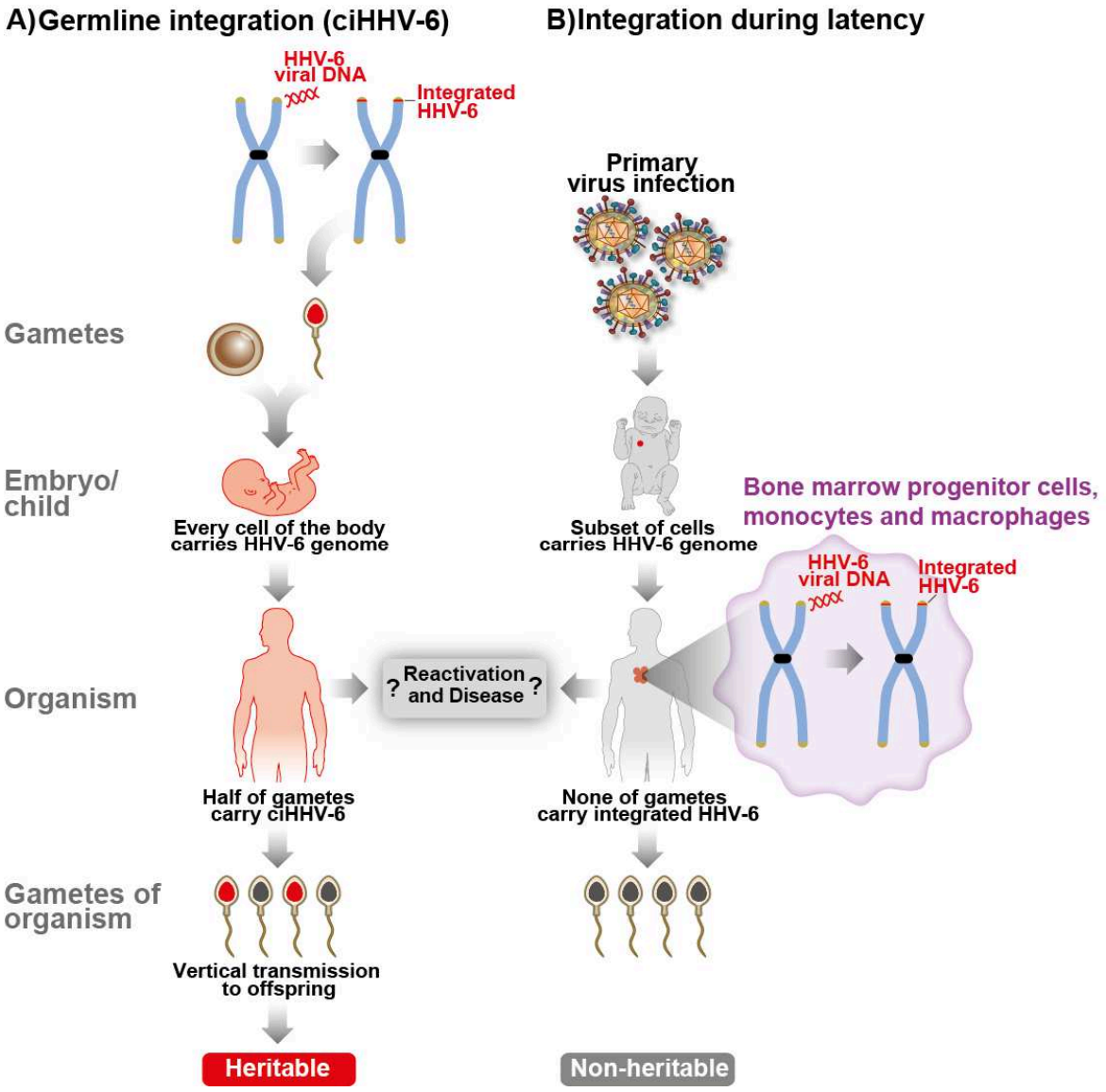


**Figure 8: HHV-6 integration into germline vs. somatic cells during latency. (A)** Germline integration of HHV-6 (sperms as well as oocytes) results in an individual with HHV-6 in every cell of the body. ciHHV-6 can subsequently be inherited to the offspring in a Mendelian manner. **(B)** Upon primary infection during early childhood, the virus establishes latency via integration in a subset of cells (non-heritable). Possible consequences of integration and the mechanism of genome mobilization during reactivation are under investigation. Modified from Osterrieder *et al.* [102].

### 5.3.3 Viral integration factors

Throughout the literature, two viral factors encoded in the HHV-6 genome have been constantly linked to its integration into the human telomeres; namely the telomeric repeats (TMRs) and the protein U94, a putative recombinase.

#### 5.3.3.1 Telomeric repeat sequences

The HHV-6 genome harbors two distinct arrays of TMRs. First, perfect TMRs are repeats of the hexanucleotide TTAGGG with the same composition as human telomere sequences, located at the right genomic terminus and the $DR_L$-U junction. And second, imperfect TMRs at the left genome terminus and at the U-$DR_R$ junction (see Figure 3) [80, 163-165]. Imperfect in this case means that the TTAGGG array is interrupted by related hexamers. The number of TMRs ranges from 15 to 180 copies (e.g. 58 for HHV-6A strain U1102) among clinical isolates and different laboratory strains [164]. The incidence of tandem TMRs is limited and specific to the two regions flanking each DR, but they are hardly ever observed elsewhere in the HHV-6 genome; only monomers of the repeat unit are sporadically distributed within the U region, but nearly absent in the DR regions. The tandem arrays are terminated with motifs for DNA packaging – called pac1 and pac2 (see Figure 3) [163]. Naturally, it is tempting to believe that homologous recombination between the viral TMRs and their host analogs permits genome integration of HHV-6 into the telomere region of the human chromosome. Reinforcing this speculation are findings for MDV, displaying severely impaired integration efficiency in the absence of its viral TMRs [166, 167]. Similar to HHV-6 integration, and therefore worth mentioning, is also the sequence-specific integration of the retrotransposable element TRAS1 (telomeric repeat-associated sequence) within the $(TTAGG)_n$ telomere repeat of the silkworm, *Bombyx mori* [168]. Cleavage of the telomere TTAGG sequence by the TRAS1 endonuclease enables integration [169].

#### 5.3.3.2 U94 protein

The second viral candidate associated with HHV-6 integration is the protein U94. The high degree of genetic conservation of the 490 amino acid protein, differing only by 2.4 % between HHV-6A and -6B, predestines it for a critical role in the HHV-6 life-cycle, nearly intolerant of sequence variation. HHV-6 U94 is unique among human herpesviruses [46, 170], but it exhibits homology to the human parvovirus adeno-associated virus 2 (AAV-2) Rep78/68 protein, sharing 24 % amino acid sequence identity with its counterpart. Due to a HHV-6 helper virus function for AAV-2 infection, the possibility that HHV-6 has snatched the *Rep* gene by non-homologous recombination with AAV-2 replicative intermediates or integrated provirus is more appealing than the assumption of a common ancestral origin or convergence in sequence evolution [171].

Rep78/68 is essential for AAV-2 replication and beyond that regulates viral gene expression. It harnesses its site- and strand specific endonuclease, along with its DNA-binding, helicase as well as ATPase activity for the site-specific integration of AAV-2 into chromosome 19q13.4 [172-178]. Rep-deficient AAV-2 integrates merely inefficiently and

randomly [177]. Interestingly, HHV-6 U94 expression could complement replication of a Rep-deficient AAV-2 virus [179]; strongly suggestive for similar biological functions of the two proteins. The C-terminus of *U94* ORF corresponds to the helicase and ATPase domain of *Rep*, whereas, the N-terminus strongly resembles the DNA binding and endonuclease domain [110]. Mutational analysis of AAV-2 Rep furthermore identified several key amino acids essential for such tasks, all of which are conserved within U94 [180, 181]. U94 has been shown to possess ssDNA-binding activity [182], which was lately reassured and extended to dsDNA with a preference for TTAGGG repeats. In addition, ATPase, helicase and 3'-5' exonuclease activity against 3' recessive ends could be proven *in vitro* using maltose-binding protein (MBP)-fusion proteins of both HHV-6A and -6B [183]. Moreover, several studies indicate a function of U94 on multiple levels of gene expression or replication/transcription itself [184-187]. Purified U94 localizes to the nucleus and seems to be a negative regulator of viral replication; at least for HHV-6 and other betaherpesviruses [188]. This fits the observation that U94 is only expressed at very low levels during lytic infection [170, 182], but could be detected in latently infected PBMCs of healthy individuals in the absence of other transcripts [96].

Altogether, U94 meets all requirements for a potential recombinase during the HHV-6 integration process establishing and/or maintaining latency.

## 5.4 Project outline

In need of a proper genetic system, Borenstein and Frenkel published the first attempt to clone the HHV-6A genome into a bacterial artificial chromosome (BAC) in 2009. This allows genome maintenance and mutagenesis of the virus genome in *E.coli* and lays the groundwork for the analysis of viral proteins and sequences. Their approach comprised the direct cloning of the BAC sequences into the HHV-6A (strain U1102) *U2* gene region via a unique restriction site. The generated BAC only contained a single, shorter DR region (with intact packaging signals) that is predicted to be rescued/duplicated upon reconstitution; however, this BAC construct turned out to be not infectious [189, 190]. Only one year later, the Mori laboratory finally succeeded in constructing the first infectious BAC clone for HHV-6A. CBMCs (cord blood mononuclear cells) were transfected with a plasmid (containing genes essential for the stable maintenance in *E. coli*, a GFP-marker and flanking sites homologous to the HHV-6 genome for recombination) and co-cultivated with HHV-6A (strain U1102) infected cells; giving rise to recombinant virus, which was introduced into *E. coli*. Infectious virus is obtained by transfection of the BAC DNA into mammalian cells and can be visualized by GFP-expression (CMV-promoter driven) [191]. To date, there is no BAC available for HHV-6B.

As described in section 5.3.3, the TMRs and the U94 protein are the two viral factors hypothesized to be of fundamental importance for HHV-6 integration. However, no studies have been conducted to address this on a molecular level, as of yet. In order to elucidate the actual role of the TMR motifs and the protein U94 in HHV-6 integration, I made use of the HHV-6A BAC and deleted the corresponding regions of interest via *en passant* mutagenesis. Upon reconstitution, the mutant viruses were first characterized *in vitro* for their replication kinetics in a human T-cell line. To ultimately determine integration efficiency of generated mutants, an *in vitro* latency/integration model was established and samples studied with fluorescence *in situ* hybridization (FISH) and qPCR. Wherever possible, clonal cell lines were generated for further, more in-depth experiments. My study provides the first evidence of the viral factors involved in HHV-6 integration and will allow to shed light on the reactivation process in future studies.

# 6 Materials and Methods

## 6.1 Materials

All chemicals listed below were used according to the manufacturer´s instructions. Buffers and media for cell and bacterial culture are indicated separately.

### 6.1.1 Chemicals, consumables and equipment

**Chemicals**

| Name | Catalog Number | Manufacturer |
|---|---|---|
| Acetic acid | Cat.No. 20103.295 | VWR, Dresden |
| Agar (agar bacteriological) | Cat.No. 2266.2 | Roth, Karlsruhe |
| Agarose- Standard Roti® grade | Cat.No. 3810.4 | Roth, Karlsruhe |
| Ampicillin Sodium-salt | Cat.No. K029.2 | Roth, Karlsruhe |
| Arabinose L (+) | Cat.No. A11921 | Alfa Aesar, Karlsruhe |
| BSA (albumin bovine fraction V) | Cat.No. A6588.0100 | Applichem, Darmstadt |
| CDP-Star Ready-to-use | Cat.No. 12041677001 | Roche, Mannheim |
| $CH_3COOH$ (acetic acid) | Cat.No. A3686, 2500 | Applichem, Darmstadt |
| Chloramphenicol | Cat.No. 3886.1 | Roth, Karlsruhe |
| KaryoMAX® Colcemid™ Solution in PBS | Cat.No. 15212-012 | Gibco Life Technologies, Darmstadt |
| Dextran Sulphate Sodium salt | Cat.No. 17-0340-01 | Pharmacia Biotech, Uppsala |
| Dimethyl sulfoxide (DMSO) | Cat.No. 1.02952.2500 | Merck, Darmstadt |
| dNTP Mix (10mM total) | Cat.No. BIO-39053 | Bioline, Luckenwalde |
| EDTA (ethylendiamine tetraacetic acid) | Cat.No. A2937, 1000 | Applichem, Darmstadt |
| Ethidium bromide 1% | Cat.No. 2218.2 | Roth, Karlsruhe |
| $EtOH_{den.}$ Absolute | Cat.No. A1613 | Applichem, Darmstadt |
| FACS Rinse | Cat.No. 340346 | BD, San Jose |
| FACS Clean | Cat No. 340345 | BD, San Jose |
| Formamide deionized Molecular biology grade | Cat No. A2156 | Applichem, Darmstadt |
| Glycerol | Cat No. A2926,2500 | Applichem, Darmstadt |
| HCl 37% (hydrochloric acid) | Cat.No. 4625.2 | Roth, Karlsruhe |
| Interleukin-2 (IL-2) | Cat.No. 11011456001 | Roche, Mannheim |
| Isopropyl alcohol (2-propanol) | Cat.No. A0892 | Applichem, Darmstadt |
| Kanamycin sulphate | Cat.No. T832.2 | Roth, Karlsruhe |

| | | |
|---|---|---|
| $KCH_3CO_2$ (potassium acetate) | Cat.No. A4279,0100 | Applichem, Darmstadt |
| Lipofectamine 2000 | Cat.No. 11668027 | Life Technologies, Carlsbad |
| β-mercaptoethanol (2-mercaptoethanol) | Cat.No. 28625 | Serva, Heidelberg |
| Maleic Acid | Cat.No. A1841 | Applichem, Darmstadt |
| Methanol | Cat.No. 20847.320 | VWR, Dresden |
| $MgCl_2$ (magnesium chloride hexahydrate) | Cat.No. 5833.025 | Merck, Darmstadt |
| Mounting Medium Vectashield with DAPI | Cat.No. H-1200 | Vector Laboratories Inc, Burlingame |
| NaCl (sodium chloride) | Cat.No. A3597,5000 | Applichem, Darmstadt |
| NaOH (sodium hydroxide) | Cat.No. 1.06462 | Merck, Darmstadt |
| Nonfat dried milk powder | Cat.No. A0830 | Applichem, Darmstadt |
| OptiMEM | Cat.No. 31985062 | Life Technologies, Carlsbad |
| Paraformaldehyde | Cat.No. P6148 | Sigma-Aldrich, St. Louis |
| PHA | Cat.No. 00-4977-93 | Affymetrix, Santa Clara |
| Pepsine from porcine gastric mucosa | Cat.No. P7012 | Sigma-Aldrich, St. Louis |
| Peptone/Tryptone | Cat.No. A2210,0250 | Applichem, Darmstadt |
| Rad51 inhibitor RI-1 | Cat.No. 553514 | Merck, Darmstadt |
| Roti® Mount FluorCare DAPI | Cat.No. HP20.1 | Roth, Karlsruhe |
| Roti™-Phenol | Cat.No. 0038.3 | Sigma-Aldrich, St. Louis |
| Sodium butyrate | Cat.No. 286367-68-8 | Sigma-Aldrich, St. Louis |
| SDS (sodium dodecyl sulfate) | Cat.No. 75746 | Sigma-Aldrich, St Louis |
| Sodium Phosphate, monobasic, monohydrate | Cat.No. S9638 | Sigma-Aldrich, St Louis |
| *di*-Sodium Hydrogenophsohate dodecahydrate | Cat.No. A3906 | Applichem, Darmstadt |
| *tri*-Sodium Citrate dehydrate | Cat.No. A1357 | Applichem, Darmstadt |
| Temed | Cat.No. 2367.3 | Roth, Karlsruhe |
| Tetradecanoylphorbol acetate | Cat.No. P8139 | Sigma-Aldrich, St. Louis |
| Trichostatin A | Cat.No. T8552 | Sigma-Aldrich, St. Louis |
| Tris | Cat.No. A1086,5000 | Applichem, Darmstadt |
| Triton X-100 detergent | Cat.No. 8603 | Merck, Darmstadt |
| Tween-20 | Cat.No. 9127.2 | Roth, Karlsruhe |
| Water Molecular biology grade | Cat.No. A7398 | Applichem, Darmstadt |
| Yeast extract granulated | Cat.No. 212750 | Becton-Dickinson, Heidelberg |

**Consumables**

| **Name** | **Features/Cat.No.** | **Manufacturer** |
|---|---|---|
| Cell culture dishes | 6-well, 24-well, 96-well | Sarstedt, Nümbrecht |
| Cell culture flasks | 25 ml, 75 ml | Sarstedt, Nümbrecht |
| Conical test tubes 17x120 | 15 ml | Sarstedt, Nümbrecht |
| Conical test tubes 30x115 | 50 ml, with and without feet | Sarstedt, Nümbrecht |
| Cryotubes | 1.8 ml | Nunc, Roskilde |
| Eppendorf tubes 1.5 and 2 ml | 1.5 and 2 ml | Sarstedt, Nümbrecht |
| Expendable cuvettes | 1mm | Biodeal, Markkleeberg |
| Latex gloves | Size S | Unigloves, Troisdorf |
| Kimtech Science, Precision Wipes | Cat.No. 05511 | Kimberly-Clark, Roswell |
| Microscope cover glasses | Cat.No. ECN631-1569 | VWR, Sacramento |
| Nitrile gloves | Size S | Hansa-Medical 24, Hamburg |
| Nytran®SPC | Cat.No. 10416296 | Whatman, Maidstone |
| Parafilm® M | | Bems, Neenah |
| Pipettes for Pipetboy | 5, 10, 25 ml | Sarstedt, Nümbrecht |
| Pipette tips | P1000, 200, 100 and 10 | VWR International, West Chester |
| Pierce™ Concentrators, 150 MWCO, 20ml | Cat.No. 89921 | ThermoFisher, Waltham |
| Petri dishes for cell culture | 60 mm, 100 mm, 150 mm | Sarstedt, Nümbrecht |
| Petri dishes for bacteria | | Sarstedt, Nümbrecht |
| Polystyrene round-bottom tube 5ml | Cat.No. 352063 | VWR, Dresden |
| Polystyrene round-bottom tube with cellstrainer cap 5ml | Cat.No. 352235 | VWR, Dresden |
| PVDF membrane | Cat.No. T830 | Roth, Karlsruhe |
| Sterile syringe filters PVDF | 0,45 µm | VWR International, West Chester |
| SuperFrost® Plus | Cat.No. J1800AMNZ | Menzel Glaser, Braunschweig |
| Transfection polypropylene tubes | | TPP, Trasadingen |

| | | |
|---|---|---|
| Whatman blotting paper | 3MM | GE Healthcare, Freiburg |

**Equipment**

| **Name** | **Features/Cat. No.** | **Manufacturer** |
|---|---|---|
| **General Equipment** | | |
| Fast Real-time PCR system | ABI Prism 7500 | Invitrogen Life Technologies, Grand Island |
| Bacterial incubator | 07-26860 | Binder, Turtlingen |
| Bacterial incubator shaker | Innova 44 | New Brunswick Scientific, New Jersey |
| Bunsen burner | Type 1020 | Usbeck, Radevormwald |
| Cell incubators | Excella ECO-1 | New Brunswick Scientific, New Jersey |
| Centrifuge 5424 | Rotor FA-45-24-11 | Eppendorf, Hamburg |
| Centrifuge 5804R | Rotors A-4-44 and | Eppendorf, Hamburg |
| Centrifuge Sorvall RC 6+ | F45-30-11 | Thermo Scientific, Dreieich |
| Cytospin3 | Shandon | Thermo Scientific, Dreieich |
| Imaging system | Chemismart 5100 | Peqlab, Erlangen |
| Electroporator | Genepulser Xcell | Bio-Rad, München |
| Electrophoresis power supply | | VWR International, West Chester |
| Flow cytometer | FACS Calibur | BD, San Jose |
| FACSsorter | FACS AriaIII | BD, San Jose |
| Freezer | -20°C | Liebherr, Bulle |
| Freezer | -80°C | GFL, Burgwedel |
| Mini centrifuge | Galaxy | VWR International, West Chester |
| Gel electrophoresis chamber | | VWR International, West Chester |
| Gel electrophoresis chamber | SUB-Cell GT | Bio-Rad, München |
| Hybridization Oven | HB-1000 | UVP Laboratory Product, Cambridge |
| Ice machine AF100 | AF100 | Scotsman, Vernon Hills |
| Pipetboy | INTEGRA | IBS Integrated Biosciences, Fernwald |
| Magnetic stirrer | RH basic KT/C | IKA, Staufen |
| Gel chambers | Mini Protean 2D | Bio-Rad, München |
| Protean Tetra Cell chambers | | Bio-Rad, München |
| Nanodrop 1000 | | Peqlab, Erlangen |
| Newbauer counting chamber | | Assistant, Sondheim/Rhön |

| | | |
|---|---|---|
| Nitrogen tank | ARPEGE70 | Air liquide, Düsseldorf |
| Nucleofector™ II | | Lonza, Basel |
| Orbital shaker | 0S-10 | Peqlab, Erlangen |
| Pipets | P1000, P200, P100, P10 | Eppendorf, Hamburg |
| Horizontal Maxi-Gel System | Perfect Blue™ | Peqlab, Erlangen |
| pH-meter | RHBKT/C WTW pH level 1 | Inolab, Weilheim |
| Sterile laminar flow | ScanLaf, Mars Safety Classe 2 | LMS, Brigachtal |
| Sterile laminar flow | | Bleymehl, Inden |
| Thermocycler | T-Gradient | Biometra, Göttingen |
| UV Transiluminator | Bio-Vision-3026 | Peqlab, Erlangen |
| Transiluminator printer P93D | P93D | Mitsubishi, Rüsselsheim |
| Transiluminator | VL-4C, 1x4W-254 nm | Vilber-Lourmat, Eberhardzell |
| Vortex Genie 2™ | | Bender&Hobein AG, Zurich |
| Water baths | TW2 and TW12 | Julabo, Seelbach |
| Water bath shaker | C76 | New Brunswick Scientific, New Jersey |
| **Microscopes and associated equipment** | | |
| Fluorescence microscope | Axiovert S 100 | Carl Zeiss MicroImaging GmbH, Jena |
| Fluorescence microscope | Axio Imager M1 | Carl Zeiss MicroImaging GmbH, Jena |
| Microscope | AE31 | Motic, Wetzlar |
| **Software** | | |
| Axiovision 4.8 software | | Carl Zeiss MicroImaging GmbH, Jena |
| Chemi-Capt | | Vilber-Lourmat, Eberhardzell |
| Graphpad Prism | Version 5 | Graphpad Software Inc, La Jolla |
| Vector NTI | Version 9 | Invitrogen Life Technologies, Grand Island |
| Vision-Capt | | Vilber-Lourmat, Eberhardzell |

### 6.1.2 Enzymes and markers

| **Enzyme** | **Catalog Number** | **Manufacturer** |
|---|---|---|
| Antarctic phosphatase | Cat. No. M0289L | New England Biolabs, Ipswich |
| *Bam*HI | Cat.No. R0136 | New England Biolabs, Ipswich |
| Benzonase | Cat.No. D00111784 | Novagen, San Diego |
| *Dpn*I | Cat.No. ER1701 | New England Biolabs, Ipswich |
| *Eco*RV | Cat.No. R0195 | New England Biolabs, Ipswich |
| *Hae*III | Cat.No. R0108S | New England Biolabs, Ipswich |
| *Hind*III | Cat.No. R0104 | New England Biolabs, Ipswich |
| *Sac*I | Cat.No.R3156 | New England Biolabs, Ipswich |
| *Xho*I | Cat.No.R0146 | New England Biolabs, Ipswich |
| *Pac*I | Cat.No. R0547 | New England Biolabs, Ipswich |
| Phusion Hot Start High-Fidelity DNA Polymerase | Cat.No. M0530S | Thermo Scientific, Rochester |
| Proteinase K | Cat.No. 7528.2 | Roth, Karlsruhe |
| RNase A | Cat.No. 2326466 | Applichem, Darmstadt |
| T4 DNA Ligase | Cat.No. 01-1020 | Peqlab, Erlangen |
| Taq DNA-Polymerase | Cat.No. 01-1020 | Peqlab, Erlangen |
| SensiFast probe lo-ROX mix 2x | Cat.No. BIO-84020 | Bioline, Luckenwalde |
| **Marker** | | |
| Generuler™ 1kb Plus DNA | Cat.No. SM0311 | Fermentas, Mannheim |
| Protein Prestained plus marker | Cat.No. 26619 | Thermo Scientific, Darmstadt |

### 6.1.3 Antibodies

| **Name** | **Catalog Number** | **Company** |
|---|---|---|
| Anti-ß-Actin | Cat.No. 49705 | CellSignaling, Cambridge |
| Anti-hDaxx | Cat.No. 631301 | Biolegend, San Diego |
| Anti-DIG-FITC | Cat.No. 11207741910 | Roche, Mannheim |
| Anti-DIG-ALP | Cat.No. 11093274910 | Roche, Mannheim |
| Anti-PML | Cat.No. A301-167A | Bethyl, Montgomery |
| Goat-anti-mouse HRP | Cat.No. Sc-2031 | Santa Cruz, Santa Cruz |
| Goat-anti-rabbit AF488 | Cat.No. A11008 | Santa Cruz, Santa Cruz |
| Goat-anti-rabbit HRP | Cat.No. 7074S | CellSignalling, Cambridge |
| Streptavidin-Cy3 | Cat.No. PA43001 | GE Healthcare, Berlin |

### 6.1.4 Kits

| Name | Catalog Number | Company |
|---|---|---|
| Amaxa Nucleofector kit V | Cat.No. VCA-1003 | Lonza, Basel |
| Biotin labeling kit | Cat.No. PP-303S-BIO | Jena Biosciences, Jena |
| CDP-Star ready-to-use | Cat.No. 12041677001 | Roche, Mannheim |
| DIG High-Prime | Cat.No. 11585606910 | Roche, Mannheim |
| DIG PCR probe synthesis kit | Cat.No. 11636090910 | Roche, Mannheim |
| DIG Wash and block Buffer set | Cat.No. 11585762001 | Roche, Mannheim |
| ECL Plus Detection kit | Cat.No. RPN2232 | GE Healthcare, Berlin |
| GF-1 AmbiClean PCR/Gel purification kit | Cat.No. GF-GC-200 | Vivantis, USA |
| Hi Yield Gel/PCR DNA Fragments Extraction Kit | Cat.No. HYDF100-1 | SLG, Gauting |
| Nucleobond BAC100 Midi kit | Cat.No. 740579 | Macherey-Nagel, Düren |
| RTP® DNA/RNA Virus Mini Kit | Cat.No. 1040100300 | STRATEC Molecular GmbH, Berlin |

### 6.1.5 Antibiotics

| Name | Working concentration | Manufacturer |
|---|---|---|
| Ampicillin (Amp) [Cat. No. K0292] | 100 µg/ml in $ddH_2O$ | Roth, Karlsruhe |
| Kanamycin sulphate (Kana) [Cat. No. T832.3] | 50 µg/ml in $ddH_2O$ | Roth, Karlsruhe |
| Chloramphenicol (Cam) [Cat. No. 3886.3] | 30 µg/ml in 96 % EtOH | Roth, Karlsruhe |
| Acyclovir [Cat.No. C10045600] | 1mM in $ddH_2O$ | Dr. Ehrenstorfer, Augsburg |
| Penicillin (P) [Cat. No. A1837] | 100 U/ml in MEM | Applichem, Darmstadt |
| Streptomycin (S) [Cat. No. A1852] | 100 U/ml in MEM | Applichem, Darmstadt |
| Puromycin (Puro) [Cat. No. A11138-03] | 1 µg/ml in RPMI | Invitrogen, Carlsbad |

### 6.1.6 Bacteria, cells, viruses and plasmids

| **Name** | **Features** | **Reference** |
|---|---|---|
| **Bacteria** | | |
| Top10 | $F^-$ mcrA Δ(mrr-hsdRMS-mcrBC) φ80lacZΔM15 ΔlacX74 nupG recA1 araD139 Δ(ara-leu)7697 galE15 galK16 rpsL($Str^R$) endA1 | Invitrogen, Carlsbad |
| GS1783 | DH10B λ cl857 Δ(cro–bioA)<>araC-$P_{BAD}$I-SceI | [192] |
| Stbl3 | $F^-$mcrB mrrhsdS20($r_B^-$, $m_B^-$) recA13 supE44 ara-14 galK2 lacY1 proA2 rpsL20($Str^R$) xyl-5 $\lambda^-$leumtl-1 | ThermoScientific,Waltham |
| **Cells** | | |
| HEK293T | Human epithelial kidney cell line, SV40 T-antigen | ATCC CRL-11268 |
| U2OS | Human epithelial osteosarcoma cell line | ATCC HTB-96 |
| JJHan | Acute T-cell leukemia-derived cell line and a subclone of the JURKAT line | HHV-6 foundation |
| **Viruses** | | |
| HHV-6A BAC | Bacterial artificial chromosome (BAC) of HHV-6A strain U1102 | [191] |
| **Plasmids** | | |
| pcDNA3 | Mammalian expression vector; T7prom, f1 ori, pBR322 ori, AmpR, pCMV, pSV40, NeoR | Invitrogen, Carlsbad |
| pEP Kan-S | Mammalian expression vector, T7prom, f1 ori, SV40 prom, KanR, I-Sce-I restriction site, AmpR, ColE1 ori, NeoR | [193] |
| pLKO-shDPS | Mammalian expression vector for shRNAs, 7SK, mU6, U6, shPML, shDaxx, shSp100, CPPT, hPGK, PuroR, sin 3'LTR, f1 ori, AmpR, pUC ori, 5'LTR, RRE | [70] |
| pCMV-dR8.91 | Mammalian expression vector for envelope, AmpR, CMV promoter, VSV-G, SV40 polyA | [70] |
| pCMV-VSV-G | Mammalian expression vector for packaging, CMV promotor, Gag-Pol, CPPT, RRE, SP6, AmpR, pBR322 ori | [70] |

| | | |
|---|---|---|
| pCGN1-pp71 | Mammalian expression vector for pp71 (HCMV), CMV promotor, AmpR, SV40 ori, HygR, M13 ori | [85] |

### 6.1.7 Buffers and media

**General buffers**

**1x Phosphate saline buffer (1x PBS)**

2 mM $KH_2PO_4$

10 mM $Na_2HPO_4$

137 mM NaCl

2.7 mM KCl, pH 7.3

**1x Tris-acetate-EDTA buffer (TAE)**

40 mM Tris

1 mM $Na_2EDTAx2H_2O$

20 mM Acetic acid 99 %, pH 8.0

**0.8 % Agarose Gel**

80 mM Agarose

1x TAE buffer

4 µl Ethidium bromide 10 mg/ml

**Media and supplements for cultivation of bacteria (*E.coli*)**

**LB medium (1l)**

10 g Bacto™ Tryptone

5 g Bacto™ Yeast Extract

10 g NaCl

15 g Bacto™ Agar

**SOB medium (1l)**

20 g Bacto™ Tryptone

5 g Bacto™ Yeast Extract

0.584 g NaCl

0.186 g KCl

pH to 7.0

**SOC medium**

SOB medium

20 mM Glucose

**Plasmid preparation solution**

**Buffer (P1)**

50 mM Tris HCL pH 8.0

10 mM EDTA

100 µg/ml RNase

**Neutralization Buffer (P3)**

3 M K-Acetate pH 5.5

**Lysis Buffer (P2)**

200 mM NaOH

1 % SDS

**Buffer TE**

10 mM Tris HCl pH 7.4

1 mM $Na_2EDTA$

**Media and supplements for cultivation of mammalian cells**

| **Name** | **Catalogue number** | **Manufacturer** |
|---|---|---|
| Biocoll Separating solution, density 1.077 g/ml | Cat.No. L6115 | Biochrom AG, Berlin<br>Sigma-Aldrich, St Louis |
| Fetal bovine serum (FBS) | Cat.No. S 0415 | Biochrom AG, Berlin |
| Fetal calf serum (FCS) | Cat.No. P30-1506 | Pan Biotech, Aidenbach |
| Minimum essential Medium Eagle (MEM) | Cat.No. F 0315 | Biochrom AG, Berlin |
| RPMI 1640 (w/o Glutamine) | Cat.No. F 1215 | Biochrom AG, Berlin |
| Trypsin | Cat.No. L 2103-20G | Biochrom AG, Berlin |

**Trypsin**

137 mM NaCl
2.7 mM KCl
8 mM $Na_2HPO_4 * 2H_2O$
1.8 mM $KH_2PO_4$
Trypsin 1:250

**Southern blot solutions**

**Transfer buffer**

0.5 M NaOH
1.5 M NaCl

**Church Buffer**

0.25 M Sodium Phosphate Buffer pH 7.2
1 mM EDTA
1 % BSA
7 % SDS

**Low stringency buffer**

0.5x SSC
0.1% SDS

**High stringency buffer**

2x SSC
0.1 % SDS

**Southern I**

0.1 M Maleic acid
0.15 M NaCl pH 7.5
0.3 % Tween-20

**Southern II**

1x Maleic acid buffer
1 % Blocking reagent (Roche)

**Southern III**

0.1 M Tris-HCl
0.1 M NaCl, pH 9.5

**Fluorescence *in situ* hybridization (FISH) solutions**

**Hypotonic solution**

0.075 M KCl

autoclaved

**20x SSC**

87.6 g NaCl

44.1 g TriNaCitrate dehydrate

to 500 ml in $ddH_2O$, pH to 7.4

**Fixative**

Methanol:Acetic acid 3:1

**Stringency wash solution**

50 % 2x SSC

50 % Deionized formamide

**Detergent wash solution**

4x SSC

0.5 % Tween-20

**Pepsine solution**

0.01 % Pepsin in 10 mM HCl

**Hybridization buffer**

50 % Deoinized formamide (v/v)

10 % Dextran sufate (v/v)

2x SSC

1 x Phosphate buffer, pH 7.0

Probe

Salmon sperm

**Western blot solutions**

**10x SDS PAGE running buffer**

250 mM Tris

1.9 M Glycine

1 % SDS

**2x Stripping buffer**

50 mM Glycine

2 % SDS

pH 2

**10x Lämmli buffer**

1.25 M Tris-HCl pH 6.8

10 % SDS

0.2 % Bromophenol blue

**Transfer buffer**

25 mM Tris

192 mM Gycine

20 % (v/v) MeOH

**RIPA buffer**

20 mM Tris-HCl

150 mM NaCl

1 % (v/v) Nonidet P-40

0.5 % (w/v) Sodium deoxycholate

0.1 % (w/v) SDS

Complete® Mini protease/phosphatase

inhibitor cocktail

### 6.1.8 Primers

**Table 2: Primers HHV-6A TMR project**

| | | |
|---|---|---|
| **Mutagenesis primers** | | |
| ΔpTMR | for | GGTGGCCTGGCACGGTGCCAAAGGAAACCACCGGCTAACCCATCCCCCAACGCGTAGGGATAACAGGGTAATCGATTT |
| | rev | CTCCCATAGCGGCGTGCGCGCGCGCGTTGGGGGATGGGTTAGCCGGTGGTTTCCTTTGGCCAGTGTTACAACCAATTAACC |
| ΔpTMRrevertant | for | TACACACGCAGACACACAGACA |
| | rev | ATACCGTCGTCCGCTCTTTC |
| Kana-in wt pTMR | for | ATCCCCCCACGCGCGCGCGCACGCCGCTATGGGAGGCGCCGTGTTTTTCACCAACACGCGCGCCGCTGCGAGACTAGGGATAACAGGGTAATCGATTT |
| | rev | GTCTCGCAGCGGCGCGCGTGTTGGTGAAAAACACGGCGCCAGTGTTACAACCAATTAACC |
| ΔimpTMR | for | CAAATCCCCCGGGGGGGGCTAAAAAAAGGGGGGGTAATAACGCTGCCCCTCTTTCACACTAGGGATAACAGGGTAATCGATTT |
| | rev | GAAGCGGCAGGGGGGTGATGGTGTGAAAGAGGGGCAGCGTTATTACCCCCCCTTTTTCAGTGTTACAACCAATTAACC |
| ΔimpTMRrevertant | for | GACTCCTTTTTTGTTTCGTTTTCC |
| | rev | CCCAAGAGTAGCCACCAATAAT |
| Kana-in wt impTMR | for | CTTTCACACCATCACCCCCTGCCGCTTCAACTTCACCTTCTTCCTCCATCTCGCCCCGCTTGTTTCTACATAGGGATAACAGGGTAATCGATTT |
| | rev | GGACAAGTGTAGAAACAAGCGGGGCGAGATGGAGGAAGCCAGTGTTACAACCAATTAACC |
| **Sequencing primers** | | |
| pTMR region | for | TACACACGCAGACACACAGACA |
| | rev | ATACCGTCGTCCGCTCTTTC |
| impTMR region | for | GACTCCTTTTTTGTTTCGTTTTCC |
| | rev | CCCAAGAGTAGCCACCAATAAT |
| **Other primers** | | |
| TMR probe | for | TACACACGCAGACACACAGACA |
| | rev | ATACCGTCGTCCGCTCTTTC |

**Table 3: Primers HHV-6A U94 project**

| | | |
|---|---|---|
| **Mutagenesis primers** | | |
| ∆U94 | for | TAAAAGTGGTCTTTTAAGATGTTGTTAAATATATAGTTAACCG TTTGCGCCTCCCAAGTAGGGATAACAGGGTAATCGATT |
| | rev | CGTATACAACTATAAAAAACTTGGGAGGCGCAAACGGTTAA CTATATATTTAACAACGCCAGTGTTACAACCAATTAACC |
| ∆U94revertant | for | ATTTTAAAAGTGGTCTTTTAAGATGTTGTTAAATATATAGTTA TAAAATTTTCGGAACCG |
| | rev | CCGTATACAACTATAAAAAACTTGGGAGGCGCAAACGGTAT GTTTTCCATAATAAATCCG |
| U94stop | for | GGATTTCTGCCTCCCACTCCACGGGGCCTTTGATAGTCAA CTAGATATATTTGTCCTTAGTCCTAGGGATAACAGGGTAATC GATTT |
| | rev | AATCCAAGTGATGATTTTTGGACTAAGGACAAATATATCTAG TTGACTATCAAAGGCCCCGTGCCAGTGTTACAACCAATTAA CC |
| U94stop2 | for | CGGCAGTTTTATTATTCCAGTAATTGAGTATGACATCGATCT ATTTGGTACATGCAGTTATCCTAGGGATAACAGGGTAATCG ATTT |
| | rev | GGGAGCGCCCGATATTAAATGGATAACTGCATGTACCAAAT AGATCGATGTCATACTCAATTAGCCAGTGTTACAACCAATTA ACC |
| U94stoprevertant | for | TTCTTCTGCTAACTCGGACGC |
| | rev | TGTTTTCGTCACACGTGGAC |
| **Sequencing primers** | | |
| U94 region | for | TTCTTCTGCTAACTCGGACGC |
| | rev | TGTTTTCGTCACACGTGGAC |
| **Other primers** | | |
| Shuttle plasmid U94 | for | CGCACTTAAGCTTGGTATGTTTTCCATAATAAATCCGAGTG |
| | rev | CGACGATGGATCCTTATAAAATTTTCGGAACCGTGTAGTC |
| Kana-in U94 | for | GACTTTTAATTAATAGGGATAACAGGGTAATCGATTT |
| | rev | CTGTATTAATTAATACGCCCCTGATTTCCGTTGTGTGTTTTC CTATCGTTGCGGCCAGTGTTACAACCAATTAACC |
| U94 probe 1 | for | CCCTCTGTGATAGATTTATTTTGTG |
| | rev | CCATAGGGCTCTATCTATAGCTAAA |
| U94 probe 2 | for | CCGTGTGTTAGCGTCAACAA |
| | rev | AATAAAGCTGGCAGACCCTC |

**Table 4: qPCR primers**

| | | |
|---|---|---|
| **qPCR primers** | | |
| ß2M | for | CCAGCAGAGAATGGAAAGTCAA |
| | rev | TCTCCATTCTTCAGTAAGTCAACTTCA |
| ß2M probe | | FAM-ATGTGTCTGGGTTTCATCCATCCGACA-TAMRA |
| U86 | for | TGTACATGGGCTGTAGGAGTTGA |
| | rev | ACATCCTCTGCTTCCAATCTACAATC |
| U86 probe | | FAM-TTCCGAAGCAAAGCGCACCTGG-TAMRA |

## 6.2 Methods

### 6.2.1 Molecular biology methods

#### 6.2.1.1 The Red recombination system and *en passant* mutagenesis

Bacterial artificial chromosomes (BACs) for cloning large DNA fragments of more than 300 kb were first established in the early 1990s and are based on the single-copy F-plasmid of *E.coli* [194]. The stable maintenance and easy manipulation of the cloned DNA make BACs a useful tool for many research areas including herpesvirology. Already in 1997, Messerle *et al.* cloned the first herpesvirus genome, that of MCMV (murine cytomegalovirus), into a BAC with efficient reconstitution of infectious progeny by transfection into eukaryotic cells [195]. To manipulate BACs, the Red recombination system, derived from the λ-phage, is widely used to introduce desired modifications including insertions, deletions, point mutations or tags. The recombination system consists of the Exo, Beta and Gam proteins that are controlled by a temperature-inducible promoter [196-198]. Gam inhibits the degradation of double strand breaks mediated by *E. coli* RecB/C/D enzymes [199]. The 5'-3' exonuclease Exo produces 3' single strand overhangs [200] that are protected by the Beta protein. Moreover, Beta promotes annealing of complementary single strands of DNA [201, 202]. Red recombination only requires homologous sequences of 30-50 bp in length; therefore, PCR-amplified fragments can be used as targeting cassettes and are introduced by electroporation [203]. For the markerless two-step Red-mediated recombination system used in this dissertation, an *E.coli* strain termed GS1783 was used that harbors the temperature-inducible λ-phage Rec system as well as the *I-Sce*I homing endonuclease (18 bp recognition site, originating from *Saccaromyces cerevisiae* [204]) under an arabinose-sensitive promoter [192, 193].

The initial step in the two-step Red-mediated mutagenesis, also known as *en passant* mutagenesis, is generating a linear DNA product by PCR (Figure 9). This contains the desired point mutation or deletion in combination with a resistance marker cassette, usually the *aphAI* kanamycin resistance gene and the *I-Sce*I restriction site. In their overhangs, primers comprise homologous sequences for the first Red recombination step (A/B and C/D), the mutation of interest (indicated with the X) and sequence duplications for scarless removal of the resistance marker in the second Red recombination step (B/C). Furthermore, they need to contain a specific sequence in order to anneal to the pEP Kan-S plasmid (black lines) allowing amplification.

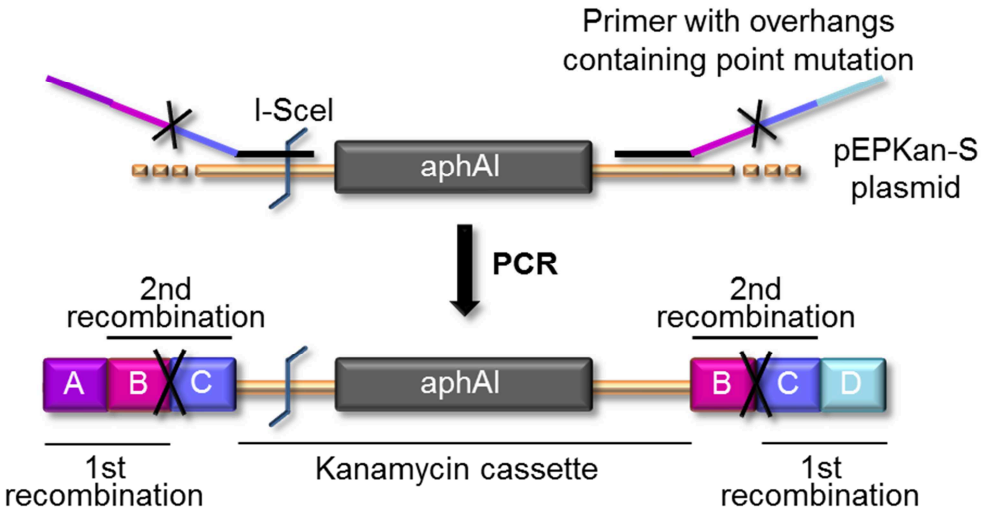


**Figure 9: PCR product amplified from pEP Kan-S for deletions and insertion of point mutations into the genome.** Symbol X indicates location for deletions or introduction of point mutations. The regions A/B and C/D, located at both extremities of the PCR product (in primer overhangs), enable integration of the electroporated PCR product into the genome's desired locus (1st Red recombination), whereas the duplicated sequences B/C allow markerless removal of *aphAI* upon *I-Sce*I cleavage during resolution (2nd Red recombination).

Following electroporation of the PCR product into competent BAC-containing GS1783 bacteria, the first Red recombination takes place via the homologous A/B and C/D sequences, inserting the entire cassette (containing the mutation/deletion) into the desired locus of the genome; giving rise to the intermediate that can be selected for via the introduced kanamycin resistance gene. Next, induction of *I-Sce*I expression generates a double-strand break (termed resolution) and allows for the second Red recombination resulting in the seamless removal of the selection marker, giving rise to the final clone (Figure 10).

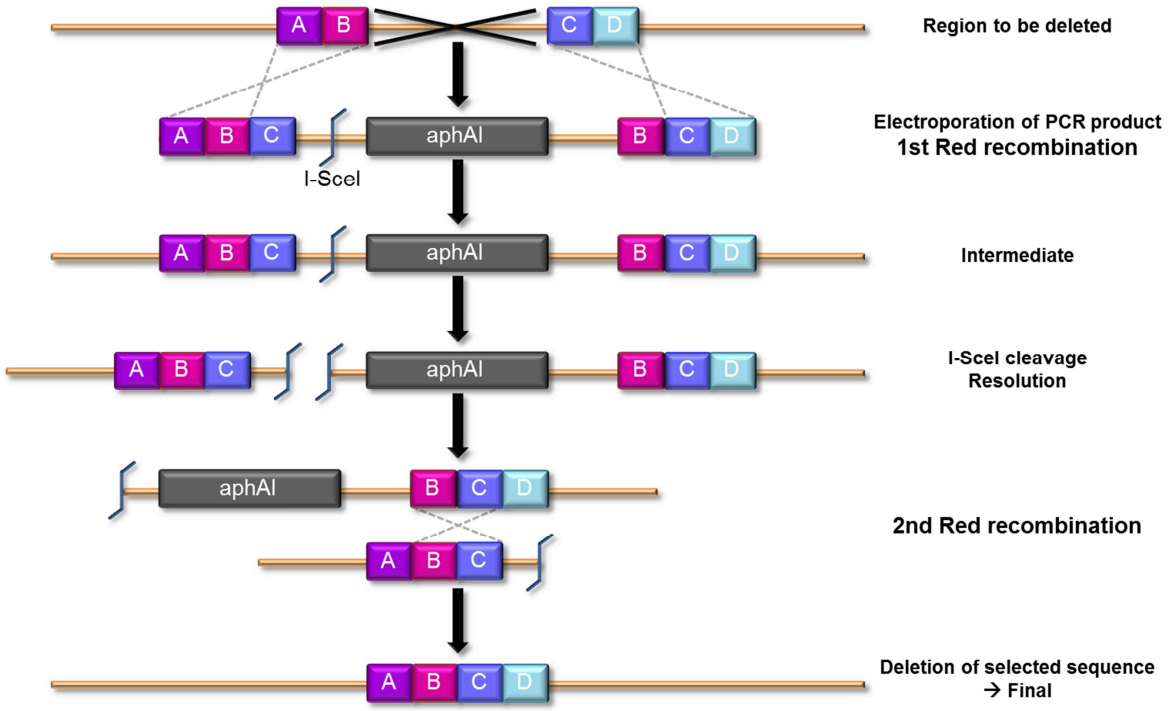


**Figure 10: Schematic overview of two-step Red-mediated recombination (*en passant* mutagenesis) for deletion of selected sequences.** Homologous flanks A/B and C/D enable the integration of the PCR product containing the kanamycin resistance gene and *I-Sce*I site into the correct locus in a first Red recombination step resulting in the intermediate, which can be selected for. Following *I-Sce*I induction with L-arabinose and incubation at 42 °C, the second Red recombination step, termed resolution, takes place, via homologous recombination between the sequences B/C. The selection marker is scarlessly removed. Modified from Tischer *et al.* [193].

For insertion of long sequences into the viral genome (to generate ΔU94 revertant), an intermediate construct (transfer plasmid) needed to be prepared (see 6.2.1.1.1). This construct harbors the kanamycin cassette with the *I-Sce*I site flanked by duplicated sequences of approximately 40 bp (for 2$^{nd}$ Red recombination) cloned into a unique restriction site within the gene of interest. This is then amplified by PCR with primers containing homologous sequences for the 1$^{st}$ Red recombination in their overhangs and electroporated into competent bacteria. The mutagenesis protocol is otherwise identical, as shown in Figure 11.

Due to cloning difficulties of the repeated sequences into a plasmid vector, I generated BAC-based transfer constructs by recombination as an intermediate step for generating the TMR revertants. In the wild type (wt) BAC background, the kanamycin cassette and the *I-Sce*I site (between duplicated sequences for 2$^{nd}$ Red recombination) were inserted in very close proximity to the pTMR or impTMRregion, respectively. This BAC intermediates

were used as a PCR template as shown in Figure 11. The resulting PCR product was used for mutagenesis as described above.

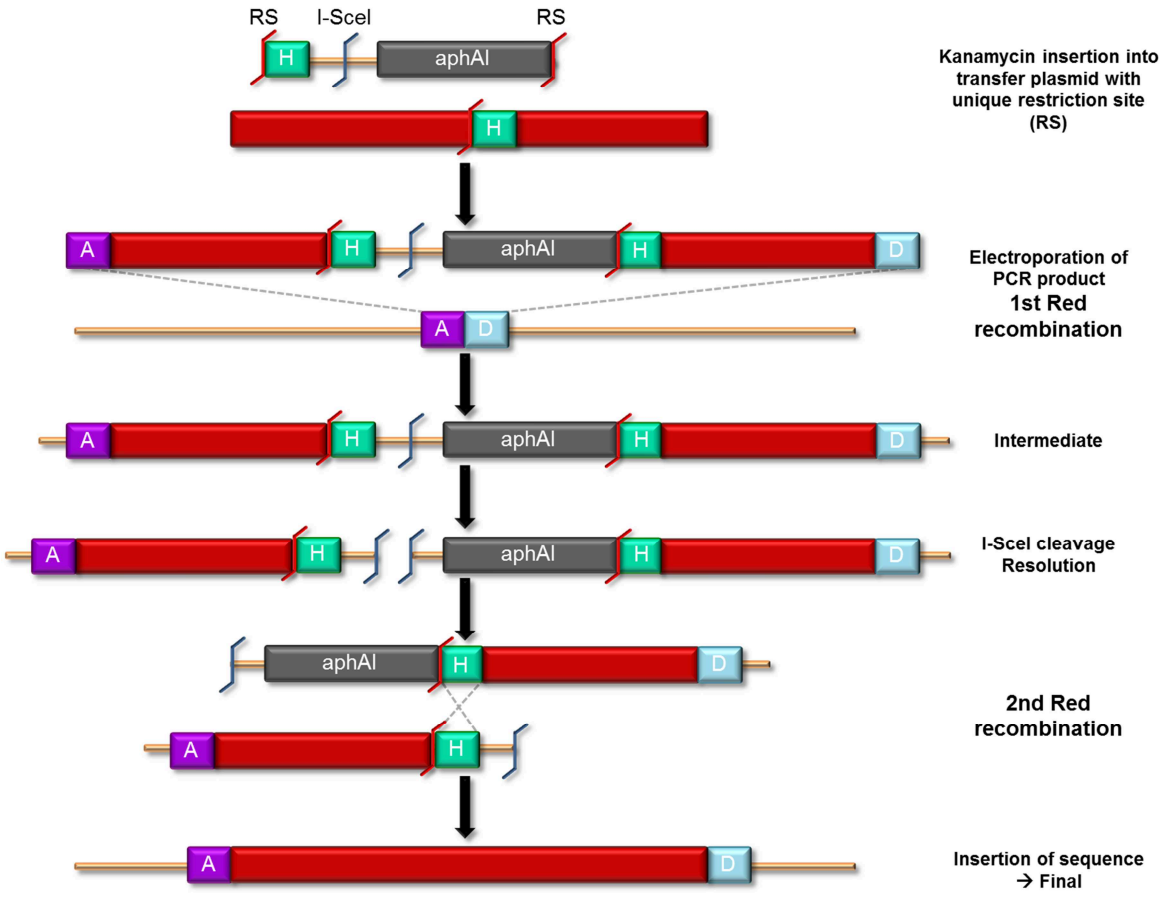


**Figure 11: Schematic representation of the two-step Red-mediated recombination (*en passant* mutagenesis) procedure for insertion of long sequences into the viral genome.** Initially, the kanamycin cassette with homologous sites (H) and *I-Sce*I restriction site needs to be cloned into a unique restriction site (RS) of the sequence/gene to be inserted, previously cloned into a plasmid. After PCR amplification with primers adding homologous flanks A/D, the first Red recombination step is performed and the PCR product is integrated into the genome. The following process is identical to the previously described procedure (Figure 10). Modified from Tischer *et al.* [193].

#### 6.2.1.1.1 Generation of recombinant plasmids

First, the entire *U94* ORF was amplified from the HHV-6A BAC and cloned into pcDNA3 between the *Bam*HI and *Hind*III sites of the multiple cloning site. All PCR products (primers in Table 3) used for cloning were column purified using Hi Yield Gel/PCR DNA Fragments Extraction Kit (SLG, Gauting) according to the manufacturer's instructions. Final concentrations of the prepared DNA were measured with the Nanodrop1000 (Peqlab, Erlangen). Insert and vector were digested for 3 h with the appropriate enzymes in the recommended buffers at 37 °C. The vector was dephosphorylated using antarctic

phosphatase for 20 min at 37 °C. Digested insert and vector were separated on a 1 % agarose gel at 100 V for 30 min and gel-purified using the Hi Yield Gel/PCR DNA Fragments extraction kit (SLG, Gauting) according to the manufacturer's instructions. Insert and vector were ligated at a ratio of 3:1. Ligation reaction was performed in 1x ligase buffer containing 5 units T4 ligase and was incubated o/n at 16 °C. Ligation mix was transformed into chemically competent Top10 *E.coli* and plated onto agar plates containing ampicillin. After mini-prep (see 6.2.1.1.2), diagnostical digests with several enzymes were performed as well as sequencing of the final construct. Subsequently, the *U94* transfer plasmid, for re-insertion of the *U94* ORF in the ΔU94 mutant, was generated by the insertion of the kanamycin resistance gene (*aphAI*) along with the *I-Sce*I site and sequence duplications for the removal of the selection marker in the 2nd Red recombination step. For this purpose, the *aphAI* kanamycin resistance gene and an *I-Sce*I restriction site were amplified from pEP Kan-S plasmid along with sequence duplications and inserted into the unique *Pac*I site of the HHV-6A *U94* gene as described above.

#### 6.2.1.1.2 DNA mini- and midi-preparation

To isolate DNA from bacteria, a standard alkaline lysis protocol was performed. For that purpose, bacterial culture was grown overnight (o/n) at 32 °C in 4 ml LB medium supplemented with the appropriate antibiotics. The next day, the culture was pelleted for 5 min at 5,000 rpm and the supernatant was discarded. The bacterial pellet was resuspended in 300 µl of P1 buffer and cells were lysed by the addition of 300 µl P2 buffer and incubated for 5 min at RT. To neutralize the reaction and to precipitate proteins, 300 µl of buffer P3 were subsequently added to the mixture. After incubation for 10 min on ice, proteins and cell debris were removed by centrifugation (10 min, 10,000 rpm). The supernatant was transferred into a new tube, and 900 µl of a phenol:chloroform solution were added to ensure the elimination of proteins. Following sample vortexing and centrifugation for 10 min at 10,000 rpm, the aqueous phase was transferred to a new tube, mixed with 450 µl of isopropanol and incubated for 10 min at -20 °C. DNA precipitation was carried out by centrifugation of the samples for 15 min at 10,000 rpm and 4 °C. After two wash steps with 70 % ethanol, residual ethanol was completely removed by heating the samples for 5 min at 37 °C. DNA was then dissolved in TE-buffer containing RNase A (final concentration 100 µg/ml) at 37 °C for 30 min. Subsequently, digestion with appropriate enzymes was performed with the extracted DNA and obtained fragments separated by a 0.8 % agarose gel electrophoresis o/n at 65 V (restriction fragment length polymorphism RFLP).

Midi DNA preparations were performed using the BAC100 Kit (Macherey-Nagel, Düren) following the manufacturer's instructions for BAC DNA.

#### 6.2.1.1.3 Electrocompetent bacteria

GS1783 bacteria containing the BAC clone of the HHV-6A strain U1102 were grown o/n at 32 °C in 1 ml LB medium with chloramphenicol (Cam). The following day, 100 ml were inoculated with the o/n culture and incubated at 32 °C under vigorous shaking (220 rpm). When the bacteria culture reached the logarithmic growth phase after 2-4 h ($OD_{600}$ 0.5-0.7), a heat shock was performed to activate the Red-recombination system. For this, bacteria were heated for 15 min to 42 °C at 220 rpm and afterwards cooled on ice for 20 min under continuous shaking. The culture was pelleted by centrifugation (5,000 rpm, 5 min at 4 °C), followed by three washing steps with an ice-cold 10 % glycerol solution. After the final wash (5,000 rpm, 5 min, 4 °C), bacteria were resuspended in a small volume of 10 % glycerol, aliquoted in 1.5 ml Eppendorf tubes and snap-frozen for storage at -80 °C.

#### 6.2.1.1.4 Generation of HHV-6A mutants

For the first Red recombination, electrocompetent GS1783 bacteria were thawed on ice and 100 ng of *Dpn*I-digested PCR product (protocol Table 5) was electroporated. Electroporation was performed at 1.25 kV, 25 µF and 200 Ω. Subsequently, 900 µl of pre-warmed LB-medium were added to the bacteria. After 1 h incubation at 32 °C and 220 rpm, cells were pelleted for 2 min at 5,000 g, most of the supernatant was discarded, bacteria were resuspended in residual media (~60 µl) and then streaked out on LB agar plates containing chloramphenicol (Cam) and kanamycin (Kana), to positively select for *E. coli* clones harboring the kanamycin resistance gene. After 48 h incubation at 32 °C, several clones were screened by RFLP for correct banding pattern.

Positive clones were cultured o/n at 32 °C in 2 ml LB+Cam+Kana for resolution/second Red recombination, to facilitate excision of the kanamycin cassette the next day. 2 ml LB+Cam were inoculated with 100 µl of the o/n culture. After 3-4 h shaking at 32 °C, 2 ml of LB+Cam containing 2 % arabinose were added to induce *I-Sce*I expression and incubated for 60 min at 32 °C and 220 rpm. To activate the Red recombination system, bacteria were incubated for 30 min at 42 °C and 220 rpm. To allow recombination, the culture was subsequently grown for another 4 h at 32 °C. $10^{-4}$ and $10^{-6}$ dilutions of the culture were prepared in LB and 20 µl distributed on agar plates with Cam+1 % arabinose. After 48 h in the 32 °C incubator, individual colonies (~20) were picked and *replica*-plated on plates containing LB+Cam and LB+Cam+Kana. Kana-sensitive clones (finals) were further screened by RFLP.

**Table 5: Two-step PCR protocol for the generation of HHV-6A mutants**

| Temperature (°C) | Time | PCR step | Cycles |
|---|---|---|---|
| 94 °C | 5 min | Initial denaturation | |
| 94 °C | 30 s | Denaturation | |
| various | 30 s | Annealing | 10 cycles |
| 72 °C | various | Elongation | |
| 94 °C | 30 s | Denaturation | |
| 68 °C | 30 s | Annealing | 30 cycles |
| 72 °C | various | Elongation | |
| 72 °C | 8 min | Extension | |

#### 6.2.1.1.5 Sequencing PCR

To confirm that the recombination occurred properly, the mutated locus was analyzed by DNA sequencing in the final clones using primers listed in Table 2 and Table 3. The protocol for the sequencing PCR is shown in Table 6.

**Table 6: Sequencing PCR protocol**

| Temperature (°C) | Time | PCR step | Cycles |
|---|---|---|---|
| 94 °C | 5 min | Initial denaturation | |
| 94 °C | 30 s | Denaturation | |
| 52 °C | 30 s | Annealing | 30 cycles |
| 72 °C | Various | Elongation | |
| 72 °C | 8 min | Extension | |

### 6.2.1.2 Southern blot

To verify the deletions of *U94* as well as of the TMR sequences in the BAC mutants, I performed southern blotting. After a 3 h digestion at 37 °C with either *Sac*I, *Eco*RV or *Hind*III, samples were separated on a 0.8 % agarose gel o/n at 65 V. Next day, the gel was stained for 40 min in a TAE bath containing ethidium bromide (1:25,000) and pictures were taken with the Vision-Capt system (Vilber-Lourmat, Eberhardzell). Afterwards, the gel was washed in dd$H_2O$ for 30 min to remove the TAE buffer and excess ethidium bromide. The DNA within the gel was depurinated using 0.25 N HCl for 10 min under continuous shaking. The gel was then briefly rinsed with water and equilibrated in transfer buffer. O/n transfer of the DNA onto a positively charged Nytran®SPC membrane (Whatman, Maidstone) was performed by an upward flow of southern blot transfer buffer. The membrane was shortly washed with 2x SSC to remove gel residues. Following a 30 min incubation at 42 °C with Church buffer, the membrane was hybridized with the DIG-labeled probe (1 µg) diluted in Church buffer at 42 °C o/n. Next, two washing steps with

low stringency buffer for 10 min at RT, two wash steps with pre-warmed high stringency buffer for 15 min at 65 °C and finally one wash with Southern I solution for 5 min at RT were performed. Blocking of the membrane was carried out for 30 min at RT with Southern II solution prior to incubation with an anti-DIG-ALP antibody (1:10,000) diluted in Southern II for 30 min at RT. Then, the membrane was washed twice at RT with Southern I for 10 min and once with Southern III for 5 min. CSP-star detection reagent was used according to the manufacturer's instruction in order to detect signals with the Chemi-Capt system (Vilber-Lourmat, Eberhardzell).

### 6.2.2 Cell culture methods

#### 6.2.2.1 Culture of eukaryotic cells

All cell types used in this project were grown at 37 °C and under 5 % $CO_2$ atmosphere. HEK293T and U2OS cells were cultured with MEM containing 10 % FCS with 1 % penicillin/streptomycin (P/S). Confluent monolayers were passaged after 1x PBS wash and detached with 0.25 % trypsin-EDTA. Trypsin was inactivated by adding 10 % FCS in growth media to detached cells; subsequently cells were either routinely split 1:4 for further passaging, seeded for specific experiments or frozen in 1.8 ml cryotubes in growth media containing 8 % DMSO. The suspension T-cell line JJHan was grown in RPMI media supplemented with 10 % FBS and 1 % P/S. At a cell density of ~1x $10^6$ cells/ml, cells were split every three days 1:4 for routine passaging.

#### 6.2.2.2 Lentiviral transduction

ND10 components in JJHan T-cells were knocked down by shRNAs delivered by a lentivirus transduction system. Lentiviruses were prepared by co-transfection of HEK293T cells with a pLKO-shDPS vector containing shRNAs against the major ND10 components PML, hDaxx and Sp100, pCMV-VSV-G (expressing the vesicular stomatitis virus (VSV) envelope protein), and pCMV-dR8.91 (expressing lentivirus helper functions), as described previously [70]. Virus supernatants were harvested 24 h and 48 h after transfection and filtered before use. Subsequently, JJHan target cells were transduced with these lentiviruses expressing shRNAs directed against the respective cellular proteins. Stable cell lines were selected using puromycin (initially 1 µg/ml and then reduced to 0.5 µg/ml during subsequent passages). The degree of PML and hDaxx silencing was monitored by both immunofluorescence and Western blotting.

#### 6.2.2.3 Immunofluorescence

Immunofluorescence staining was performed to evaluate the knockdown of PML in JJHan cells after lentiviral transduction. After initial PBS wash, cells were fixed with 4 % PFA in

PBS for 15 min at RT, permeabilized with 0.1 % Triton X-100 in PBS for 3 min at RT, and blocked with 10 % BSA in PBS for 30 min. After removing the blocking solution, cells were stained with rabbit anti-PML (1:1,000) diluted in PBS with 3 % FBS for 60 min. Cells were washed three times with PBS prior to incubation for 60 min with anti-rabbit AlexaFluor488 antibody (1:1,000) diluted in PBS with 3 % FBS. Cells were centrifuged onto glass slides using the Cytospin3 device (Thermo Scientific, Dreieich) for 5 min at 300 rpm. After mounting (containing DAPI to visualize the nuclei), pictures were taken with the Axio Imager M1 fluorescence microscope (Zeiss, Jena).

#### 6.2.2.4 Western blot

JJHan or JJHan ND10KD (knockdown) cells were harvested and lysed in radioimmunoprecipitation assay buffer (RIPA). Lysates were separated by sodium dodecyl sulfate (SDS) polyacrylamide gel electrophoresis (PAGE) using a 10 % gel for 20 min at 60 V and 90 min at 130 V, followed by transfer of the proteins onto a polyvinylidene difluoride (PVDF) membrane (Roth, Karlsruhe) using the BioRad wet blot system for 1 h at 100 V. Subsequently, membranes were blocked for 1 h at RT with 5 % nonfat dried milk powder in PBS-T and incubated o/n at 4 °C with either mouse anti-hDaxx (1:1,000) or rabbit anti-PML (1:1,000) antibody, diluted in blocking buffer. Following 3x washing with PBS containing 0.1 % Tween-20 (PBS-T), membranes were incubated for 1 h at RT with horseradish peroxidase-conjugated anti-mouse or anti-rabbit antibody, diluted 1:10,000. Finally, membranes were stained with enhanced chemiluminescence (ECL) Plus western blot detection reagent and the signal was recorded using the Chemi-Smart 5100 detection system (Peqlab, Erlangen). For consecutive staining, membranes were incubated twice for 10 min with stripping buffer at RT to remove bound antibodies, washed twice with PBS, blocked with blocking buffer and re-probed with the rabbit anti-Actin (1:1,000) antibody.

#### 6.2.2.5 Virus reconstitution

HHV-6A BAC DNA (5 µg) and the HCMV pp71-expressing plasmid pCGN1-pp71 (1 µg) were co-transfected into 5x $10^6$ JJHan ND10KD cells with transfection solution V using the Amaxa nucleofector (Lonza, Basel) following the manufacturer's protocol T-008. After 5 to 7 days, virus was reactivated by supplementing the medium with 20 ng/ml Tetradecanoylphorbol acetate (TPA) and 3 mM sodium butyrate for 24 h. The next day, cells were washed to remove the drugs and co-cultured with an equal number of JJHan ND10KD cells that were pre-stimulated for 24 h with interleukin-2 (IL-2) 1:1,000 and 5 µg/ml phytohemagglutinin (PHA). Fresh, pre-stimulated JJHan ND10KD cells were added as needed to allow accumulation of the virus by cell-to-cell spread. Virus stocks were frozen in 8 % DMSO containing medium in 1 ml aliquots. Temperature was slowly

decreased to -80°C and samples were then transferred for long-time storage to liquid nitrogen tanks.

#### 6.2.2.6 Cell-free virus production, titration and growth kinetics

200 ml supernatant of recombinant HHV-6 infected JJHan cells was concentrated 100-fold using the Pierce concentrators (ThermoFisher, Waltham). Concentrated cell-free virus stocks were used for titration and growth kinetics. For titration of each virus, 5x $10^5$ JJHan cells were infected with 100 µl of the virus stock and viral genome copies were determined by qPCR at 1 dpi. To determine the growth properties of the recombinant viruses, growth kinetic were performed. 6x $10^5$ JJHan cells were infected with each virus at 37 °C o/n at an MOI (multiplicity of infection) of 10. Upon infection, the cells were washed and divided into 6 wells and cultured in 500 µl of culture medium (RPMI medium containing 10 % FBS) in a 48-well plate. The samples were harvested at 0, 1, 4, 7, 10, and 15 dpi. To determine the number of HHV-6 genome copies in each sample, viral DNA was extracted using the RTP® DNA/RNA Virus Mini Kit (Stratec, Berlin) according to manufacturer's instructions. Viral genome copy numbers were determined by quantitative PCR (qPCR) (see 6.2.2.8).

#### 6.2.2.7 *In vitro* integration assay

To determine the integration efficiency of recombinant HHV-6 viruses, 1x $10^7$ U2OS cells were infected by co-cultivation with highly infected JJHan cells for 3 h. After extensive washing with PBS, cells were incubated for 36 h. Then, cells were detached from the dishes, washed twice with PBS, and GFP positive ($GFP^+$) infected cells were isolated using the FACS AriaIII cell sorter (BD, San Jose). The sorted cells were re-seeded in 12-well plates and cultured for 14 days. qPCR samples were taken at d0 and d14 post sort, FISH samples were prepared at d14 post sort (see 6.2.2.8 and 6.2.2.9).

#### 6.2.2.8 qPCR

For HHV-6A genome quantification, DNA was isolated using the RTP® DNA/RNA Virus Mini Kit according to manufacturer's instructions. For the qPCR reaction, a master mix was prepared containing 10 µl Master Mix, 0.12 µl of each primer (100 µM), 0.5 µl probe (10 µM) and 10 µl of DNA sample. HHV-6A genome copies were determined by qPCR on a 7500 Fast Real-Time PCR System (Invitrogen, Grand Island) using primers and a TaqMan probe specific for the HHV-6A U86 gene. U86 gene copy numbers were normalized against cellular genome copies of the ß2M gene. Primers and probe sequences are listed in Table 4 and cycling conditions are given in Table 7. For the generation of standard curves for U86 and ß2M, HHV-6A BAC DNA and a plasmid containing cellular ß2M were used, respectively, as serial 10-fold dilutions. The coefficient of regression was always > 0.99 for standard curves.

**Table 7: qPCR protocol**

| Temperature (°C) | Time | PCR step | Cycles |
|---|---|---|---|
| 95 °C | 20 s | Initial denaturation | |
| 95 °C | 3 s | Denaturation | |
| 60 °C | 30 s | Annealing | 40 cycles |

#### 6.2.2.9 Metaphase preparation and fluorescence *in situ* hybridization (FISH)

Metaphase chromosomes were prepared from infected JJHan or U2OS cells. To arrest cells in metaphase, cultures were treated with 0.1 µg/ml colcemid for 4–5 h (JJHan) or o/n (U2OS). Colcemid not only depolymerizes microtubules and limits microtubule formation, but also inactivates spindle fiber formation required to separate metaphase chromosomes. Cells were then harvested and collected by centrifugation for 8 min at 400 g and RT. Pellets were resuspended in 10 ml of hypotonic solution and incubated for 10 min at 37 °C. In order to prevent cell clumping, 1 ml of fresh ice-cold fixative was added prior to centrifugation. Cells were then pelleted for 8 min at 400 g, the supernatant was removed and the pellet was washed twice with 5 ml ice-cold fixative. Finally, the pellet was resuspended in an adequate amount of ice-cold fixative and chromosomes were stored at -20 °C until further use.

To prepare metaphase spreads, a water bath was set to 98 °C. Microscope slides were briefly passed through the water vapor and then 10 µl of chromosome suspension were dropped on the slide. Slides were passed through the vapor again and then placed on the side of a metallic plate on top of the water bath to dry, followed by ageing o/n at RT. The following day, samples were dehydrated for 5 min at RT in 100 % ethanol. Proteins were removed from the slide by incubation with a pre-warmed pepsin solution at 37 °C for 7 min. Subsequently, the RNA was degraded by incubation for 2 min in 2x SSC with RNase A. Slides were then washed twice for 1 min with 2x SSC, briefly rinsed in Millipore water and dehydrated by subsequent ethanol washes, twice for 2 min in 70 %, twice for 2 min in 90 % and once for 4 min in 100 % ethanol. Slides were aged again for 1 h at 65 °C. To generate the HHV-6A probe, 1.5 µg HHV-6A BAC DNA were first digested for 3 h at 37 °C with *Hae*III and *Dpn*I, then purified with HI-Yield Gel purification kit (SLG, Gauting) and eluted in water. Digoxigenin (DIG) labeling of the DNA was performed with DIG-High Prime (Roche, Mannheim) according to the manufacturer´s instructions. Briefly, 300 ng of digested DNA were dissolved in a final volume of 16 µl and denatured for 10 min at 98 °C. After cooling of the sample on ice, 4 µl of DIG-High prime were added to the DNA solution. The reaction was perpetuated o/n at 37 °C, stopped by heat inactivation (10 min at 65 °C) and the probe was purified once more with High-Yield PCR Purification kit (SLG, Gauting). The TMR probe was generated by PCR using the Biotin labeling kit (Jena

Biosciences, Jena) according to the manufacturer's instructions, using the HHV-6A BAC as a template and the primers listed in Table 2.

For hybridization, 1.2 µl of the HHV-6A probe (+/- TMR probe) were mixed with 30 µl of hybridization buffer. 0.5 µl of salmon sperm DNA per slide were used as competitor DNA to reduce background. The probe mix was first denatured for 10 min at 75 °C, then cooled down on ice and dropped on the aged slides. To avoid evaporation, a coverslip was placed on the probe and sealed with rubber cement. For efficient hybridization, slides were placed into a 80 °C incubator for 90 seconds, then gradually cooled to 42 °C and left o/n. Prior to detection, coverslips were removed and slides were washed sequentially at 44 °C twice for 5 min in 2x SSC, twice for 5 min in stringency wash, twice for 5 min in 2x SSC and finally twice for 5 min in detergent wash. The slides were then incubated for 30 min at 37 °C with 75 µl of anti-DIG-FITC antibody (1:500) (+/- Streptavidin-Cy3 (1:1,000)) diluted in detergent wash. The final wash was performed via three 4 min incubations in detergent wash followed by a brief rinse in water. Mounting media containing DAPI was added and samples were sealed with a coverslip prior to detection with Axio Imager M1 (Zeiss, Jena).

#### 6.2.2.10 Preparation of clonal cell lines

For the preparation of clonal U2OS cell lines harboring integrated HHV-6A, $GFP^+$ sorted U2OS cells were plated in 96-well plates at a density of one cell per well. Clonal cell lines were grown up for four weeks and tested by qPCR for the detection of HHV-6A DNA. Positive results were confirmed by FISH.

#### 6.2.2.11 Reactivation assay

Clonal U2OS cell lines were cultured in MEM medium supplemented with 10 % FCS and P/S. For virus reactivation 80 ng/mL TSA were added for the duration of 2 days. Reactivation of HHV-6A was monitored by FACS (BD, San Jose), counting the percent of $GFP^+$ cells.

#### 6.2.2.12 Statistical analysis

Statistical analysis was performed using the GraphPad Prism Software. qPCR data on HHV-6 genome copies, FISH metaphase and interphase integration counts as well as FACS results were analyzed using Mann-Whitney U test.

# 7 Results

## 7.1 Establishment of ND10 knockdown JJHan cells using lentiviral transduction

HHV-6A had previously been cloned as a bacterial artificial chromosome [191], however, the reconstitution of the virus is very inefficient. To optimize virus reconstitution from the HHV-6A BAC, I aimed to disrupt ND10 bodies, an intrinsic immune defense against herpesviruses [68]. The major ND10 components PML, hDaxx and Sp100 were knocked down by shRNAs, delivered by lentiviral transduction in the human T-cell line JJHan (JJHan ND10KD) used for virus reconstitution and propagation (Figure 12A).

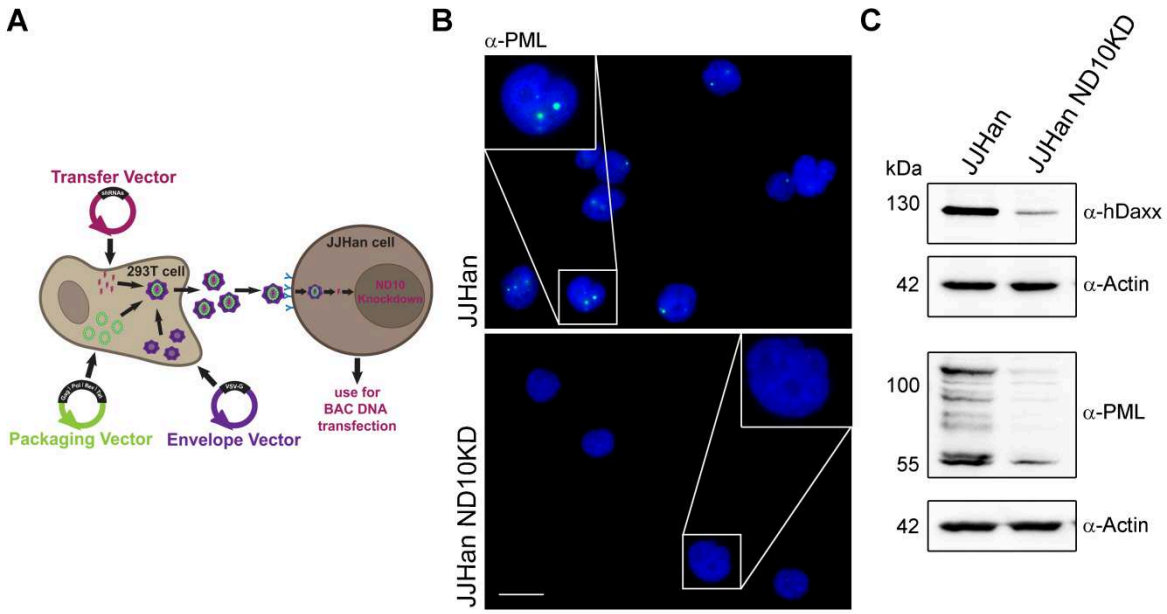


**Figure 12: ND10 knockdown in JJHan cells. (A)** Schematic representation of the lentiviral transduction system. **(B)** Indirect immunofluorescence of parental JJHan and JJHan ND10KD cells. Cells were fixed/permeabilized, subsequently stained with rabbit anti-PML, washed and incubated with secondary goat anti-rabbit AF488 antibody and DAPI to visualize the nuclei. Blue: DNA, green: PML. Scale bar correspond to 100µm. **(C)** Western blot analysis of parental JJHan and JJHan ND10KD cells. Cell lysates were separated in a 10 % SDS-PAGE followed by immunoblotting. Membranes were incubated with rabbit anti-PML or mouse anti-hDaxx, washed and incubated with secondary goat anti-rabbit/mouse HRP antibodies. For the detection of ß-Actin as a loading control, blots were stripped, blocked and re-probed with rabbit anti-Actin antibody. Positions of marker bands are indicated on the left.

Lentiviruses containing shRNAs against PML, hDaxx and Sp100 were produced in HEK293T cells. JJHan cells were infected with the lentiviruses and cultured under puromycin selection. Successful knockdown was confirmed by immunofluorescence

(Figure 12 B) and Western blotting (Figure 12C). HHV-6A wild type (wt) virus showed significantly improved growth in the ND10KD cells compared to parental JJHans (Figure 13), confirming that ND10 suppresses HHV-6A replication. The ND10KD JJHans were used for all further virus reconstitutions.

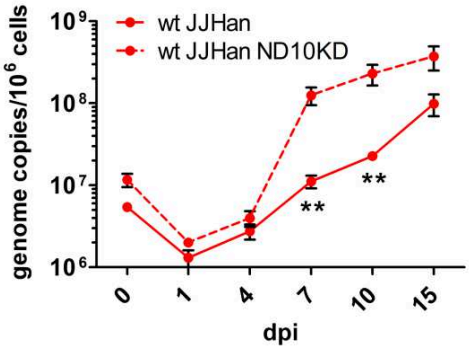


**Figure 13: Growth kinetics of HHV-6A wt virus in JJHan vs. JJHan ND10KD cells.** HHV-6A genome copy numbers were detected by qPCR. Copy numbers per 1x $10^6$ cells are shown as means of three independent experiments with corresponding standard errors (SEM). Significant differences between JJHan and JJHan ND10KD (Mann-Whitney U-test, $p < 0.01$) are indicated with asterisks (**). dpi: days post infection.

## 7.2 Evaluating the role of the HHV-6A telomeric repeats in replication and integration

The HHV-6A genome is flanked by telomeric repeats - imperfect and perfect (see Figure 3). Since HHV-6A is known to integrate into human telomeres [101], I hypothesized that integration occurs via homologous recombination between viral and cellular TMRs.

### 7.2.1 Telomeric repeats are not essential for HHV-6 replication

In order to elucidate the role of the HHV-6 TMRs in viral replication and integration, both TMR regions (perfect and imperfect) were deleted from the wt HHV-6A BAC (ΔTMR) using *en passant* mutagenesis (Figure 14A). In a first recombination round, the perfect TMRs were removed. Subsequently the imperfect TMRs were deleted. Mutants were analyzed by RFLP, sequencing and Southern blotting, using specific probes for the telomeric sequences (Figure 14B and C). Both wt and ΔTMR mutant could be successfully reconstituted in the JJHan ND10KD cells via nucleofection of BAC DNA (Figure 14D). Replication kinetics revealed that there was no difference in virus replication between parental (wild type) and ΔTMR mutant virus (Figure 14E).

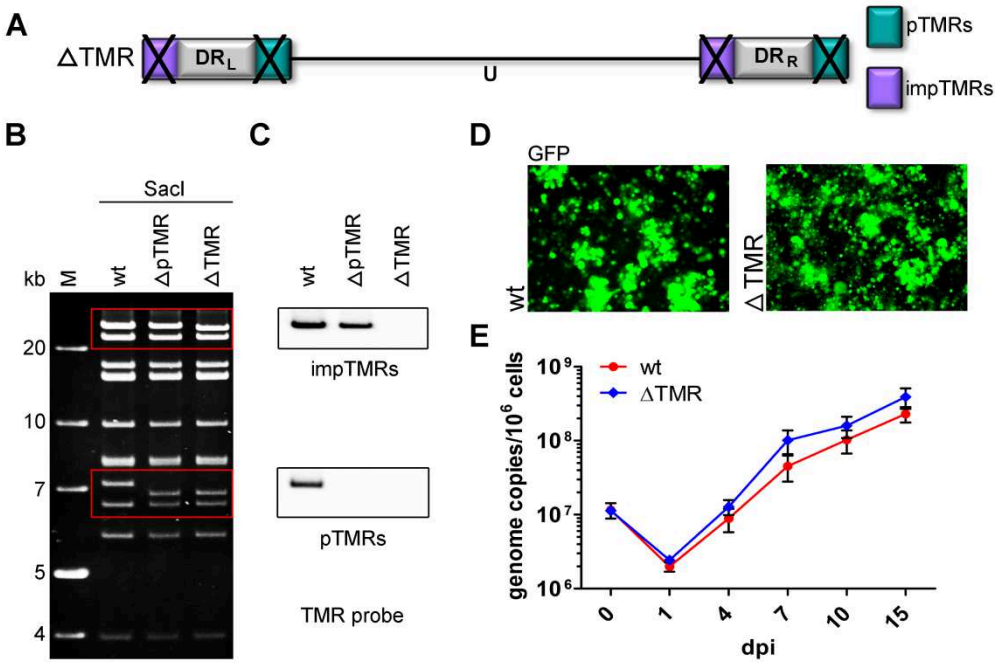


**Figure 14: Generation and characterization of the ΔTMR mutant. (A)** Schematic representation of the ΔTMR mutant. **(B)** RFLP pattern of the wt, the ΔpTMR intermediate and the double deletion mutant ΔTMR upon digestion with *Sac*I analyzed on a 0.8 % agarose gel o/n at 65 V. M = marker. Sizes of the marker fragments are indicated on the left. Red boxes highlight the fragments containing the target regions, where the expected band shifts can be observed. **(C)** Southern blot analysis detecting TMR sequences, impTMR (upper panel) and pTMR (lower panel) after *Sac*I digestion of the indicated BAC clones using a DIG-labeled TMR probe and a secondary anti-DIG-ALP antibody. **(D)** Reconstitution of wt and ΔTMR mutant in JJHan ND10KD cells. Representative images of GFP-expressing infected cells with syncytia formation are shown. **(E)** Growth kinetics comparing replication of wt and ΔTMR mutant virus in JJHan cells. HHV-6A genome copy numbers were detected by qPCR. Copy numbers per 1x $10^6$ cells are shown as means of three independent experiments with corresponding standard errors. dpi: days post infection.

### 7.2.2 Development of an *in vitro* latency/integration model

Next, I wanted to determine the integration efficiency of the generated mutant virus. For this purpose, I established an *in vitro* latency model using the human osteosarcoma cell line U2OS. U2OS cells were infected by co-seeding with infected JJHan cells (GFP-expressing viruses). JJHan cells were removed by stringent washing, $GFP^+$ U2OS cells were sorted 36 h p.i. and further cultured. The possible fate of the $GFP^+$ sorted U2OS cells is shown in Figure 15A. Cells can either i) loose the viral genome during cell division, ii) become lytically infected, eventually resulting in cell death, or iii) the virus can integrate into host telomeres and is silenced. At day 14 post sort, cells were fixed for FISH and analyzed for integration. Examples of observed phenotypes are presented in Figure 15B.

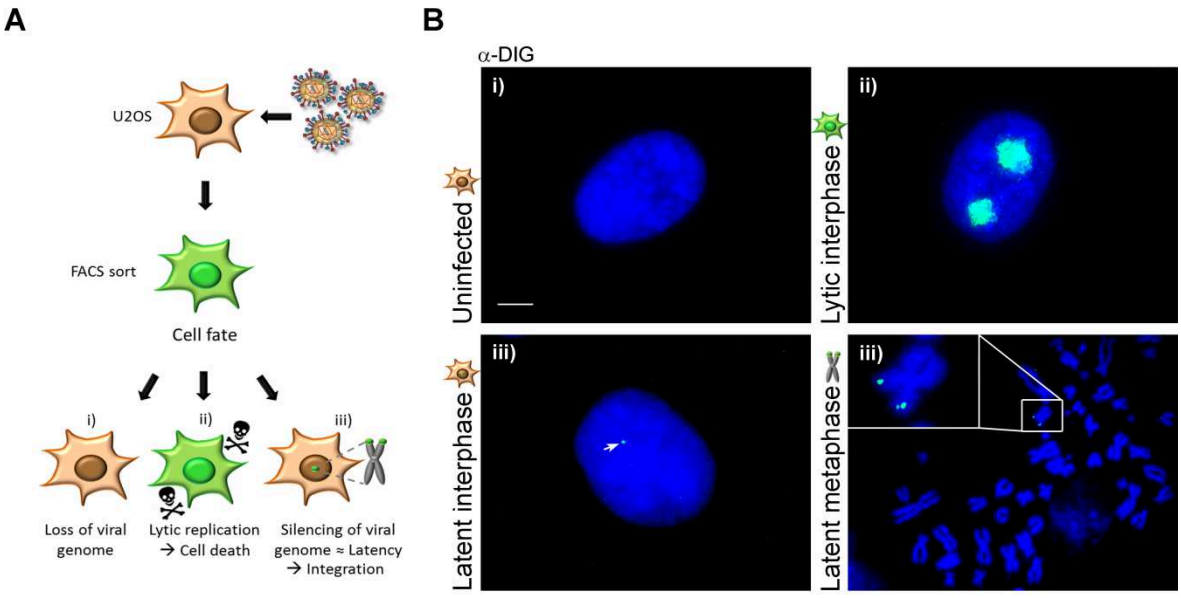


**Figure 15: Visualization of HHV-6A integration into U2OS cells using FISH. (A)** Schematic representation of the fate of U2OS cells after infection with HHV-6A and FACS sorting for $GFP^+$ cells. **(B)** Representative images of FISH analyses of i) uninfected cells, ii) lytic infected cells, iii) latently infected interphase nuclei (left) or metaphases (right). The arrow indicates the virus genome and the integration into telomeres is shown in an enlarged image. Cells were fixed, metaphase spreads were prepared, hybridized with a HHV-6A specific DIG-labeled probe, washed and incubated with a secondary anti-DIG-FITC antibody, DAPI was used to visualize the nuclei and chromosomes. Blue: DNA, green: HHV-6A genome. Scale bar corresponds to 10µm.

To ensure that the virus indeed integrated into the telomeres, a co-staining was performed using probes against the HHV-6A genome and TMR sequences (Figure 16).

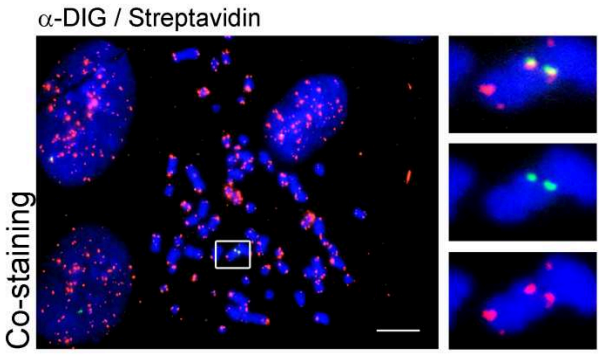


**Figure 16: Detection of co-localization of HHV-6A genome and TMRs by FISH.** Integration into telomeres is shown in enlarged images on the right. Co-staining was performed using a DIG-labeled HHV-6A probe and a Biotin-labeled TMR probe. Secondary antibodies were anti-DIG-FITC and Streptavidin-Cy3 and DAPI to visualize the chromosomes. Blue: DNA, green: HHV-6A genome, red: TMRs. Scale bar corresponds to 10 µm.

### 7.2.3 Integration of the double TMR mutant is severely impaired in U2OS cells

According to the established protocol in 7.2.2, U2OS cells were infected with wt and ΔTMR mutant virus.

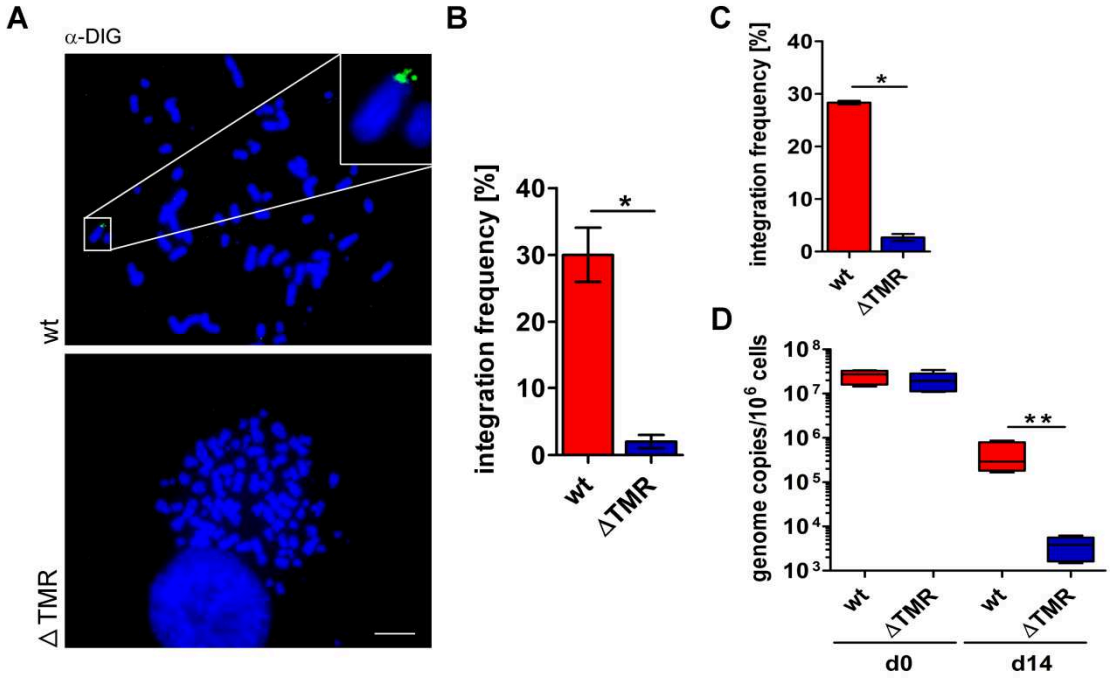


**Figure 17: Integration efficiency and genome maintenance of the ΔTMR mutant in the U2OS latency system. (A)** Representative metaphase images of wt and ΔTMR virus in U2OS cells at d14 post sort. Cells were fixed, metaphase spreads were prepared, hybridized with a HHV-6A specific DIG-labeled probe, washed and incubated with a secondary anti-DIG-FITC antibody, DAPI was used to visualize the nuclei and chromosomes. Blue: DNA, green: HHV-6A genome. Scale bar corresponds to 10µm. **(B)** Integration frequency was quantified by determining the integration status of at least 90 metaphases. Significant differences between wt and ΔTMR (Mann-Whitney U-test, $p < 0.05$) are indicated with an asterisk (*). Results are shown as means of three independent experiments (+SEM). **(C)** Likewise, 100 interphase nuclei were examined for the presence of HHV-6A to calculate the integration frequency. Significant differences between wt and ΔTMR (Mann-Whitney U-test, $p < 0.05$) are indicated with an asterisk (*). Results are shown as means of three independent experiments (+SEM). **(D)** Maintenance of the HHV-6A genome was determined by qPCR analysis at d0 and d14 post sort. Copy numbers per 1x $10^6$ cells are shown as means of three independent experiments with corresponding standard errors. Significant differences between wt and ΔTMR (Mann-Whitney U-test, $p < 0.01$) are indicated with asterisks (**). d:day.

At d14 post sort cells were prepared for FISH and integration efficiency was determined in metaphases (Figure 17A and B) and interphases (Figure 17C). Integration of wt virus was

observed in 30 % of the metaphases, but was nearly abolished in the ΔTMR mutant virus. The same was observed in interphase nuclei. Likewise, genome copy numbers were significantly lower at d14 for the ΔTMR virus compared to the wt virus, even though both viruses had comparable starting levels at d0 (Figure 17D). The data demonstrate that the viral genome cannot be maintained in the absence of the viral TMRs due to the inability of the virus to integrate into host telomeres.

### 7.2.4 The pTMRs are crucial for HHV-6 integration

Furthermore, the perfect (ΔpTMR) and imperfect TMRs (ΔimpTMR) were deleted individually to investigate their distinct contribution in the integration process.

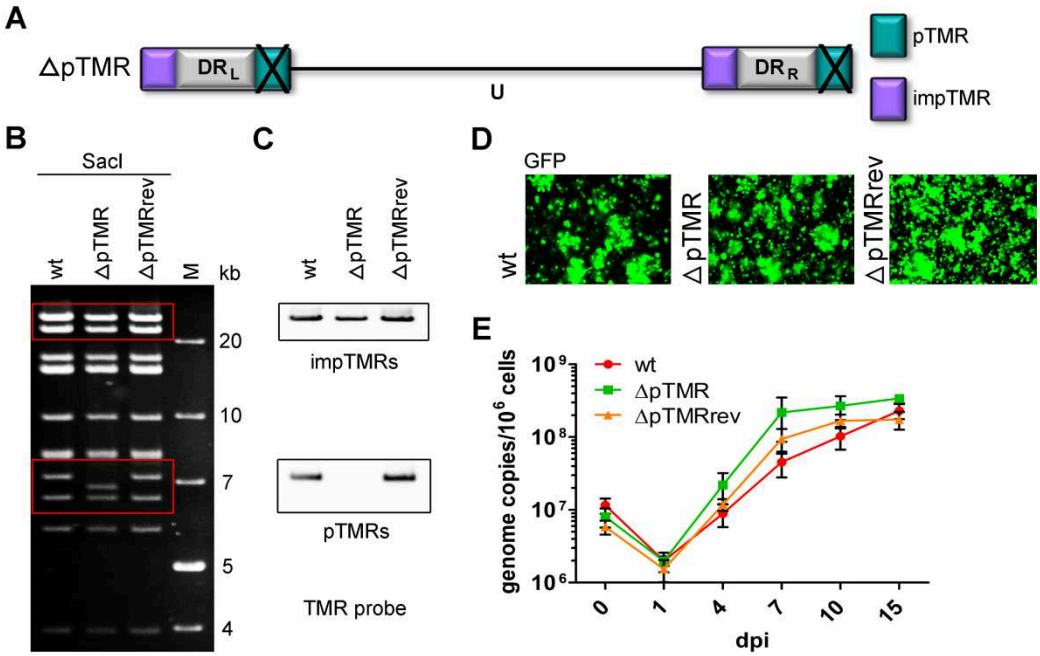


**Figure 18: Generation and characterization of the ΔpTMR mutant. (A)** Schematic representation of the ΔpTMR mutant. **(B)** RFLP pattern of the wt, the ΔpTMR and the ΔpTMRrev upon digestion with *Sac*I. M = marker. Sizes of the marker fragments are indicated on the right. Red boxes highlight the fragments containing the target regions, where the expected band shifts can be observed. **(C)** Southern blot analysis detecting TMR sequences, impTMR (upper panel) and pTMR (lower panel) after *Sac*I digestion of the indicated BAC clones using a DIG-labeled TMR probe and a secondary anti-DIG-ALP antibody. **(D)** Reconstitution of wt, ΔpTMR mutant and ΔpTMRrev in JJHan ND10KD cells. Representative images of GFP-expressing infected cells with syncytia formation are shown. **(E)** Growth kinetics comparing replication of wt, ΔpTMR mutant and ΔpTMRrev virus in JJHan cells. HHV-6A genome copy numbers were detected by qPCR. Copy numbers per 1x $10^6$ cells are shown as means of three independent experiments with corresponding standard errors. dpi: days post infection.

In Figure 18, the generation and characterization of the ΔpTMR mutant is depicted. pTMR sequences were deleted using *en passant* mutagenesis. In addition, a revertant virus (ΔpTMRrev) was generated, in which the perfect TMRs were restored in order to rule out that secondary mutations were introduced during the mutagenesis process. BAC mutants were checked by RFLP (Figure 18B) and confirmed by Southern blotting (Figure 18C) and sequencing of the mutated locus. After successful reconstitution (Figure 18D), growth kinetics revealed that the ΔpTMR mutant replicated comparable to wt and revertant virus (Figure 18E).

The integration efficiency of the ΔpTMR virus was determined using again the U2OS *in vitro* integration system. Integration of ΔpTMR was severely impaired, while the wt and revertant virus consistently integrated in about 30 % of the metaphases (Figure 19A and B). Comparable results were obtained when analyzing interphase nuclei (Figure 19C). As observed for the ΔTMR mutant, the genome copies of the ΔpTMR mutant were significantly lower at d14 compared to wt and revertant (Figure 19D). In summary, it appears that the pTMRs are crucial for integration and that the impTMRs alone are not sufficient for integration.

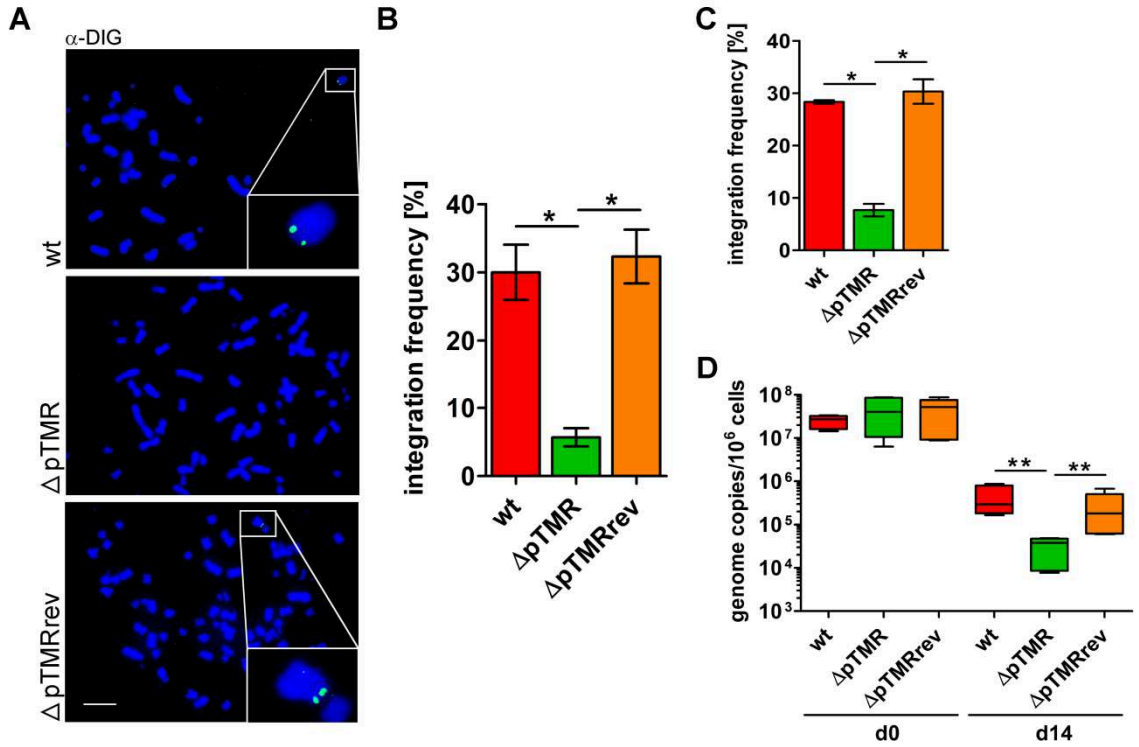


**Figure 19: Integration efficiency and genome maintenance of the ΔpTMR mutant in the U2OS latency system. (A)** Representative metaphase images of wt, ΔpTMR and ΔpTMRrev virus in U2OS cells at d14 post sort. Cells were fixed, metaphase spreads were prepared, hybridized with a HHV-6A specific DIG-labeled probe, washed and incubated with a secondary anti-DIG-FITC antibody, DAPI was used to visualize the nuclei and chromosomes. Blue: DNA, green: HHV-6A genome. Scale bar corresponds to 10µm. **(B)**

Integration frequency was quantified by determining the integration status of at least 90 metaphases. Significant differences between wt and ΔpTMR, as well as ΔpTMR and ΔpTMRrev (Mann-Whitney U-test, $p < 0.05$) are indicated with an asterisk (*). Results are shown as means of three independent experiments (+SEM). **(C)** Likewise, 100 interphase nuclei were examined for the presence of HHV-6A to calculate the integration frequency. Significant differences between wt and ΔpTMR, as well as ΔpTMR and ΔpTMRrev (Mann-Whitney U-test, $p < 0.05$) are indicated with an asterisk (*). Results are shown as means of three independent experiments (+SEM). **(D)** Maintenance of the HHV-6A genome was determined by qPCR analysis at d0 and d14 post sort. Copy numbers per 1x $10^6$ cells are shown as means of three independent experiments with corresponding standard errors. Significant differences between wt and ΔpTMR, as well as ΔpTMR and ΔpTMRrev (Mann-Whitney U-test, $p < 0.01$) are indicated with asterisks (**). d:day.

Concerning the impTMRs, I observed in various restriction digests that the fragment containing the impTMR region was always larger than expected (data not shown). Furthermore, in the standard sequencing PCR a faint band, roughly triple the size of the expected 0.7 kb, became apparent under prolonged extension time, using either wt BAC DNA or viral DNA as a PCR template (Figure 21C, wt lane). This result suggests that the wt contains multiple copies of the impTMR region, which I was unaware off yet (Figure 20).

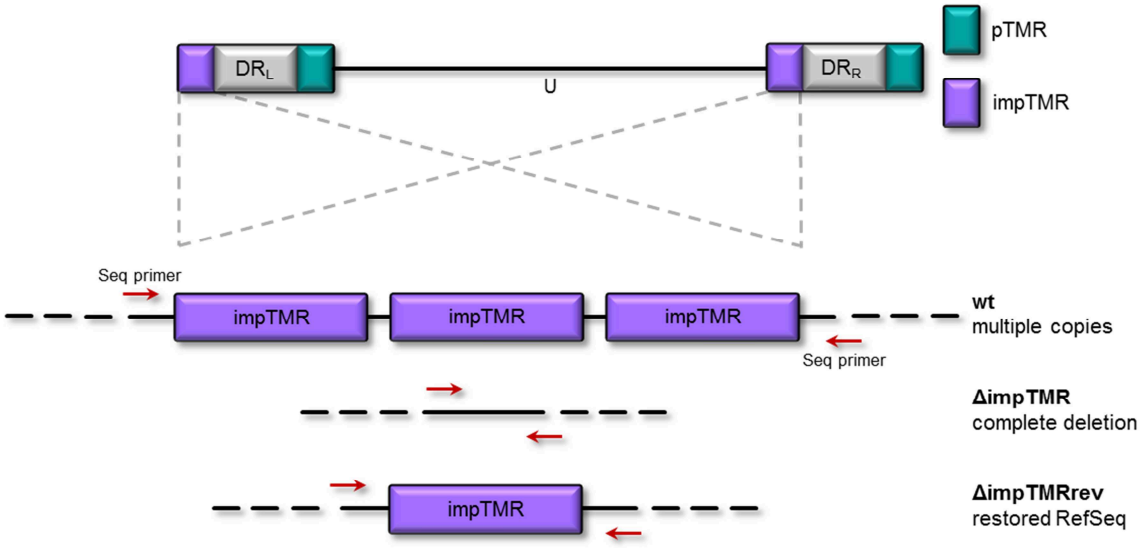


**Figure 20: Schematic representation of the impTMR region in the wt, ΔimpTMR and ΔimpTMR rev BAC/virus.** Red arrows indicate sequencing primers used for PCR in Figure 21C. Not drawn to scale.

In the ΔimpTMR mutant, the entire sequence was deleted; however, in the generated revertant (ΔimpTMRrev) only a single impTMR was re-introduced to restore the NCBI reference sequence and analyze possible effects of the extended impTMR region in the

wt. Preliminary sequencing studies confirmed the hypothesis; further approaches are currently ongoing, but are very laborious in a repeated region.

RFLP and Southern blotting was performed for the generated BAC clones (Figure 21A and B). Using *EcoR*V it is evident that the original wt BAC fragment containing the impTMRs ran higher, while the revertant could be detected at the predicted size. This observation was confirmed by Southern blotting. In addition, the stronger staining of the wt fragment indicates the presence of more TMR sequences (Figure 21B, lower box). PCR analysis amplifying the impTMR region of wt, ΔimpTMR and ΔimpTMRrev was performed using primers depicted in Figure 20. Whereas the bands for the ΔimpTMR and the ΔimpTMRrev displayed a single and clear band matching the predicted sizes, the wt, as described above, gives a smear of larger size (Figure 21C).

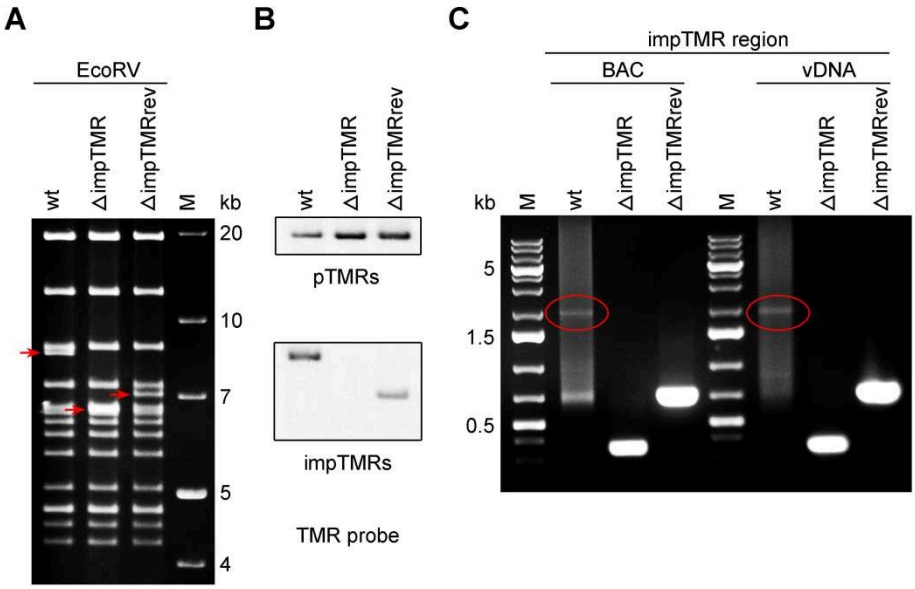


**Figure 21: Analysis of the impTMR region in wt and revertant genome. (A)** RFLP pattern of the wt, the ΔimpTMR and the ΔimpTMRrev upon digestion with *Eco*RV. M = marker. Sizes of the marker fragments are indicated on the right. Red arrows highlight the important band, where shifts can be observed. **(B)** Southern blot analysis detecting TMR sequences, pTMR (upper panel) and impTMR (lower panel) after *Eco*RV digestion of the indicated BAC clones using a DIG-labeled TMR probe and a secondary anti-DIG-ALP antibody. **(C)** 1 % agarose gel with products from sequencing PCR of the impTMR region. M = marker. Sizes of the marker fragments are indicated on the left. Red circles show the faint band and smear appearing in the wt samples after long extension time in BAC DNA as well as vDNA.

Recombinant BAC clones were characterized as described above for the ΔpTMR (Figure 22A-E). The removal of the impTMRs had no influence on the replication of the virus.

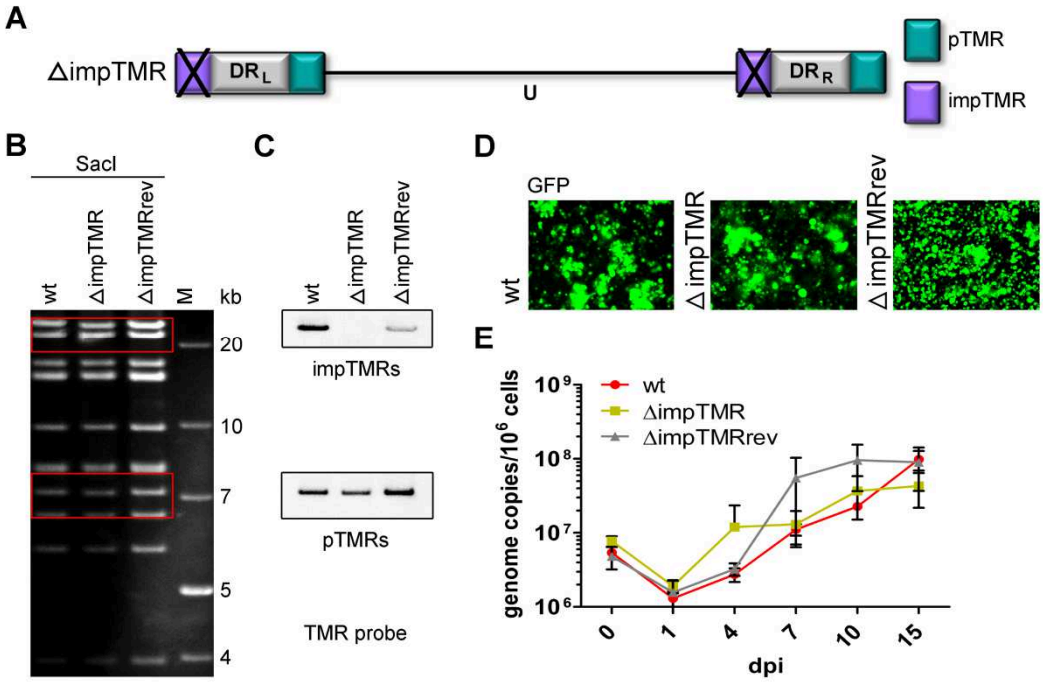


**Figure 22: Generation and characterization of the ΔimpTMR mutant. (A)** Schematic representation of the ΔimpTMR mutant. **(B)** RFLP pattern of the wt, the ΔimpTMR and the ΔimpTMRrev upon digestion with *Sac*I. M = marker. Sizes of the marker fragments are indicated on the right. Red boxes highlight the fragments containing the target regions, where the expected band shifts can be observed. **(C)** Southern blot analysis detecting TMR sequences, impTMR (upper panel) and pTMR (lower panel) after *Sac*I digestion of the indicated BAC clones using a DIG-labeled TMR probe and a secondary anti-DIG-ALP antibody. **(D)** Reconstitution of wt, ΔimpTMR mutant and ΔimpTMRrev in JJHan ND10KD cells. Representative images of GFP-expressing infected cells with syncytia formation are shown. **(E)** Growth kinetics comparing replication of wt, ΔimpTMR mutant and ΔimpTMRrev virus in JJHan cells. HHV-6A genome copy numbers were detected by qPCR. Copy numbers per 1x $10^6$ cells are shown as means of three independent experiments with corresponding standard errors. dpi: days post infection.

To determine the role of the impTMRs in integration, I analyzed the integration efficiency of the recombinant viruses by FISH. The ΔimpTMR mutant had only a twofold reduction in virus integration compared to the wt virus (Figure 23B). Similar results could be observed in interphases (Figure 23C) and genome copy levels (Figure 23D). Surprisingly, reversion of the impTMR region to the NCBI reference sequence in the ΔimpTMRrev did not restore the integration to the level of the wt virus, indicating that the extended impTMR region in the wt further increases integration capacity. Taken together, it is obvious that the impTMRs seem to play a minor role during the integration process of HHV-6.

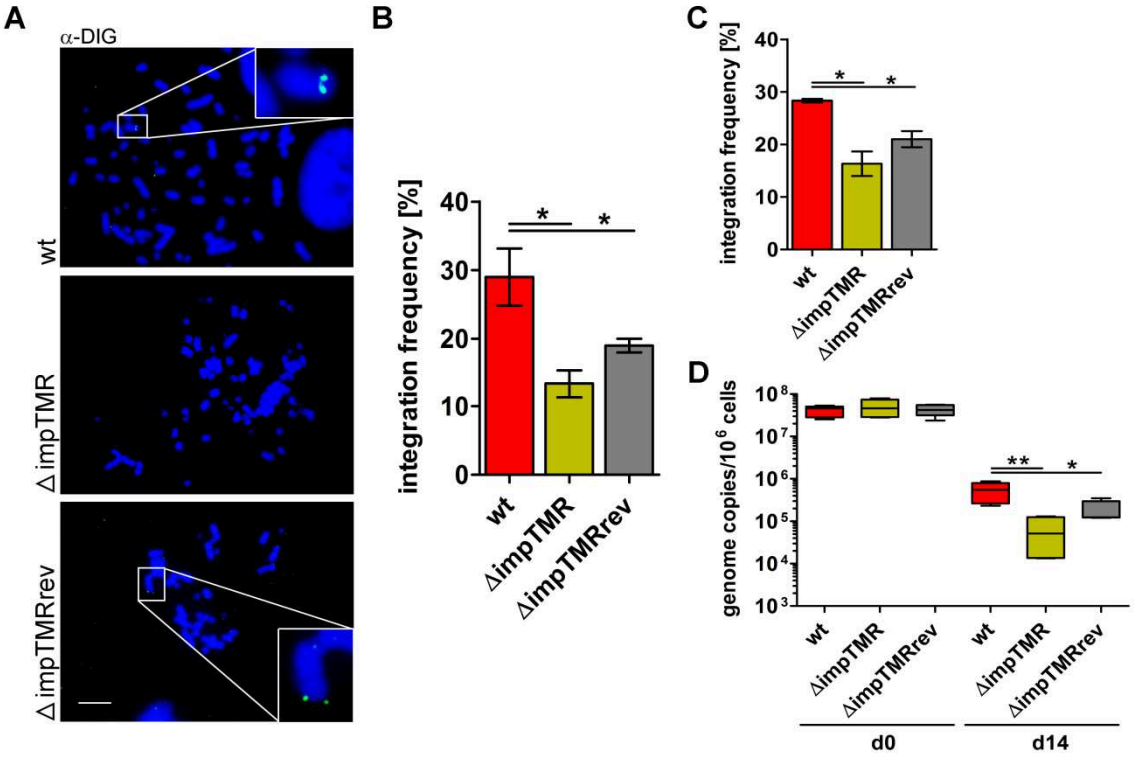


**Figure 23: Integration efficiency and genome maintenance of the ΔimpTMR mutant in the U2OS latency system. (A)** Representative metaphase images of wt, ΔimpTMR and ΔimpTMRrev virus in U2OS cells at d14 post sort. Cells were fixed, metaphase spreads were prepared, hybridized with a HHV-6A specific DIG-labeled probe, washed and incubated with a secondary anti-DIG-FITC antibody, DAPI was used to visualize the nuclei and chromosomes. Blue: DNA, green: HHV-6A genome. Scale bar corresponds to 10µm. **(B)** Integration frequency was quantified by determining the integration status of at least 90 metaphases. Significant differences between wt and ΔimpTMR, as well as wt and ΔimpTMRrev (Mann-Whitney U-test, $p < 0.05$) are indicated with an asterisk (*). Results are shown as means of three independent experiments (+SEM). **(C)** Likewise, 100 interphase nuclei were examined for the presence of HHV-6A to calculate the integration frequency. Significant differences between wt and ΔimpTMR, as well as wt and ΔimpTMRrev (Mann-Whitney U-test, $p < 0.05$) are indicated with an asterisk (*). Results are shown as means of three independent experiments (+SEM). **(D)** Maintenance of the HHV-6A genome was determined by qPCR analysis at d0 and d14 post sort. Copy numbers per 1x $10^6$ cells are shown as means of three independent experiments with corresponding standard errors. Significant differences between wt and ΔimpTMR, as well as wt and ΔimpTMRrev (Mann-Whitney U-test, $p < 0.05$ or $p < 0.01$) are indicated with asterisks (* or **). d:day.

### 7.2.5 Integration analysis of TMR mutant viruses in clonal U2OS cell lines

Next, I prepared clonal cell lines for the TMR mutants, to identify the exact integration sites or to elucidate if deletion of the viral TMRs results in integration elsewhere in the host chromosomes aside the telomeres.

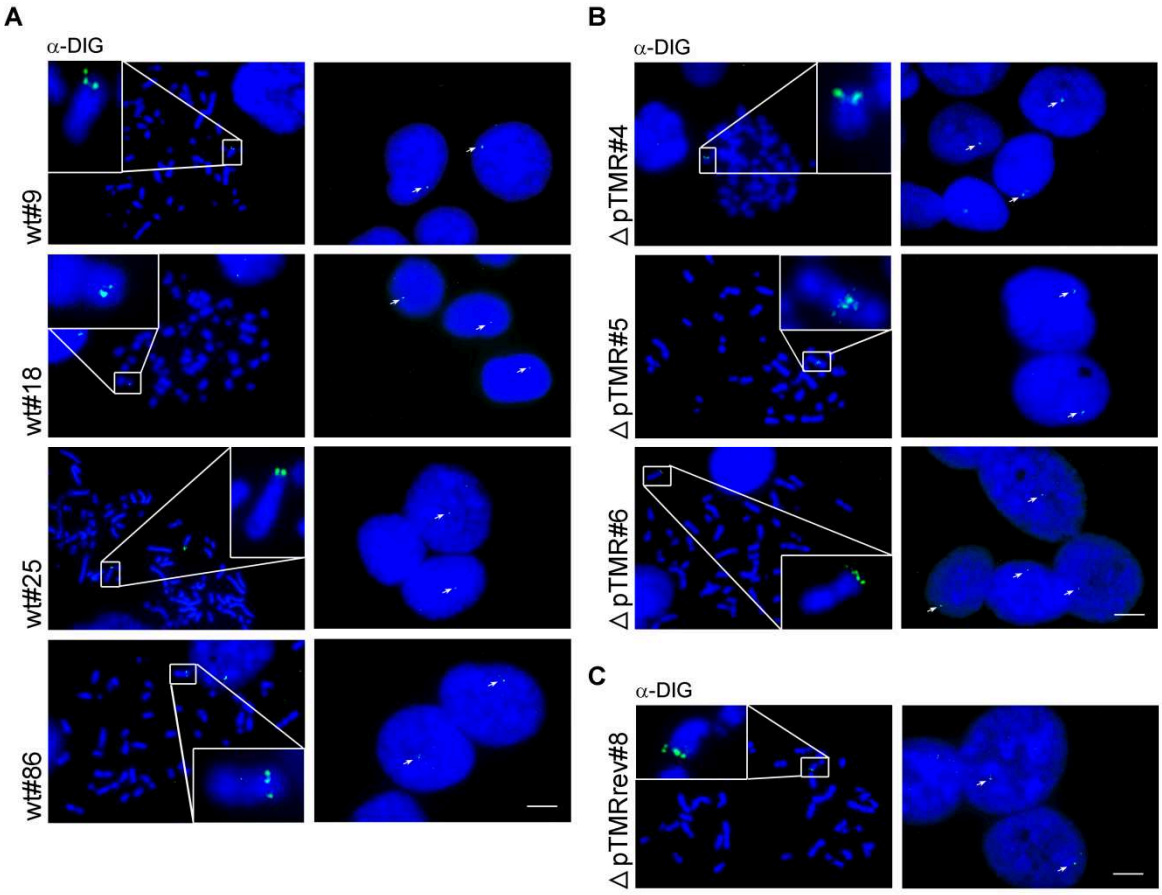


**Figure 24: Generation of clonal U2OS cell lines containing wt, ΔpTMR and ΔpTMRrev virus. (A-C)** Representative images of clonal U2OS cell lines for wt, ΔpTMR and ΔpTMRrev. Left = metaphase, right = interphase nuclei. Cells were fixed, metaphase spreads were prepared, hybridized with a HHV-6A specific DIG-labeled probe, washed and incubated with a secondary anti-DIG-FITC antibody, DAPI was used to visualize the nuclei and chromosomes. Blue: DNA, green: HHV-6A genome. Scale bar corresponds to 10µm.

For this purpose, $GFP^+$ sorted U2OS cells were plated in 96-well plates at a density of 1 cell per well. Clonal cell lines were grown up and tested by qPCR to detect the presence of the HHV-6A genome. Out of >100 clonal cell lines obtained from ΔTMR infected U2OS cells, none was positive for HHV-6A in the qPCR analysis, confirming that the viral genome is not maintained if integration is abolished. For the ΔpTMR mutant, however, few clonal cell lines could be established (5 out of ~100), suggesting that the impTMRs alone might allow integration at a very low frequency or that the virus integrated elsewhere in the host genome. Cell lines for wt and revertant viruses could be readily established and

were used as controls. FISH analyses revealed that wt and revertant viruses integrated efficiently at the end of the host chromosomes (Figure 24). Intriguingly, in the ΔpTMR clones integration was also observed. Whether this integration indeed occurred in the telomeres is currently under investigation by additional methods such as PFGE (pulsed-field gel electrophoresis). qPCR analysis were conducted and the HHV-6A genome could be detected (Figure 25); however, all ΔpTMR derived clones showed higher levels, suggesting that the ΔpTMR mutant virus might integrate as concatemers, as previously observed for MDV lacking TMR sequences [166].

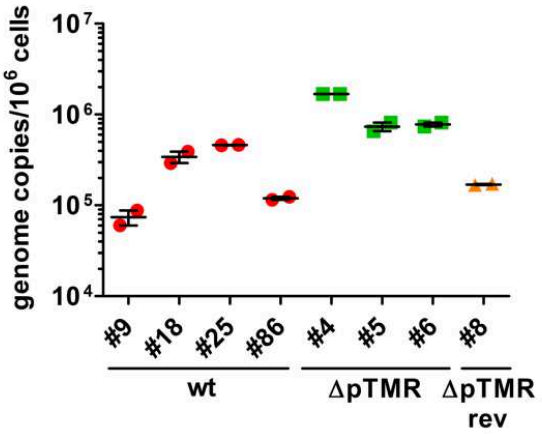


**Figure 25: qPCR analysis of clonal U2OS cell lines.** HHV-6A genome copy numbers per 1x $10^6$ cells are shown as means.

## 7.3 Evaluating the role of the HHV-6A protein U94 in replication and integration

I could demonstrate that the TMR sequences are crucial for the integration of HHV-6A into telomeres, however, the viral proteins that mediate this recombination event are still unknown. One of the candidates encoded by HHV-6 is the putative recombinase U94, an ortholog of the AAV-2 Rep recombinase. We and collaborators recently demonstrated that U94 possesses all functions required for recombination *in vitro*: DNA-binding, ATPase, helicase and exonuclease activity [183].

### 7.3.1 Disruption of U94 expression

In order to elucidate the role of the HHV-6A U94 protein in viral replication and integration, I disrupted this ORF by seamless *en passant* mutagenesis in the HHV-6A BAC.

#### 7.3.1.1 Complete deletion of open reading frame leads to growth defect

At first, the entire open reading frame for *U94* was deleted (ΔU94) from the HHV-6A genome (Figure 26A). In addition, I generated a revertant virus to ensure that no secondary mutations occurred during the mutagenesis process. RFLP pattern and Southern blotting confirmed that *U94* was completely deleted in the ΔU94 mutant (Figure 26B and C), while the sequences were restored in the revertant (ΔU94rev). All mutants were confirmed by DNA sequencing of the *U94* region. After successful reconstitution (Figure 26D), replication kinetics revealed that the ΔU94 mutant has a significant growth defect (Figure 26E).

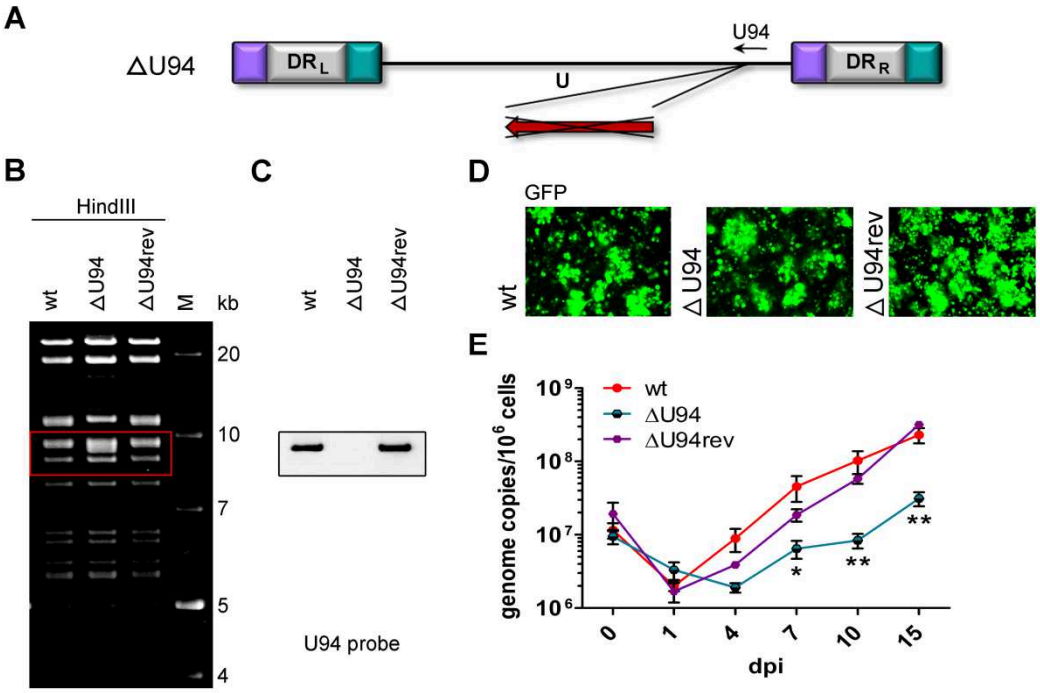


**Figure 26: Generation and characterization of the ΔU94 mutant. (A)** Schematic representation of the ΔU94 mutant. **(B)** RFLP pattern of the wt, the ΔU94 and the ΔU94rev upon digestion with *Hind*III. M = marker. Sizes of the marker fragments are indicated on the right. Red box highlights the fragments containing the target region, where the expected band shifts can be observed. **(C)** Southern blot analysis detecting U94 sequences, after *Hind*III digestion of the indicated BAC clones using a DIG-labeled U94 probe and a secondary anti-DIG-ALP antibody. **(D)** Reconstitution of wt, ΔU94 mutant and ΔU94rev in JJHan ND10KD cells. Representative images of GFP-expressing infected cells with syncytia formation are shown. **(E)** Growth kinetics comparing replication of wt, ΔU94 mutant and ΔU94rev virus in JJHan cells. HHV-6A genome copy numbers were detected by qPCR. Copy numbers per 1x $10^6$ cells are shown as means of three independent experiments with corresponding standard errors. Significant differences between wt and ΔU94 as well as ΔU94 and ΔU94rev (Mann-Whitney U-test, $p < 0.05$ or $p < 0.01$) are indicated with asterisks (* or **). dpi: days post infection.

This reduction in replication might either be due to the lack of U94 or could also be due to effects of the deletion on neighboring genes such as the *U95 IE* gene, which plays an important role in virus replication [205]. The two genes do not overlap, however the promoter of *U95* is likely located within the *U94* sequences due to the close proximity (Figure 27). Alternatively, *U95* has been suggested to be a spliced gene [206], suggesting that deletion of *U94* sequences could interfere with correct splicing of *U95*.


**Figure 27: Schematic representation of the HHV-6A genome segment containing the ORFs *U94* and *U95*.** A scale bar indicates the size of the genes.

### 7.3.1.2 Introduction of stop codon mutations to abrogate U94 expression

To determine if the growth defect upon deletion is due to the absence of the *U94* sequence or the protein I generated a mutant virus in which the second and third predicted start codons of *U94* were changed to stop codons (U94stop) (Figure 28A).

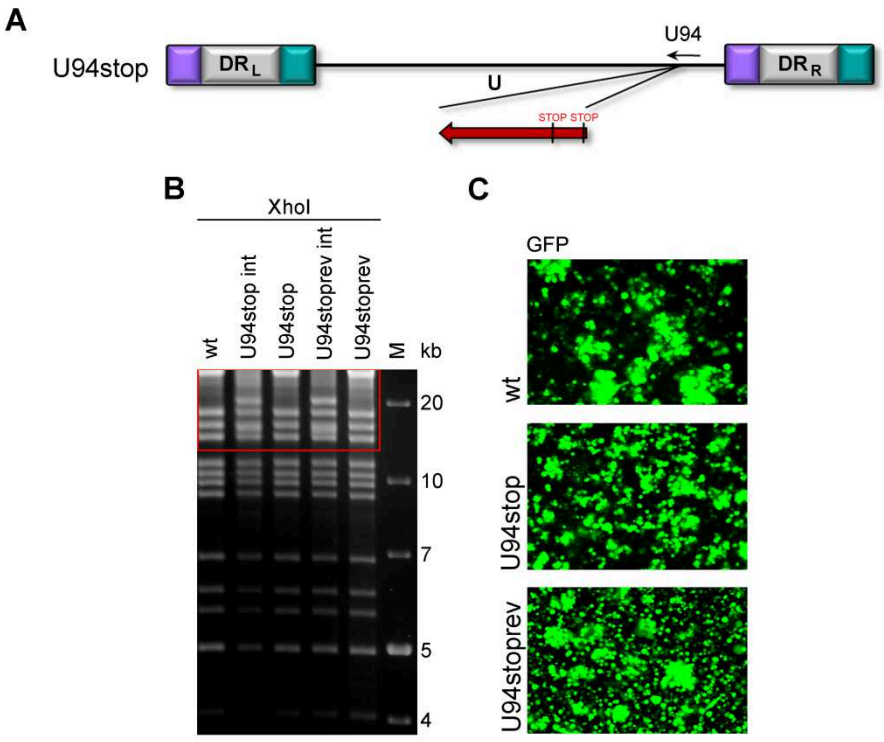


**Figure 28: Generation and characterization of the U94stop mutant. (A)** Schematic representation of the U94stop mutant. **(B)** RFLP pattern of the wt, U94stop int, U94stop, U94stoprev int and U94stoprev upon digestion with *Xho*I. M = marker. Sizes of the marker fragments are indicated on the right. Red box highlights the fragments containing the target region, where the expected band shifts can be observed. **(C)** Reconstitution of wt, U94stop

and U94stoprev in JJHan ND10KD cells. GFP expression shows infected cells with syncytia formation.

RFLP analysis of wt, intermediate, final U94stop, intermediate revertant and final U94stop revertant are shown in Figure 28B. The viruses were successfully reconstituted and efficiently replicated in culture (Figure 28C). To confirm that the expression of U94 was indeed abrogated in the U94stop virus, a polyclonal antibody specific for U94 is currently being produced and optimized in chickens by Prof. Louis Flamand and Dr. Annie Gravel (Laval University, Quebec), since tagging the protein was not successful (data not shown).

### 7.3.2 Integration of HHV-6A is not altered in the absence of U94

To determine the integration efficiency of HHV-6A in the absence of U94 and to elucidate if U94 is indeed the putative recombinase, I used my well established U2OS integration system. Both mutants (ΔU94 and U94stop) (Figure 29A-D and Figure 30A-D) integrated as efficient as wt and revertant viruses.

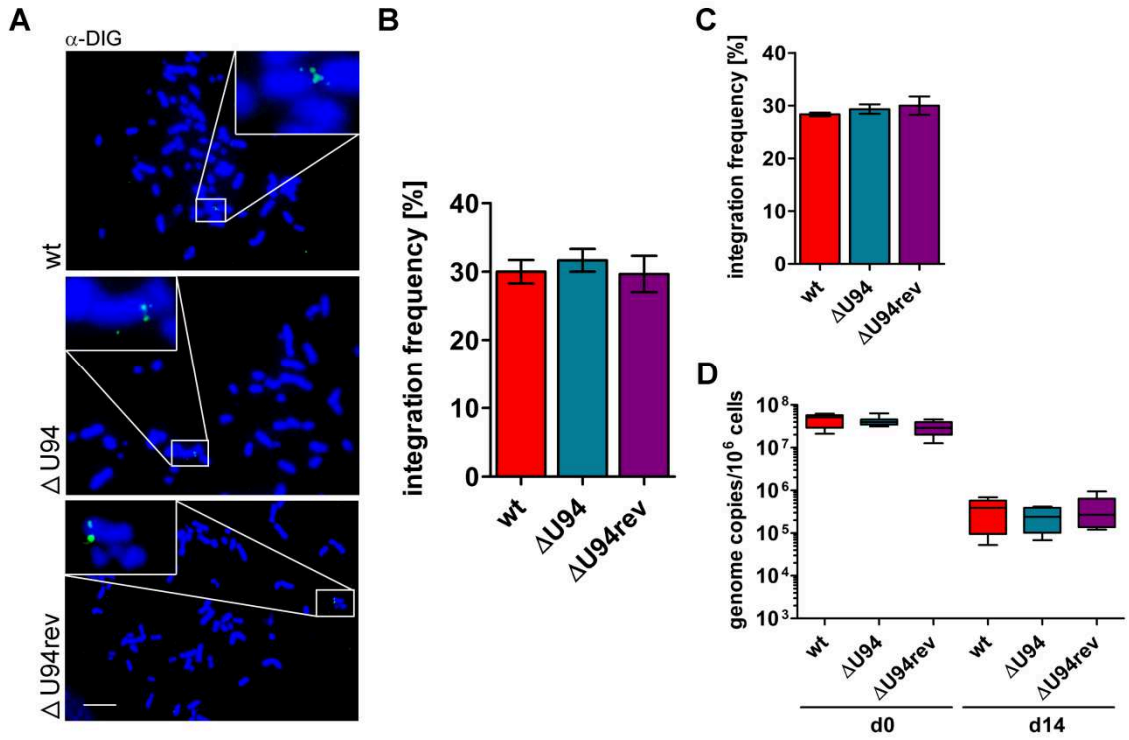


**Figure 29: Integration efficiency and genome maintenance of the ΔU94 mutant in the U2OS latency system. (A)** Representative metaphase images of wt, ΔU94 and ΔU94rev virus in U2OS cells at d14 post sort. Cells were fixed, metaphase spreads were prepared, hybridized with a HHV-6A specific DIG-labeled probe, washed and incubated with a secondary anti-DIG-FITC antibody, DAPI was used to visualize the nuclei and chromosomes. Blue: DNA, green: HHV-6A genome. Scale bar corresponds to 10µm. **(B)** Integration frequency was quantified by determining the integration status of at least 90 metaphases. Results are shown as means of three independent experiments (+SEM). **(C)**

Likewise, 100 interphase nuclei were examined for the presence of HHV-6A to calculate the integration frequency. Results are shown as means of three independent experiments (+SEM). **(D)** Maintenance of the HHV-6A genome was determined by qPCR analysis at d0 and d14 post sort. Copy numbers per 1x $10^6$ cells are shown as means of three independent experiments with corresponding standard errors. d:day.

In addition, qPCR analyses revealed that genome maintenance was not altered upon abrogation of U94. My data demonstrates that U94 is not essential for HHV-6A integration in the U2OS system.

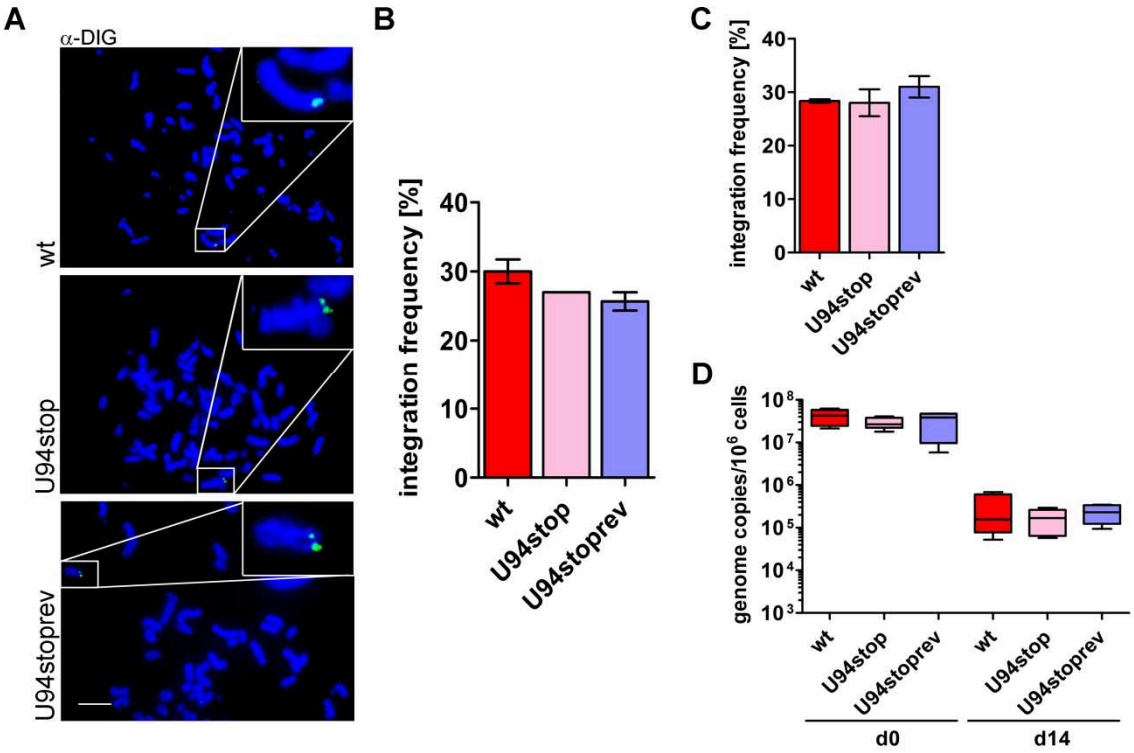


**Figure 30: Integration efficiency and genome maintenance of the U94stop mutant in the U2OS latency system. (A)** Representative metaphase images of wt, U94stop and U94stoprev virus in U2OS cells at d14 post sort. Cells were fixed, metaphase spreads were prepared, hybridized with a HHV-6A specific DIG-labeled probe, washed and incubated with a secondary anti-DIG-FITC antibody, DAPI was used to visualize the nuclei and chromosomes. Blue: DNA, green: HHV-6A genome. Scale bar corresponds to 10µm. **(B)** Integration frequency was quantified by determining the integration status of at least 90 metaphases. Results are shown as means of three independent experiments (+SEM). **(C)** Likewise, 100 interphase nuclei were examined for the presence of HHV-6A to calculate the integration frequency. Results are shown as means of three independent experiments (+SEM). **(D)** Maintenance of the HHV-6A genome was determined by qPCR analysis at d0 and d14 post sort. Copy numbers per 1x $10^6$ cells are shown as means of three independent experiments with corresponding standard errors. d:day.

Next, I investigated whether the cellular recombinase Rad51 [207] is involved in the integration of HHV-6A and if it allows integration in the absence of U94. Therefore, I performed *in vitro* integration assays in the presence or absence of the specific Rad51 inhibitor RI-1 [208] with wt and ΔU94 mutant viruses. Both wt and the ΔU94 mutant were still able to integrate into U2OS cells (Figure 31A), however with a slightly decreased frequency in metaphases and interphases (Figure 31B and C).

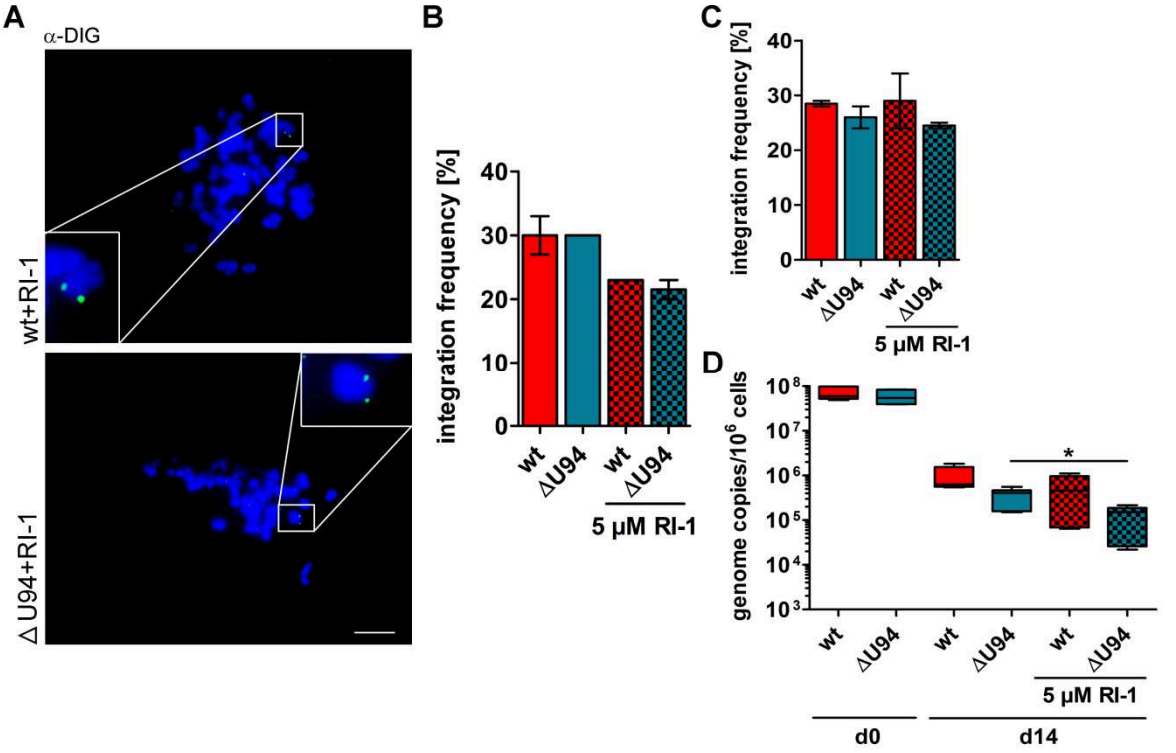


**Figure 31: Integration efficiency and genome maintenance of the wt and the ΔU94 mutant with or without Rad51 inhibition in the U2OS latency system. (A)** Representative metaphase images of wt and ΔU94 virus in U2OS cells treated with 5 µM RI-1 over the entire duration of the experiment at d14 post sort. Cells were fixed, metaphase spreads were prepared, hybridized with a HHV-6A specific DIG-labeled probe, washed and incubated with a secondary anti-DIG-FITC antibody, DAPI was used to visualize the nuclei and chromosomes. Blue: DNA, green: HHV-6A genome. Scale bar corresponds to 10µm. **(B)** Integration frequency was quantified by determining the integration status of at least 90 metaphases. Results are shown as means of two independent experiments (+SEM). **(C)** Likewise, 100 interphase nuclei were examined for the presence of HHV-6A to calculate the integration frequency. Results are shown as means of two independent experiments (+SEM). **(D)** Maintenance of the HHV-6A genome was determined by qPCR analysis at d0 and d14 post sort. Copy numbers per 1x $10^6$ cells are shown as means of three independent experiments with corresponding standard errors. Significant differences between ΔU94 and ΔU94 + RI-1 (Mann-Whitney U-test, $p < 0.05$) are indicated with an asterisk (*).d:day.

These minor differences are likely due to the toxicity of the Rad51 inhibitor. Similarly, qPCR analyses revealed a minor reduction in HHV-6A genome copies (Figure 31D). My data suggests that Rad51 does not play a major role in the integration of HHV-6A in U2OS cells.

### 7.3.3 Role of U94 in the integration into T-cells

U2OS cells have been previously shown to use the ALT mechanism for telomere length maintenance that could complement the function of U94. Therefore, I tested the integration efficiency in another cell type. HHV-6 also integrates into ALT negative JJHan T-cells that commonly support lytic infection of the virus [101]. For this experiment, $GFP^-$ cells of an exponentially growing, highly infected JJHan culture were sorted and fixed for FISH analysis. The cells showed no signs of lytic replication, but HHV-6A integrated in a small subset of cells (Figure 32A). Moreover, I obtained detectable and comparable levels of HHV-6A genome copies by qPCR for wt, ΔU94 and ΔU94rev (Figure 32B).

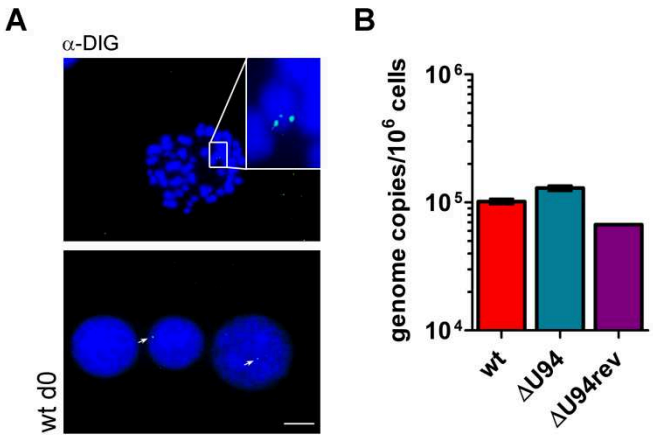


**Figure 32: Integration of wt, ΔU94 and ΔU94rev in JJHan cells. (A)** Representative FISH images (interphase nuclei and metaphase) of wt $GFP^-$ sorted JJHan cells at d0 post sort. Cells were fixed, metaphase spreads were prepared, hybridized with a HHV-6A specific DIG-labeled probe, washed and incubated with a secondary anti-DIG-FITC antibody, DAPI was used to visualize the nuclei and chromosomes. Blue: DNA, green: HHV-6A genome. Scale bar corresponds to 10 µM. **(B)** qPCR analysis for HHV-6A genome copies at d0 post sort. Copy numbers per 1x $10^6$ cells are shown as means with corresponding standard errors. One of three independent experiments is shown representatively. d:day.

At d6 post sort, the cells were again monitored via FISH, now displaying tremendous lytic infection in nearly all cells (Figure 33A, lower picture). qPCR analysis, in the presence or absence of the antibiotic Acyclovir, that is e.g. used to drive HSV-1 into latency, verified re-initiation of lytic infection at d6 (Figure 32B). GFP expression steadily increased as well over the days following the sort (data not shown). It is evident that the wt, U94 mutant and

revertant virus behave quite comparable in all settings. GFP$^-$ sorted cells are assumed to have a low percentage of supposedly integrated virus, which through the stress of sorting could be reactivated to lytic infection. Alternatively, it cannot be ruled out that some of the GFP$^-$ sorted cells might have been infected so recently that they do not yet express the GFP protein (under a CMV IE promoter), and that those are the ones re-starting lytic replication. Further experiments are needed to gain more insights on that matter.

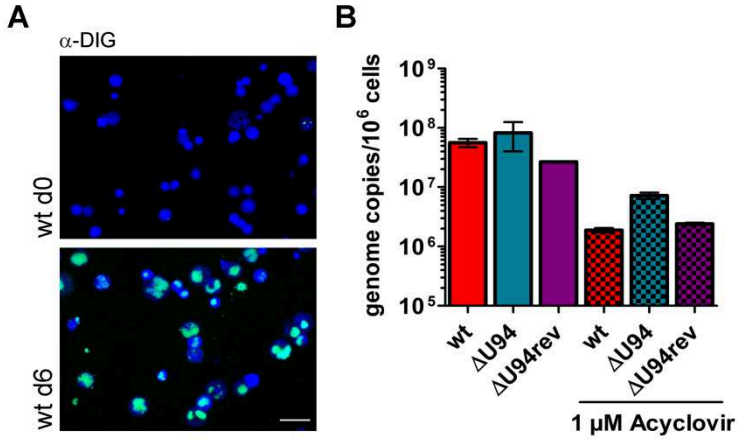


**Figure 33: Reactivation of wt, ΔU94 and ΔU94rev in JJHan cells. (A)** Representative FISH images of wt GFP$^-$ sorted JJHan cells at d0 and d6 post sort. Cells were fixed, metaphase spreads were prepared, hybridized with a HHV-6A specific DIG-labeled probe, washed and incubated with a secondary anti-DIG-FITC antibody, DAPI was used to visualize the nuclei and chromosomes. Blue: DNA, green: HHV-6A genome. Scale bar corresponds to 50 µM. **(B)** qPCR analysis for HHV-6A genome copies at d6 post sort with or without acyclovir treatment. Copy numbers per 1x $10^6$ cells are shown as means with corresponding standard errors. One of three independent experiments is shown representatively. d:day.

Furthermore, GFP$^+$ sorted cells were kept in culture for a prolonged period of time. All cells that survived the peak of infection lost the GFP signal (became GFP$^-$ again), suggesting that the cells either established latent infection or lost the viral genome. FISH analyses of these polyclonal GFP$^+$ sorted cells after more than 30 days (d30+) showed that the virus genome seems to be integrated in some cells (Figure 34A). Viral genome copies were still detectable by qPCR for both wt and ΔU94, indicating that the virus can be maintained in the latently infected cells in the absence of U94 (Figure 34B). Intriguingly, the ΔTMR mutant did not give rise to a GFP$^-$ cell population at d30+ after sorting in two independent experiments (data not shown), proposing that integration is important for cell survival in this setting.

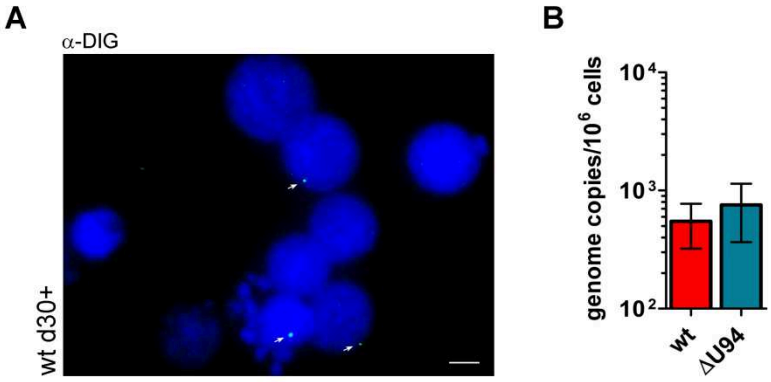


**Figure 34: Integration of wt, ΔU94 and ΔU94rev in JJHan cells after peak of lytic infection. (A)** Representative FISH image of wt at d30+. Cells were fixed, metaphase spreads were prepared, hybridized with a HHV-6A specific DIG-labeled probe, washed and incubated with a secondary anti-DIG-FITC antibody, DAPI was used to visualize the nuclei and chromosomes. Blue: DNA, green: HHV-6A genome. Scale bar corresponds to 10 µM. **(B)** qPCR analysis for HHV-6A genome copies at d30+ post sort. Copy numbers per 1x $10^6$ cells are shown as means of three independent experiments with corresponding standard errors.

### 7.3.4 Establishment of clonal cell lines for the ΔU94 mutant

Next, clonal U2OS cell lines obtained upon infection with the ΔU94 mutant virus were established in collaboration with Prof. Louis Flamand and Dr. Annie Gravel (Laval University, Quebec), as described above for the ΔpTMR virus (see 7.2.5).

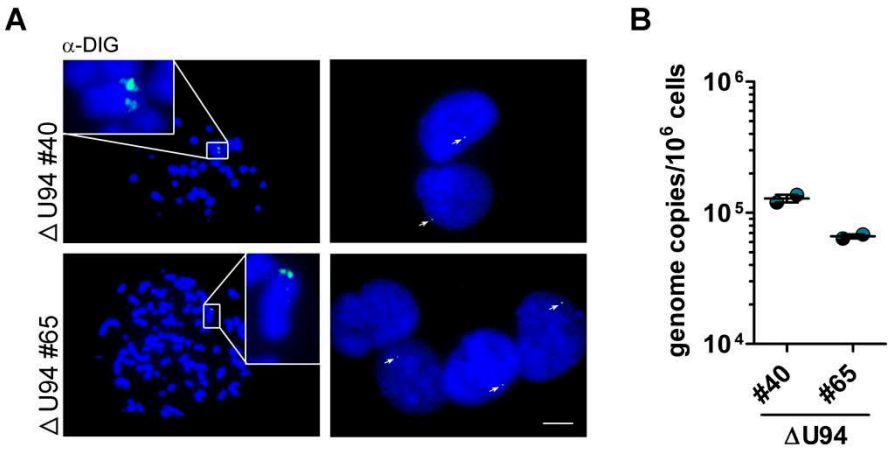


**Figure 35: Generation of clonal U2OS cell lines containing the ΔU94 virus. (A)** FISH analysis of clonal U2OS cell lines for the ΔU94 mutant with detection of integration. Cells were fixed, metaphase spreads were prepared, hybridized with a HHV-6A specific DIG-labeled probe, washed and incubated with a secondary anti-DIG-FITC antibody, DAPI was used to visualize the nuclei and chromosomes. Blue: DNA, green: HHV-6A genome. Scale bar corresponds to 10 µM. **(B)** qPCR analysis of HHV-6A genome copy numbers of clonal U2OS cell lines. Copy numbers per 1x $10^6$ cells are shown as means.

Clonal cell lines were amplified and the HHV-6A genome copies quantified by qPCR (Figure 35B). Several were obtained for the ΔU94 mutant and integration was confirmed by FISH analysis (Figure 35A).

### 7.3.5 Reactivation of HHV-6A in latently infected cells

Finally, I investigated if U94 is involved in the reactivation of HHV-6A, as previously suggested. The clonal wt and ΔU94 cell lines were treated with 80 ng/ml of the HDAC inhibitor TSA for 48 h. As iHHV-6 U2OS cells express GFP upon reactivation, I analyzed the cells by immunofluorescence (Figure 36A) and FACS analysis (Figure 36B). Preliminary experiments show that HHV-6A efficiently reactivates in several cell lines upon TSA treatment (in one out of four wt cell lines and in two out of two ΔU94 cell lines). Comparable results were obtained upon reactivation with TPA/sodium butyrate (data not shown). Further qPCR and FISH analyses are currently ongoing.

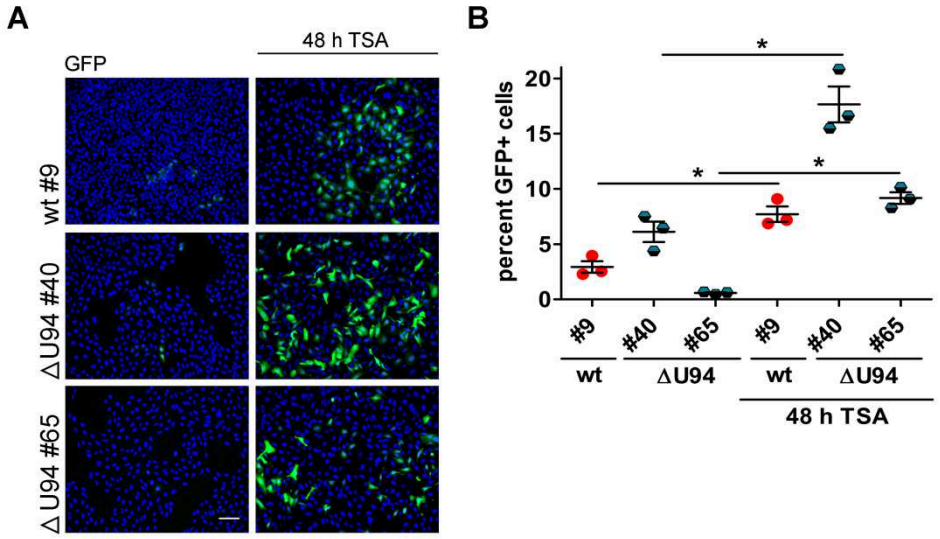


**Figure 36: Reactivation of latent HHV-6A. (A)** GFP expression of clonal cell lines of wt and ΔU94 mutant without (left panel) and with (right panel) 48 h TSA treatment (80ng/µl) observed under the fluorescent microscope. Scale bar corresponds to 100 µM. **(B)** GFP expression observed with the FACS Calibur. Significant differences between wt and ΔU94, treated vs. untreated (Mann-Whitney U-test, $p < 0.05$) are indicated with an asterisk (*). Results are shown as means of three independent experiments with corresponding standard errors.

# 8 Discussion

## 8.1 ND10 knockdown cells as tool for more efficient virus reconstitution

Considerable efforts had been devoted previously to achieve a more efficient virus reconstitution of the HHV-6A BAC clone. To enhance this reconstitution process, I disrupted ND10 bodies in the nucleus of the commonly used T-cell line JJHan. ND10s (or PML bodies) have been shown to be involved in antiviral processes of the cell hampering initiation of viral replication [64]. The major components of ND10 bodies namely PML, hDaxx and Sp100 were knocked down using RNA interference with shRNAs introduced into the cells by lentiviral transduction (Figure 12). These ND10 knockdown JJHan cells (JJHan ND10KD) allowed a more efficient replication of HHV-6A (Figure 13), making them a useful tool for virus reconstitution, which is currently the rate-limiting step in the generation of recombinant viruses for HHV-6A.

## 8.2 TMRs are required for HHV-6A integration

A number of viruses, including retroviruses or adeno-associated viruses, integrate their genome into chromosomes of the host as a compulsory part of their natural life-cycle. The central dogma for herpesviruses has always been that they maintain their viral genome as extra-chromosomal circular episomes during their dormant stages termed latency- the unifying principle of all herpesviruses [102]. Intriguingly, in 2010 Arbuckle *et al.* found *in vitro* no evidence for viral episomes during HHV-6 infection and instead saw that the virus integrated into host telomeres [101]. Since this discovery, a notion began to build that targeted integration may be mandatory for the successful establishment of HHV-6 latency. Until this point, the occasional integration observed for some herpesviruses (like EBV [104]) was thought to be an unintended and accidental event that rarely occurs during the course of viral infection.

Several groups proposed that the TMRs, present in the DR region of the HHV-6 genome and identical to human telomere sequences [165], are required for both integration (to establish latency) and excision (to reactivate from latency). This hypothesis was based on sequencing analysis of PBMCs isolated from ciHHV-6 carriers (harboring integrated HHV-6 in their germline cells). In all sequenced patient samples, the pTMRs of the $DR_R$ were located at the virus-host junction within the human subtelomere/telomere region (see Figure 6). Hence, a single copy of an entire viral genome is integrated containing both DRs [101, 107-109, 132]. TMRs are indeed an obvious suspect to facilitate homologous

recombination (HR) between virus and host, but since no experiments looking at the precise molecular mechanism had been conducted, their actual role remained unknown.

Using the HHV-6A BAC [191] and the *en passant* mutagenesis technique, I generated virus mutants lacking either the impTMRs (ΔimpTMR) or the pTMRs (ΔpTMR) and both in combination (ΔTMR). Lytic replication in JJHan cells was not influenced by any of the deletions (Figure 14, Figure 18 and Figure 22), illustrating that the TMRs are dispensable for viral growth. Integration efficiency of these mutants in comparison to wt virus was subsequently investigated with an *in vitro* latency/integration system using U2OS cells. As expected, integration of the ΔTMR mutant into telomeres was nearly abolished (Figure 17). In addition, the ΔpTMR mutant also displayed significantly impaired integration capacity (Figure 19), indicating that the perfect TMRs play a major role in the HHV-6 integration process. This is consistent with observations in ciHHV-6 patients (mentioned above) where in nearly all cases the pTMRs were the site of virus integration. The impTMRs alone were not sufficient for thorough viral integration, as only very few integration events occurred. The residual integration observed for the ΔpTMR mutant virus could be explained by recombination of the remaining impTMRs with the host telomeres. This explanation is entirely plausible, since one ciHHV-6 patient in the study by Ohye *et al.* was identified with the impTMRs at the site of integration [107]. Deletion of the impTMRs only had a minor impact on HHV-6A integration frequencies, suggesting that the impTMRs are of little importance for the HHV-6A integration process. Intriguingly, the extended impTMR region (multiple copies) I discovered in the HHV-6A wt BAC positively affected integration efficiency compared to the revertant virus, in which the impTMRs were restored according to the NCBI reference sequence (Figure 23).

For further in-depth experiments, I attempted to generate clonal U2OS cell lines containing the integrated TMR mutants. However, despite tremendous efforts, I was unable to generate clonal cell lines for the ΔTMR mutant virus that harbor the HHV-6 genome (tested by qPCR). This is in line with and further supports my previous results obtained from the HHV-6 latency system, clarifying the inability of the ΔTMR mutant to maintain the viral genome in the absence of integration. For the ΔpTMR mutant I successfully established several clonal cell lines due to residual integration (mentioned above). In qPCR and FISH analysis, they were positive for the HHV-6A genome as well as integration (Figure 24 and Figure 25). Whether the ΔpTMR mutant still integrates into the telomeres, possibly via the remaining impTMRs, remains unknown. Alternatively the virus genome could also integrate randomly in the human genome. Pinpointing this issue and investigating whether the HHV-6A ΔpTMR integrates as a single copy or as concatemers, as shown for an equivalent mutant in MDV (as described below in 8.3), will be addressed in the future by pulsed-field gel electrophoresis.

A method to determine the exact sequence of the virus-host junctions in the generated clonal cell lines is currently established with our collaborators Drs. Alex Greenwood and David Alquezar (Leibniz-Institut für Zoo- und Wildtierforschung, Berlin). In this method, genomic DNA is fragmented into 4 kb pieces that get circularized, amplified with virus-specific bidirectional primers and sequenced using PacBio next-generation sequencing.

Another intriguing aspect worth investigating is the minimal number of TMRs required for efficient integration of HHV-6. Although this experiment is beyond the scope of this work, it could be addressed using techniques established in this study.

In conclusion, the proposed model of HHV-6 integration by HR between viral TMRs and host telomeres is depicted in Figure 37. Considering that HR is a native process occurring in cells, in the absence of infection, one might argue that viral proteins are dispensable for integration. Furthermore, if the model holds true, other herpesviruses that possess TMRs could potentially also insert their genome into host telomeres.

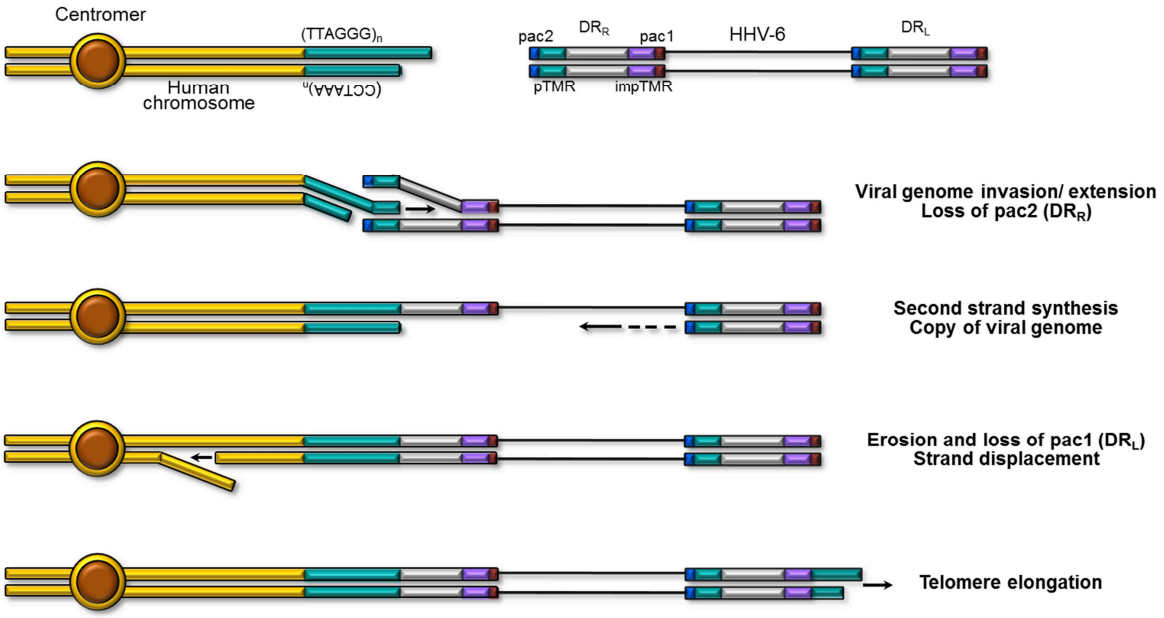


**Figure 37: Working model for HHV-6 genome integration into host telomeres.** A mechanism using homologous recombination would enable invasion of the 3' end of the chromosome into the viral genome at the $DR_R$ pTMR, followed by extension and second strand synthesis. The $DR_R$ pac2 as well as the $DR_L$ terminal pac1 sequences would be lost. The adjacent impTMR of $DR_L$ could be used to form a neo-telomere at the end. This integration process is conceivably independent of further viral proteins (modified from Kaufer and Flamand [209]).

## 8.3 Presence of TMRs in a number of herpesviruses

Major advances in sequencing methods have led to a tremendous increase in the number of sequenced virus genomes. Intriguingly, this has helped to identify a number of other herpesviruses harboring TMRs in their genome, mostly at the genome termini. Among those are representatives of all genome classes and herpesvirus subfamilies, even members of the *Alloherpesviridae*, which infect fish (Table 8).

**Table 8: Members of the order *Herpesvirales* harboring telomeric repeat sequences in their genomes.** Modified from Osterrieder *et al.* [102].

| Species | Genome type | Telomere integration |
|---|---|---|
| ***Herpesviridae*** | | |
| ***Alphaherpesvirinae*** | | |
| **Marek's disease virus (MDV) [gallid herpesvirus 2 (GaHV-2)]** | E | Yes [105] |
| **Gallid herpesvirus 3 (GaHV-3)** | E | Unknown |
| **Herpesviurs of turkeys (HVT) [meleagrid herpesvirus 1 (MeHV-1)]** | E | Unknown |
| **Duck enteritis virus (DEV) [anatid herpesvirus 1 (AHV-1)]** | D | Unknown |
| **Marmoset herpesvirus (MarHV) [saimiriine herpesvirus 1 (SaHV-1)]** | D | Unknown |
| ***Betaherpesvirinae*** | | |
| **Human herpesvirus 6A (HHV-6A)** | A | Yes [101] |
| **Human herpesvirus 6B (HHV-6B)** | A | Yes [132] |
| **Human herpesvirus 7 (HHV-7)** | A | Unknown |
| **Macaca nemestrina herpesvirus 6 (MneHV-6)** | A | Unknown |
| **Macaca nemestrina herpesvirus 7 (MneHV-7)** | A | Unknown |
| ***Gammaherpesvirinae*** | | |
| **Equine herpesvirus 2 (EHV-2)** | A | Unknown |
| **Ovine herpesvirus 2 (OvHV-2)** | C | Unknown |
| ***Alloherpesviridae*** | | |
| **Cyprinid herpesvirus 1 (CyHV-1)** | A | Unknown |
| **Cyprinid herpesvirus 2 (CyHV-2)** | A | Unknown |
| **Cyprinid herpesvirus 3 (CyHV-3)** | A | Unknown |

Such wide conservation of these repeats suggests that they perform an important function for herpesviruses. However, for most of these viruses it remains unknown if they integrate into telomeres and if integration is key for the maintenance of the virus genome in latently infected cells. While much investigation remains to be done, speculatively, it could be that integration is a common, yet unappreciated mechanism to achieve latency for a

multiplicity of herpesviruses. A point that would unhinge the central dogma of episomal herpesvirus genomes during latent stages [102].

One example of a TMR containing virus is Marek's disease virus (MDV), a member of the *Alphaherpesvirinae*, which causes various clinical symptoms including polyneuritis and multiple lymphoma formation in its natural host, the chicken. Its class E genome contains two unique regions ($U_L$ and $U_S$) bracketed by inverted repeats termed terminal and internal repeats long ($TR_L$ and $IR_L$) and terminal and internal repeats short ($TR_S$ and $IR_S$) [210]. During viral latency in $CD4^+$ T-cells, MDV is exclusively found in an integrated state in one or multiple chromosomes [105]. MDV harbors two arrays of TMRs termed multiple TMRs (mTMRs- ranging from 27 to 100 repeats) and short TMRs (sTMRs- with a fixed number of six TTAGGG repeats) [165]. In 2011, Kaufer and colleagues could show that the mTMRs facilitate genome integration of MDV into chicken telomeres *in vivo*, while the deletion had no influence on lytic replication. Furthermore, this study proved that integration is a prerequisite for the establishment of latency and lymphoma formation in the chicken. In addition, integration into telomeres allowed efficient reactivation and genome mobilization from its dormant state. Viruses with deleted mTMRs merely displayed random chromosome integration in the form of concatemers [166]. The sTMRs play a minor role in MDV integration, which appears to be similar to the impTMRs in HHV-6; since mutations in that region did not abolish integration, however, correlated with a remote decrease in the number of viral integration sites in tumor cells [167]. Current conjectures also attribute vTR an auxiliary role in the integration process of MDV by promoting telomeric elongation, possibly required upon integration. vTR is the viral homolog of telomerase RNA (TERC) that shares 88 % sequence identity with its chicken counterpart and in combination with TERT forms the telomerase complex required for telomere maintenance [210]. Of note, HHV-6 does not encode a telomerase RNA ortholog in its genome.

The closest relative of HHV-6 is HHV-7, the third member of the *Roseolovirus* genus that was isolated from healthy individuals in 1990 [211]. HHV-7, like HHV-6 is a ubiquitous pathogen and infects over 90 % of the population in early childhood. Disease associations strongly resemble those of HHV-6, though usually display milder clinical symptoms. The HHV-7 genome is co-linear to HHV-6 across the entire length and nucleic acid sequence identity ranges from 40 % to 75 % depending on the region [212]. Only one gene is unique for HHV-7, when compared to HHV-6, and that is ORF *U55B* [213]. The DR region of HHV-7 harbors both perfect and imperfect TMRs that are somewhat more complex than the ones found in the HHV-6 genome. Interestingly, for HHV-7, the number of TMR repeats is the dominant reason for inter- and intra-strain genome size heterogeneity [214].

HHV-7 integration has not yet been published, despite the presence of TMRs and the considerable similarity to HHV-6. Intriguingly, HHV-7 does not encode an equivalent of the HHV-6 Rep homolog U94, suggesting that this protein could be the decisive factor- tipping the scales towards integration [215].

This model is in conflict with a recent finding by our collaborator Dr. Bhupesh Prusty (University of Würzburg, personal communication), who found that the HHV-7 laboratory strains JI and RK integrate into human chromosomes, both at the telomeres and elsewhere in the chromosome. Additionally, individuals have been identified potentially harboring the HHV-7 genome in the germline, a condition bearing resemblance to ciHHV-6. One explanation why previous studies on HHV-7 integration have not revealed virus integration may be due to the narrow tropism of the virus for CD4 positive cells [216]. In this regard, relatively few cells would be latently infected with HHV-7, making it more technically challenging to isolate these cells from individuals and to determine the status of the virus genome.

## 8.4 U94 is dispensable for HHV-6A integration

If HHV-7 can also integrate without encoding an *U94* ortholog, it seems plausible that U94 might not mediate integration after all- at least not on its own. The high conservation level between *U94* from HHV-6A and HHV-6B and its uniqueness among human herpesviruses points to an important function of this protein during the HHV-6 life-cycle [46, 170]. Several lines of evidence suggest that U94 is a potential recombinase. HHV-6 U94 has a strong homology to the AAV-2 Rep protein. Rep in AAV-2 induces the targeted integration into chromosome 19 by utilizing its DNA-binding, helicase, ATPase and endonuclease activity [175]. Making use of MBP-fusion proteins of both HHV-6A and -6B U94, Trempe *et al.* investigated the biological and enzymatic activities of U94. The U94 protein displayed ATPase, helicase, 3'-5' exonuclease and DNA-binding (preferential to TMRs) activities and destabilized telomere D-loops. Therefore, U94 exhibits activities that could facilitate integration and excision (reactivation) of HHV-6 [183].

Conservationally speaking, two more herpesviruses encode *U94/Rep* homologs. The rat cytomegalovirus (RCMV) encodes a non-essential DNA-binding protein r127 with genomic position and orientation similar to that of the HHV-6 *U94* gene. This suggests that the gene may have been acquired from parvoviruses by a common ancestor of herpesviruses, rather than by two independent events. Why closely related viruses (MCMV, HCMV, HHV-7) do not possess *U94* homologs can only be speculated, for example due to a lack of positive selection pressure [217]. The second homolog is present in a novel bat herpesvirus MsHV (*Minipterus schreibersii*). The predicted protein B125 is

located in the same position in the MsHV genome as the *U94* gene of HHV-6 and the protein has 27 % amino acid identity with HHV-6 U94, indicating a likely common origin [218]. However, it should be noted that both viruses lack TMRs and so far nothing is known about their integration potential.

In this thesis, an apparent discrepancy can be seen between the *in vitro* findings for purified U94, strongly suggesting a role of U94 in HHV-6 integration and the results I have obtained with the U94 mutant viruses. In the *in vitro* latency system using U2OS cells, ΔU94 and U94stop mutant viruses exhibited integration efficiencies comparable to wt and the respective revertant viruses (Figure 29 and Figure 30), arguing against a role for U94 in HHV-6 integration. Moreover, preliminary results using JJHan cells also point to the same conclusion (Figure 32). Other cell types, however, should be tested to rule out a cell type dependent effect. The human osteosarcoma cell line U2OS was chosen based on studies by our collaborators Prof. Louis Flamand and Dr. Annie Gravel (Laval University, personal communication). They tested a number of cell lines (U2OS, GM847, Hela, HCT-116, NIH3T3, HEK293T) and demonstrated that U2OS have the highest integration rate of approximately 30 %.

One reason for the high integration frequency could be that U2OS cells are the prototypic ALT (alternative lengthening of telomeres) positive cells; ALT is a mechanism that involves frequent recombination events at the telomeres [127]. Therefore, the ALT activity could compensate for the loss of U94 in the U94 deletion mutants. Usually, telomere length is maintained by telomerase, an enzyme complex that is capable of adding TTAGGG repeats to the chromosome termini *de novo* [117]. Only a small subset of cells uses ALT to counteract telomere shortening. This recombination–mediated synthesis of new telomeric DNA is accomplished by HR using the same telomere, a sister chromatid, the telomere of other chromosomes, linear extra-chromosomal telomeric, or t-circle DNA as a template. The latter could be resembled by linear or circular HHV-6 genomes present in the cell [128, 129]. ALT makes use of various DNA repair proteins (MRN complex, SMC5/6 complex or BLM helicase) to elongate telomeres. DNA ends get joined together, which in turn facilitates 5' to 3' resection of DNA ends resulting in 3' overhangs necessary for strand invasion during HR [127, 128].

There are currently no commercial ALT inhibitors available, but several factors were proven to play an important role and could already be experimentally abrogated. This led to the repression of the ALT mechanism, measured by telomere shortening. Amongst them are the SMC5/6 subunits [219] and the MRN complex including the NBS1 protein, which have been reduced by RNA interference [220]. In addition, overexpression of Sp100 also abolished a functional MRN complex [221]. These approaches could be used

in my integration system to assess the impact of ALT on HHV-6 telomere integration. Nevertheless, using more natural settings for further *in vitro* studies would be preferable. ALT$^-$ cells (e.g. HEK293T cells or MO3.13) as well as primary monocytes or macrophages were previously shown to allow for the establishment of HHV-6 latency. Use of primary monocytes and macrophages would be ideal, as these cell types represent the natural reservoir for HHV-6 latency *in vivo*.

## 8.5 Other viral and cellular factors potentially involved in integration

Besides U94, there is a plethora of other conceivable factors that could aid in the integration process of HHV-6. Redundancy in biological systems is often key for the continuation of processes crucial to an organism's survival. The integration process of HHV-6, allowing establishment of virus latency, may therefore be protected by several redundant pathways to ensure that this fundamental step can occur. This hypothesis could be tested by simultaneous knockdown or deletion of several candidate integration factors.

HHV-6 encodes a unique set of genes that lack clear counterparts in the closely related CMV, which does not integrate, but forms episomes during latency. Those genes include the ORFs *U13*, *U15*, *U20*, *U26* and *U95* that could be responsible for HHV-6 specific features such as integration. Since hardly any information is available on any of these genes, knockout viruses have recently been generated in our lab to elucidate their role in HHV-6 replication and/or integration.

The orthologs of HSV-1 *UL12* and *UL29* (ICP8) in HHV-6 (*U41* and *U70*) are also worth to be analyzed, as their gene products facilitate recombination during HSV-1 replication [222, 223]. UL12 is a 5'-3' exonuclease that generates 3' ssDNA overhangs, whereas the ICP8 protein (*UL29*) is a single strand binding protein that allows annealing of ssDNA to complementary sequences. Their interaction *in vitro* closely resembles the Red recombination system of bacteriophage λ; with UL12 matching functions of the lambda exonuclease (Exo) and ICP8 displaying similarity to the Beta component [224, 225]. Direct interaction has been proven between UL12 and elements of the MRN complex [223], which senses dsDNA breaks and perpetuates general telomere length [226]. HSV-1 has recently been shown to remodel telomeres to promote viral replication by forming ICP8-associated pre-replication foci [227]. In another context, it was speculated that ICP8 of HSV-1 could interact with Rep of AAV-2, the homolog of HHV-6 U94 [228]. Considering these aspects, it seems reasonable that the HHV-6 homologs of *UL12* and *UL29* could participate in HHV-6 integration as a redundant mechanism or in collaboration with U94. Both components will be knocked down by RNA interference (*U41* and *U70* independently

and/or in combination with a *U94* knockdown) in the integration system to resolve this issue.

Besides virus-encoded factors, cellular components could also be engaged in integration. Commercial inhibitors, shRNAs or CRISPR/Cas9 (explained in more detail below in 8.9) could be used to target cellular factors and address their involvement in integration. TRF2 for instance, which is part of the telomere-protective shelterin complex and binds to TTAGGG repeats, could associate with the HHV-6 TMRs. This would enable the linear viral genome to sit in close proximity to the telomere as a prelude to HR. Arguing for this view, was the finding that TRF2 can bind to the EBV encoded TTAGGGTTA repeat within the viral origin of plasmid replication [229].

Another cellular factor that could be involved is the cellular recombinase Rad51, which is essential for HR and repair of DSBs. Rad51 is mobilized to the site of damage and binds the 3' ss ends, resulting in formation of nucleofilaments that enable strand invasion and repair by binding to homologous DNA sequences. Rad51 expression is elevated in various human tumors [207, 230, 231] and active in both meiosis and mitosis. The recombinase possesses ATPase and DNA-binding activities, required for catalyzing strand-exchange reactions with homologous templates. Five paralogs of Rad51 have been identified in mammals (Rad51B, Rad51C, Rad51D, Xrcc2 and Xrcc3), which form a complex and initiate ssDNA processing at DSBs [232]. In Figure 31, I used the specific Rad51 inhibitor RI-1 after infection of U2OS cells. The RI-1 inhibitor was previously used in U2OS cells and covalently binds to the Rad51 protein (at cysteine 319), thereby inhibiting Rad51 oligomerization into filaments in the initial steps of HR [208]. RI-1 treatment did not significantly reduce the integration efficiency of wt virus nor the ΔU94 mutant, indicating that Rad51 is not essential for HHV-6A integration. Moreover, the observed minor differences in integration frequencies were most likely due to the marginal cytotoxic effects of the inhibitor. Our collaborators Prof. Louis Flamand and Dr. Annie Gravel (Laval University, personal communication) also tested a second commercial Rad51 inhibitor called B02, however, they were unable to observe any effect on HHV-6 integration efficiency.

Another quest to be solved is that of the integration kinetics. How quickly after infection does integration occur and is it dependent on prior virus replication?

## 8.6 Why telomeres?

Integration poses many advantages to a virus. For example, it allows faithful maintenance of the genome during cell division to ensure long-term persistence in the host. But virtually a philosophical question is why telomeres were 'selected' by HHV-6 and other

herpesviruses as the site for integration. Telomeres are repetitive regions at the termini of chromosomes that protect the chromosome ends from unwarranted repair by DDR components, which are initiated upon recognition of DSBs. Therefore, they guarantee genomic stability. In humans, telomeres consist of up to 15 kb of tandem repeats of the TTAGGG hexanucleotide which are bound by specific proteins (shelterin complex) [117]. The tremendous size of herpesvirus genomes (up to 240 kbp) stands to reason that integration of such large fragments of foreign DNA elsewhere in the chromosome could not be tolerated.

Besides, telomeres are believed to be transcriptionally inactive or 'silenced'. Only the long non-coding RNAs, called TERRA (telomeric repeat-containing RNA) of varying lengths (up to 9 kb in mammals [233]) are generated from different subtelomeric locations towards the chromosome ends [234]. The overall heterochromatic nature of the telomere region contributes to telomeres as the location of choice for HHV-6 integration; as it is beneficial for the virus to silence lytic genes during latency periods in order to minimize unwanted immune detection. A number of repressive histone modifications such as trimethylation of histone H3 at lysine K9 (H3K9me3) and H4 at lysine 20 (H4K20me3) are highly elevated in telomeric regions [116]. These observations can be recapitulated in a phenomenon termed telomere position effect (TPE). TPE leads to reversible dampening of gene expression near telomeres and was originally identified in *Saccaromyces cerevisiae* [235]. This effect has also been confirmed in human cells. A 10-fold reduction in expression of a luciferase reporter introduced adjacent to the telomeres was detected compared to integrations that were elsewhere in the chromosome. This suppression could be rescued by treatment with the histone de-acetylase inhibitor TSA. The intensity of TPE is dependent on the telomere length and correlates with alterations in the recruitment of chromatin remodeling factors [236]. The conservation of TPE from yeast to humans indicates a crucial role in telomere biology and chromosome integrity [237]. Harnessing TPE, lytic genes of iHHV-6 would be silenced during latency. However, it remains unknown if HHV-6 utilizes this silencing mechanism or if TPE could potentially be disturbed upon virus integration.

As telomeres gradually shorten with time, which could result in loss of integrated viral sequences, the virus choice perhaps seems rather counter-intuitive at first glance. In ciHHV-6 patients, however, it was shown that the impTMRs in the $DR_L$ form a neo-telomere adjacent to the integrated virus genome [107], ensuring at least in part that the virus is initially protected from telomere shortening over numerous rounds of cell division. To date 10 differential telomeric integration sites were identified for HHV-6 using fluorescence *in situ* hybridization (FISH): 17p13.3 [98, 100, 101, 142, 143], 18q23 [101, 132], 22q13.3 [9, 99, 101, 134], 9q34.3, 10q26.3, 11p15.5, 19q13.4 [100], 1q44 [9, 131,

144, 145], 11q, 2p [132]. This raises the questions as to whether all telomeres are equal when it comes to virus integration or whether there are indeed preferential sites/chromosome's telomeres for HHV-6 integration? The explanations range from accessibility issues or heterochromatic structure to the assumption that some chromosome ends are too fragile to withstand such a drastic alteration, resulting in instability. In the observed sites however, iHHV-6 seems to have marginal impact on the existing telomere/shelterin complex.

Lastly, the telomeres may be an optimal 'hiding-place' for HHV-6 as they are highly dynamic and harbor many homologous sites [116], increasing the number of sites where integration could occur. Taken together, telomeres provide high copy numbers as well as a protected and silenced region of the chromosome, which is perfectly suited for a virus to hide. Besides, the dynamics of the telomeres offer good prospects for HHV-6 to rather effortless enter and exit the host chromosomes, allowing the establishment of latency but also reactivation of the virus.

## 8.7 ciHHV-6 disease associations

A fascinating feature of HHV-6 is the integration into the germline (ciHHV-6), resulting in individuals that harbor the integrated virus genome in every nucleated cell of their body. This is then passed on to their children by Mendelian inheritance. HHV-6 was shown to bind to spermatozoa acrosomes and was the predominant herpesvirus found in semen samples collected from sperm donors [238]. One explanation could be the high prevalence of the CD46 receptor on the inner acrosomal membrane of spermatozoa [239]. ciHHV-6 affects approximately 70 million individuals (~1 % of the population) on earth [141], which means twice as many people as are currently living with human immunodeficiency virus 1 (HIV-1) (UNAIDS.org, 2014 global statistics). In various studies, the actual percentages ranged from 0.2 % to 2.1 %, depending on geographic location as well as health status of the probands [134-140]. Overall, it appears that ciHHV-6 is more common in diseased individuals [141].

Specific disease associations are hard to assess, since different chromosome locations found for ciHHV-6 could cause multiple unrelated pathologies or dysfunctions. Nevertheless, a study from Pantry *et al.* in 2013 concluded that a number of ciHHV-6 carriers are prone to increased incidence of infection with exogenous HHV-6 strains, leading to a wide range of neurological symptoms including long-term fatigue [152]. In a recent large-scale analysis, ciHHV-6 was found to be a predisposing factor for the development of angina pectoris. Patients displayed 10 % shorter telomeres compared to age-matched controls, leading to the conclusion that diminished telomeres could cause

cardiovascular disease [153]. This finding is supported by another study, showing increased risk of myocarditis in case of a ciHHV-6 status [135]. Furthermore, a wide variety of indirect HHV-6 effects (like bacterial superinfections or allograft rejection) could be observed after transplantation in ciHHV-6 individuals [154].

Telomeres containing ciHHV-6 are often the shortest, promoting instability and telomere truncations [109]. These altered telomeric regions may cause precocious aging, leading to organ dysfunctions or alternatively favor cancer development [240]. Similarly, subtelomeric rearrangements, microdeletions and chromosome-end truncations have been identified as a major cause of mental retardation and developmental malformations [237, 241-243]. Several locations that were also shown to potentially harbor ciHHV-6 are etiologic for cases of delayed mental development: 1q44, 17p13.3 (Miller-Dieker syndrome), 18q23 (de Grouchy syndrome) and 22q13.3 [241]. Even though HHV-6 is unlikely the cause of these diseases, the possibility of similar chromosomal alterations caused by HHV-6 integration in these and other areas of interest exists, since each chromosome end could produce a distinct phenotype [244].

Finally, there is an active debate to whether standard testing for ciHHV-6 should be performed for transplant donors and recipients. At the very least, awareness about ciHHV-6 should be disseminated amongst clinicians to prevent misinterpretation of high viral loads as substantial active infection and subsequent administration of harmful antiviral therapy [140, 143, 150, 245].

## 8.8 Virus reactivation from its integrated state

Integration of the HHV-6 genome into the telomeres of human chromosomes represents a means to maintain its genome during latency and is not a dead end, as the virus can mobilize its genome from the integrated state during reactivation to re-initiate production of virus particles.

This thesis has presented preliminary results regarding *in vitro* reactivation of integrated HHV-6A from the U2OS cell line. After 48 h TSA treatment in several clonal iHHV-6 U2OS cell lines, I observed the initiation of GFP expression (Figure 36). However, the stimulus was not sufficient to induce genome replication as analyzed by qPCR. No signs of lytic infection were detected by FISH either. Therefore, it is possible that the chromatin de-condensation mediated by the HDAC inhibitor TSA was not sufficient to induce full reactivation. Thus, longer exposure times or other drugs may be needed to initiate virus replication. Furthermore, some integrated viruses could be defective in reactivating, while others readily reactivate only under certain conditions. Other groups previously accomplished reactivation of integrated HHV-6 (in: Katata Burkitt's lymphoma cell line,

HEK293T cells, monocytes, myeloid cell line and an astrocytoma cell line) upon treatment with various reagents: TPA, sodium butyrate, TSA, hydrocortisone or *chlamydia trachomatis* infection [88, 90, 91, 99, 101, 108]. Reactivation has been suggested to occur via t-circle formation, when the ss telomeric 3' overhang incidentally invades into the internal HHV-6 $DR_R$-pTMR region. HHV-6 could be released, giving rise to a circular full-length HHV-6 genome lacking one DR region but in possession of intact packaging and cleavage sites. This would permit rolling-circle replication and formation of viral particles [108, 109].

Reactivation of ciHHV-6 *in vivo* has been documented in a number of publications. The majority has dealt with assumed reactivation of ciHHV-6 caused by other previous clinical conditions. All patients displayed a positive response to antiviral treatment, easing the HHV-6 induced symptoms [135, 157, 159, 160]. Furthermore, ciHHV-6 reactivation was detected in a patient following cord blood transplantation [158]. Convincing data from two independent studies demonstrated that HHV-6 can be transmitted from ciHHV-6 positive mothers via the placenta to the embryo, likely derived from their integrated virus upon reactivation [161, 162].

Cellular factors involved in reactivation could be identified using a genome-wide CRISPR/Cas9 knockout (GeCKO v2) library. The library targets the 5' constitutive exons of 18,080 genes using 64,751 specific guide sequences resulting in directed loss-of function mutations in genomic DNA (see 8.9) [246]. Besides cellular targets, U94 may also be involved in the maintenance of latency. The clonal U2OS cell lines with integrated wt HHV-6A or the ΔU94 mutant virus could be used to address this question (Figure 35).

## 8.9 Therapeutic intervention

Therapeutic intervention to treat or cure patients is the ultimate goal in all biomedical research. However, it is often a long and treacherous path. The work highlighted in this thesis has furthered the understanding of HHV-6 integration and has begun to delve into the processes underlying reactivation of the virus. Moreover, my studies have laid the groundwork for future experiments aimed at the discovery of novel treatments against HHV-6 integration and reactivation. I could show that the virus-encoded TMR sequences are necessary for virus integration, whereas the putative viral recombinase, U94, appears to be dispensable for the integration process. However, much work remains to be done in order to decipher the precise mechanism of HHV-6 integration and target this process for therapeutic intervention. One approach for translational research in the future is to eventually develop strategies to circumvent integration of HHV-6. As latency is an

essential part of the herpesvirus life-cycle, therapies targeting formation of this dormant state are highly desirable.

Alternatively, it may be possible to excise and eliminate the integrated genome using the CRISPR/Cas9 technology. CRISPR (clustered regularly interspaced short palindromic repeats) and its associated protein Cas9 have been adapted to molecular biology from the immune system of bacteria like *Streptococcus pyogenes*. Two components are required to be introduced into the cell for this system, usually delivered using lentiviral or adeno-associated virus vectors: the Cas9 protease and a short guide RNA (gRNA). This gRNA sequence, complementary to the target DNA (which contains a protospacer adjacent motif (PAM) 3' to the target site) directs the Cas9 nuclease to the desired genome location. Upon binding, Cas9 induces blunt-end DSBs causing repair by HR or NHEJ (non-homologous end joining), resulting in insertions or deletions at the target site. Any site can be targeted with this approach, including genes, promoters, enhancers, introns or intergenic regions [247-249]. The importance of this technique for biomedicine is emphasized by the fact that it is applicable to a vast array of problems such as the repair of genetic mutations, which are the cause of many inherited disorders [250].

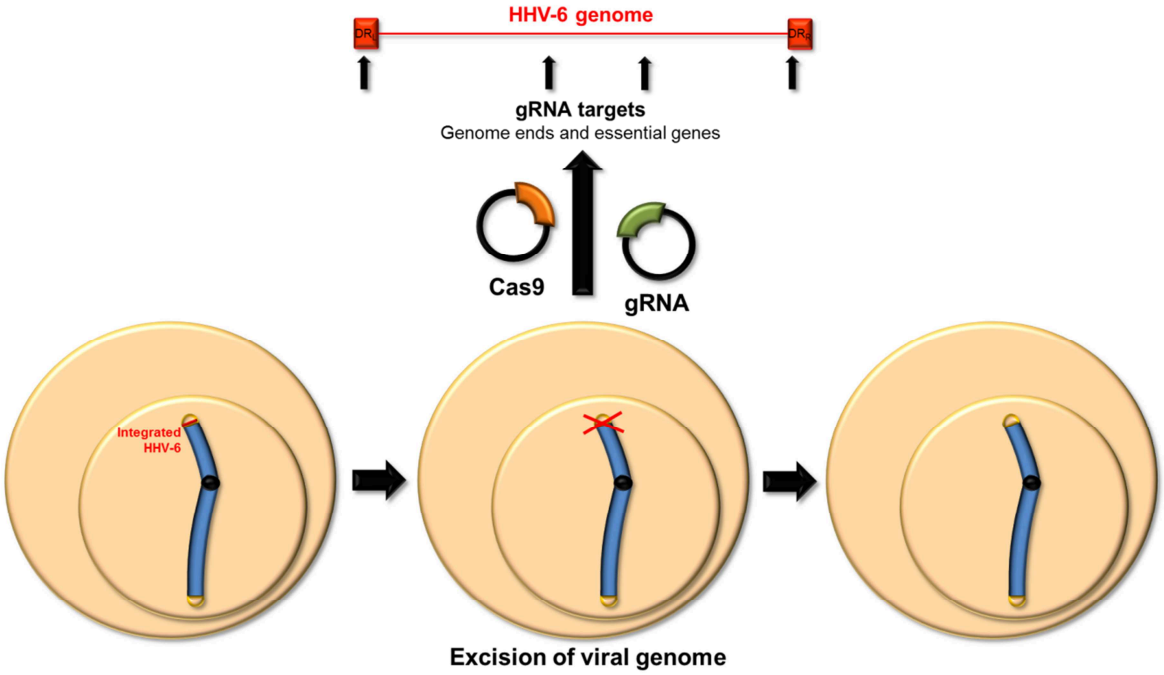


**Figure 38: Approach to excise integrated HHV-6 from human chromosomes using CRISPR/Cas9 technology.** Potential target sites for attack by Cas9 would be genome ends, essential genes and other repeated regions.

Indeed, now the first attempts to excise the integrated HIV-1 (human immunodeficiency virus 1) genome have been published, accomplishing the removal of fragments of the integrated viral DNA [251, 252]. Latent herpesviruses have also been targeted using this

strategy. Wang *et al.* showed drastic reduction in viral load during EBV infections by targeting the viral genome and deleting large segments [253]. Furthermore, the first studies using this technology on HCMV and HSV-1 have already been conducted (IHW 2015, Robert Lebbink). Before clinical trials, the hurdle of off-target effects leading to non-specific gene modifications certainly must be addressed. However, the CRISPR/Cas9 technology will be a great tool for gene therapy and could find a future therapeutic use in the elimination of integrated virus genomes like HHV-6 (Figure 38).

# 9 Summary

Human herpesvirus 6 (HHV-6) is a betaherpesvirus related to the human cytomegalovirus. It is the causative agent of *roseola infantum*, a febrile illness in infants, and has a seroprevalence of over 90 % worldwide. Upon primary infection, HHV-6 establishes a persistent infection in the host for life termed latency, mostly in bone marrow progenitor cells, monocytes and macrophages. Reactivation from latency preferentially occurs in immunocompromised individuals and is associated with several diseases including encephalitis, multiple sclerosis, graft rejection as well as a more rapid AIDS progression. HHV-6 has previously been shown to integrate its genetic material into telomeres of human chromosomes, a mechanism that allows vertical transmission of the virus via the germline, resulting in individuals that harbor the integrated virus in every single cell of their body. This condition is termed ciHHV-6 (chromosomally integrated HHV-6) and is present in roughly 1 % of the human population. The molecular mechanism and the factors involved in HHV-6 integration remain completely unknown.

Intriguingly, HHV-6 and several other herpesviruses harbor arrays of telomeric repeats (TMRs) at their genome termini that are identical to human telomere sequences. The TMRs in HHV-6 have been termed perfect TMRs (pTMRs) and imperfect TMRs (impTMRs), and have been proposed to facilitate homologous recombination (HR). Furthermore, HHV-6 encodes the *U94* gene that contains all conserved domains of the Rep recombinase of Adeno-associated virus 2 (AAV-2). Expression of U94 restores replication of a Rep-deficient AAV-2, suggesting that both proteins have similar functions. Indeed, recently it was confirmed that a purified MBP-U94 fusion protein has DNA-binding, ATPase, helicase and exonuclease activities as described for Rep. However, the actual role of U94 and the TMRs in HHV-6 replication and integration remains elusive.

To determine whether the TMRs are involved in HHV-6 integration, I deleted the two distinct sets of TMRs, individually or simultaneously, in a bacterial artificial chromosome (BAC) of HHV-6A by *en passant* mutagenesis. As reconstitution of HHV-6A from BAC DNA is very challenging, I disrupted nuclear domains 10 (ND10s), which are part of the cellular antiviral defense machinery, to achieve a more efficient reconstitution. Knock-down of the major ND10 components PML, hDaxx and Sp100 using lentivirus-transduced shRNAs in the T-cell line JJHan (ND10KD) enhanced replication of HHV-6A. Upon reconstitution in ND10KD cells, the TMR mutant viruses replicated comparable to wild type (wt) and revertant viruses, indicating that the TMRs are not essential for HHV-6A replication. To assess the integration properties of the recombinant viruses, I established an *in vitro* latency system that allows assessment of integration efficiency and genome maintenance in latently infected U2OS cells. Fluorescence *in situ* hybridization (FISH) analyses revealed that integration is severely impaired in the absence of the TMRs. The

genome of the TMR mutants was poorly maintained in latently infected cells, suggesting that integration is crucial for the maintenance of the virus genome.

To investigate the role of the putative HHV-6 recombinase, the ORF *U94* was either deleted entirely from the HHV-6A BAC or its expression was abrogated by introducing a premature stop codon. Integration efficiencies of the U94 mutants were not altered compared to wt and revertant viruses in the U2OS integration assay, suggesting that U94 is not essential for HHV-6A integration. In addition, inhibiting the cellular recombinase Rad51, using a specific inhibitor, also did not significantly change the integration frequencies of the viruses, indicating that other viral or cellular recombinases can complement the function of U94 and Rad51 in HHV-6A integration. Clonal cell lines were generated for all mutant viruses harboring integrated HHV-6A (iHHV-6) for further in-depth analysis of integration sites and reactivation properties.

Taken together, my data show that the HHV-6A TMRs are dispensable for virus replication, but are crucial for integration and maintenance of the virus genome in latently infected cells. In addition, I could demonstrate that the putative viral recombinase U94 and the cellular recombinase Rad51 are not necessary for HHV-6A integration into host telomeres. Further studies will be performed to investigate if this is a cell type dependent effect.

# 10 Zusammenfassung

Das Humane Herpesvirus 6 (HHV-6) gehört zu den Betaherpesviren und ist eng verwandt mit dem humanen Cytomegalievirus. HHV-6 verursacht die Kinderkrankheit *Roseola Infantum* und hat eine weltweite Seroprävalenz von über 90 %. Nach überstandener Primärinfektion kann HHV-6 im Wirt eine persistierende Infektion ausbilden, die sich durch lebenslange Latenz des Virus in Knochenmark-Vorläuferzellen, Monozyten und Makrophagen auszeichnet. Eine Reaktivierung des Virus tritt häufig bei immunsupprimierten Patienten auf und wird in diesen Fällen mit Krankheitsbildern wie Enzephalitis, Multipler Sklerose, Transplantatabstoßung und einem schnelleren Vorschreiten von HIV zu AIDS in Verbindung gebracht. Es wurde gezeigt, dass HHV-6 sein genetisches Material in die Telomere von humanen Chromosomen einbauen kann. Dieser Mechanismus erlaubt die vertikale Übertragung des Virus durch die Keimbahn, was dazu führt, dass in betroffenen Individuen das integrierte Virus in jeder Körperzelle vorzufinden ist. Dieser Zustand wird als chromosomal integriertes HHV-6 (ciHHV-6) bezeichnet und kann in circa 1 % der Weltbevölkerung nachgewiesen werden. Bis heute sind der Integrationsmechanismus, sowie die benötigten Faktoren gänzlich unbekannt.

Interessanterweise besitzen HHV-6 und einige andere Herpesviren Telomersequenzen (TMRs) an ihren Genomenden, die identisch mit den Sequenzen humaner Telomere sind. In HHV-6 werden diese als perfekte TMRs (pTMRs) und nicht-perfekte TMRs (impTMRs) bezeichnet und es wird angenommen, dass sie homologe Rekombination zwischen Virus und Wirt ermöglichen. Des Weiteren kodiert HHV-6 für das Gen *U94*, das alle konservierten Domänen der Rekombinase Rep des Adeno-assoziierten Virus 2 (AAV-2) aufweist. Die Expression von U94 konnte nachweislich die Replikation eines Rep-defizienten AAV-2 wiederherstellen, was darauf hindeutet, dass beide Proteine vergleichbare Funktionen ausüben. In der Tat wurde vor kurzem gezeigt, dass U94 *in vitro* DNA-bindungs-, ATPase-, Helikase- und Exonuklease-Aktivitäten besitzt, wie sie auch für Rep beschrieben ist. Die tatsächliche Rolle dieser beiden viralen Faktoren im Verlauf der Integration von HHV-6 ist aber immer noch ungeklärt.

Um die Funktion der TMRs während der HHV-6 Integration aufzuschlüsseln, wurden beide TMR Sequenzen, entweder einzeln oder gleichzeitig, in einem bakteriellen artifiziellen Chromosom (BAC) des HHV-6A mit Hilfe der *en passant* Mutagenese Methode beseitigt. Da die Virus-Rekonstitution sehr anspruchsvoll ist, habe ich es mir zur Aufgabe gemacht, die nukleären Domänen 10 (ND10) zu zerstören, die an der zellulären antiviralen Abwehr beteiligt sind, um dadurch eine effizientere Rekonstitution zu bewerkstelligen. Mit Hilfe lentiviraler Transduktion von shRNAs konnten die Hauptkomponenten der ND10s PML, hDaxx und Sp100 in der T-Zelllinie JJHan (ND10KD) herunterreguliert werden; dies führte zu einer gesteigerten Replikation von

HHV-6A. Nach erfolgreicher Rekonstitution in ND10KD Zellen, replizierten die TMR Mutanten vergleichbar mit dem Ursprungsvirus (wt), was dafür spricht, dass die TMR Sequenzen nicht zwingend notwendig für die Replikation von HHV-6A sind. Um die Integrationseigenschaften der rekombinanten Viren zu untersuchen, habe ich ein *in vitro* Latenzsystem entwickelt, dass es mir ermöglicht die Integrationseffizienz, sowie den Erhalt des viralen Genoms in latent infizierten U2OS Zellen zu analysieren. Fluoreszenz *in situ* Hybridisierungs-Analysen (FISH) zeigten, dass die Integration der TMR Mutanten stark beeinträchtigt war im Vergleich zum Wildtyp Virus. Das Genom der TMR Mutanten wurde in den latent infizierten Zellen nur unzureichend erhalten, was dafür spricht, dass Integration essenziell für den Erhalt des Virusgenoms ist.

Um Aufschluss über die Rolle der vermeintlichen Rekombinase zu erhalten, wurde zudem der offene Leserahmen von *U94* gänzlich aus dem HHV-6A BAC beseitigt oder die Proteinexpression durch das Einfügen eines verfrühten Stopkodons außer Kraft gesetzt. Die resultierenden U94 Mutanten zeigten in meinen Integrationsanalysen einen vergleichbaren Phänotyp wie das Wildtyp Virus. Dies deutet darauf hin, dass U94 nicht essentiell für die Integration von HHV-6A ist. Zusätzlich zeigte auch eine Inhibierung der zellulären Rekombinase Rad51, mit Hilfe eines spezifischen Hemmstoffes, keine signifikanten Unterschiede im Bezug auf die Integrationsfrequenzen meiner Viren. Diese Ergebnisse legen nahe, dass es weitere zelluläre oder virale Rekombinasen gibt, die an der Integration von HHV-6A beteiligt sind. Des Weiteren wurden für alle Mutanten klonale Zelllinien angezüchtet, die das integrierte HHV-6A (iHHV-6) beinhalten, um weiterführende Versuche zur Bestimmung der Integrationsstellen und der Reaktivierungseigenschaften durchzuführen.

Zusammenfassend zeigen meine Ergebnisse, dass die TMR Sequenzen von HHV-6A für virale Replikation verzichtbar sind, aber unerlässlich für Integration und Genomerhalt. Die vermeintliche HHV-6 Rekombinase U94, sowie die zelluläre Rekombinase Rad51 spielen in U2OS Zellen keine zentrale Rolle während der Telomer-Integration von HHV-6A; ob dies nur ein Zelltyp-spezifischer Effekt ist, werden weitere Untersuchungen zeigen.

# 11 References


1. Aswad, A. and A. Katzourakis, *The first endogenous herpesvirus, identified in the tarsier genome, and novel sequences from primate rhadinoviruses and lymphocryptoviruses.* PLoS Genet, 2014. **10**(6): p. e1004332.

2. Feschotte, C. and C. Gilbert, *Endogenous viruses: insights into viral evolution and impact on host biology.* Nat Rev Genet, 2012. **13**(4): p. 283-96.

3. Aiewsakun, P. and A. Katzourakis, *Endogenous viruses: Connecting recent and ancient viral evolution.* Virology, 2015. **480**: p. 26-37.

4. Taylor, D.J. and J. Bruenn, *The evolution of novel fungal genes from non-retroviral RNA viruses.* BMC Biol, 2009. **7**(88): p. 1741-7007.

5. Koonin, E.V., *Taming of the shrewd: novel eukaryotic genes from RNA viruses*: BMC Biol. 2010 Jan 12;8:2. doi: 10.1186/1741-7007-8-2.

6. Katzourakis, A. and R.J. Gifford, *Endogenous viral elements in animal genomes.* PLoS Genet, 2010. **6**(11): p. 1001191.

7. Holmes, E.C., *The evolution of endogenous viral elements.* Cell Host Microbe, 2011. **10**(4): p. 368-77.

8. Morissette, G. and L. Flamand, *Herpesviruses and chromosomal integration.* J Virol, 2010. **84**(23): p. 12100-9.

9. Daibata, M., et al., *Inheritance of chromosomally integrated human herpesvirus 6 DNA.* Blood, 1999. **94**(5): p. 1545-9.

10. Davison, A.J., *Evolution of the herpesviruses.* Vet Microbiol, 2002. **86**(1-2): p. 69-88.

11. Fields, B.N., D.M. Knipe, and P.M. Howley, *Fields virology*2007, Philadelphia: Wolters Kluwer Health/Lippincott Williams & Wilkins.

12. Baltimore, D., *Expression of animal virus genomes.* Bacteriol Rev, 1971. **35**(3): p. 235-41.

13. Davison, A.J., et al., *A novel class of herpesvirus with bivalve hosts.* J Gen Virol, 2005. **86**(Pt 1): p. 41-53.

14. Savin, K.W., et al., *A neurotropic herpesvirus infecting the gastropod, abalone, shares ancestry with oyster herpesvirus and a herpesvirus associated with the amphioxus genome.* Virol J, 2010. **7**(308): p. 7-308.

15. Davison, A.J., et al., *The order Herpesvirales.* Arch Virol, 2009. **154**(1): p. 171-7.

16. Davison, A.J., *Herpesvirus systematics.* Vet Microbiol, 2010. **143**(1): p. 52-69.

17. Pellett, P.E., *Trunkloads of viruses.* J Virol, 2014. **88**(23): p. 13520-2.

18. Salahuddin, S.Z., et al., *Isolation of a new virus, HBLV, in patients with lymphoproliferative disorders.* Science, 1986. **234**(4776): p. 596-601.

19. Ablashi, D.V., et al., *Genomic polymorphism, growth properties, and immunologic variations in human herpesvirus-6 isolates.* Virology, 1991. **184**(2): p. 545-52.

20. Ablashi, D., et al., *Human herpesvirus-6 strain groups: a nomenclature.* Arch Virol, 1993. **129**(1-4): p. 363-366.

21. Adams, M.J. and E.B. Carstens, *Ratification vote on taxonomic proposals to the International Committee on Taxonomy of Viruses (2012).* Arch Virol, 2012. **157**(7): p. 1411-22.

22. Hall, C.B., et al., *Congenital infections with human herpesvirus 6 (HHV6) and human herpesvirus 7 (HHV7).* J Pediatr, 2004. **145**(4): p. 472-7.

23. Levy, J.A., et al., *Frequent isolation of HHV-6 from saliva and high seroprevalence of the virus in the population.* Lancet, 1990. **335**(8697): p. 1047-50.

24. Okuno, T., et al., *Seroepidemiology of human herpesvirus 6 infection in normal children and adults.* J Clin Microbiol, 1989. **27**(4): p. 651-3.

25. Zerr, D.M., et al., *A population-based study of primary human herpesvirus 6 infection.* N Engl J Med, 2005. **352**(8): p. 768-76.

26. Lusso, P. and R.C. Gallo, *Human herpesvirus 6.* Baillieres Clin Haematol, 1995. **8**(1): p. 201-23.

27. Yamanishi, K., et al., *Identification of human herpesvirus-6 as a causal agent for exanthem subitum.* Lancet, 1988. **1**(8594): p. 1065-7.

28. Hall, C.B., et al., *Human herpesvirus-6 infection in children. A prospective study of complications and reactivation.* N Engl J Med, 1994. **331**(7): p. 432-8.

29. McCullers, J.A., F.D. Lakeman, and R.J. Whitley, *Human herpesvirus 6 is associated with focal encephalitis.* Clin Infect Dis, 1995. **21**(3): p. 571-6.

30. Bates, M., et al., *Predominant human herpesvirus 6 variant A infant infections in an HIV-1 endemic region of Sub-Saharan Africa.* J Med Virol, 2009. **81**(5): p. 779-89.

31. Flamand, L., et al., *Review, part 1: Human herpesvirus-6-basic biology, diagnostic testing, and antiviral efficacy.* J Med Virol, 2010. **82**(9): p. 1560-8.

32. Caselli, E. and D. Di Luca, *Molecular biology and clinical associations of Roseoloviruses human herpesvirus 6 and human herpesvirus 7.* New Microbiol, 2007. **30**(3): p. 173-87.

33. De Bolle, L., L. Naesens, and E. De Clercq, *Update on human herpesvirus 6 biology, clinical features, and therapy.* Clin Microbiol Rev, 2005. **18**(1): p. 217-45.

34. Kosuge, H., *HHV-6, 7 and their related diseases.* J Dermatol Sci, 2000. **22**(3): p. 205-12.

35. Reynaud, J.M. and B. Horvat, *Animal models for human herpesvirus 6 infection.* Front Microbiol, 2013. **4**: p. 174.

36. Horvat, B., B.K. Berges, and P. Lusso, *Recent developments in animal models for human herpesvirus 6A and 6B.* Curr Opin Virol, 2014. **9**: p. 97-103.

37. Leibovitch, E., et al., *Novel marmoset (Callithrix jacchus) model of human Herpesvirus 6A and 6B infections: immunologic, virologic and radiologic characterization.* PLoS Pathog, 2013. **9**(1): p. e1003138.

38. Reynaud, J.M., et al., *Human herpesvirus 6A infection in CD46 transgenic mice: viral persistence in the brain and increased production of proinflammatory chemokines via Toll-like receptor 9.* J Virol, 2014. **88**(10): p. 5421-36.

39. Lusso, P., et al., *Human herpesvirus 6A accelerates AIDS progression in macaques.* Proc Natl Acad Sci U S A, 2007. **104**(12): p. 5067-72.

40. Lusso, P., et al., *In vitro susceptibility of T lymphocytes from chimpanzees (Pan troglodytes) to human herpesvirus 6 (HHV-6): a potential animal model to study the*

*interaction between HHV-6 and human immunodeficiency virus type 1 in vivo.* J Virol, 1990. **64**(6): p. 2751-8.

41. Higashi, K., et al., *Presence of antibody to human herpesvirus 6 in monkeys.* J Gen Virol, 1989. **70**(Pt 12): p. 3171-6.

42. Lacoste, V., et al., *Simian homologues of human gamma-2 and betaherpesviruses in mandrill and drill monkeys.* J Virol, 2000. **74**(24): p. 11993-9.

43. Lacoste, V., et al., *A novel homologue of Human herpesvirus 6 in chimpanzees.* J Gen Virol, 2005. **86**(Pt 8): p. 2135-40.

44. Staheli, J.P., et al., *Discovery and biological characterization of two novel pig-tailed macaque homologs of HHV-6 and HHV-7.* Virology, 2014. **471-473C**: p. 126-140.

45. Gompels, U.A., et al., *The DNA sequence of human herpesvirus-6: structure, coding content, and genome evolution.* Virology, 1995. **209**(1): p. 29-51.

46. Dominguez, G., et al., *Human herpesvirus 6B genome sequence: coding content and comparison with human herpesvirus 6A.* J Virol, 1999. **73**(10): p. 8040-52.

47. Isegawa, Y., et al., *Comparison of the complete DNA sequences of human herpesvirus 6 variants A and B.* J Virol, 1999. **73**(10): p. 8053-63.

48. Davison, A.J., D.J. Dargan, and N.D. Stow, *Fundamental and accessory systems in herpesviruses.* Antiviral Res, 2002. **56**(1): p. 1-11.

49. Stern-Ginossar, N., *Decoding viral infection by ribosome profiling.* J Virol, 2015. **89**(12): p. 6164-6.

50. Stern-Ginossar, N., et al., *Decoding human cytomegalovirus.* Science, 2012. **338**(6110): p. 1088-93.

51. Hudson, A.W., *Roseoloviruses and their modulation of host defenses.* Curr Opin Virol, 2014. **9**: p. 178-87.

52. Grinde, B., *Herpesviruses: latency and reactivation - viral strategies and host response.* J Oral Microbiol, 2013. **5**.

53. Wang, F.Z. and P.E. Pellett, *HHV-6A, 6B, and 7: immunobiology and host response*.

54. Horvat, R.T., M.J. Parmely, and B. Chandran, *Human herpesvirus 6 inhibits the proliferative responses of human peripheral blood mononuclear cells.* J Infect Dis, 1993. **167**(6): p. 1274-80.

55. Flamand, L., et al., *Immunosuppressive effect of human herpesvirus 6 on T-cell functions: suppression of interleukin-2 synthesis and cell proliferation.* Blood, 1995. **85**(5): p. 1263-71.

56. Iampietro, M., et al., *Inhibition of interleukin-2 gene expression by human herpesvirus 6B U54 tegument protein.* J Virol, 2014. **88**(21): p. 12452-63.

57. Frenkel, N., et al., *Cellular and growth-factor requirements for the replication of human herpesvirus 6 in primary lymphocyte cultures.* Adv Exp Med Biol, 1990. **278**: p. 1-8.

58. Frenkel, N., et al., *T-cell activation is required for efficient replication of human herpesvirus 6.* J Virol, 1990. **64**(9): p. 4598-602.

59. Lusso, P., et al., *In vitro cellular tropism of human B-lymphotropic virus (human herpesvirus-6).* J Exp Med, 1988. **167**(5): p. 1659-70.

60. Takahashi, K., et al., *Predominant CD4 T-lymphocyte tropism of human herpesvirus 6-related virus.* J Virol, 1989. **63**(7): p. 3161-3.

61. Dockrell, D.H., *Human herpesvirus 6: molecular biology and clinical features.* J Med Microbiol, 2003. **52**(Pt 1): p. 5-18.

62. Everett, R.D., *The use of fluorescence microscopy to study the association between herpesviruses and intrinsic resistance factors.* Viruses, 2011. **3**(12): p. 2412-24.

63. Everett, R.D., *Interactions between DNA viruses, ND10 and the DNA damage response.* Cell Microbiol, 2006. **8**(3): p. 365-74.

64. Tavalai, N. and T. Stamminger, *New insights into the role of the subnuclear structure ND10 for viral infection.* Biochim Biophys Acta, 2008. **11**(21): p. 16.

65. Everett, R.D. and M.K. Chelbi-Alix, *PML and PML nuclear bodies: implications in antiviral defence.* Biochimie, 2007. **89**(6-7): p. 819-30.

66. Maul, G.G., *Nuclear domain 10, the site of DNA virus transcription and replication.* Bioessays, 1998. **20**(8): p. 660-7.

67. Tavalai, N. and T. Stamminger, *Interplay between Herpesvirus Infection and Host Defense by PML Nuclear Bodies.* Viruses, 2009. **1**(3): p. 1240-64.

68. Tavalai, N. and T. Stamminger, *Intrinsic cellular defense mechanisms targeting human cytomegalovirus.* Virus Res, 2011. **157**(2): p. 128-33.

69. Ishov, A.M., et al., *PML is critical for ND10 formation and recruits the PML-interacting protein daxx to this nuclear structure when modified by SUMO-1.* J Cell Biol, 1999. **147**(2): p. 221-34.

70. Glass, M. and R.D. Everett, *Components of promyelocytic leukemia nuclear bodies (ND10) act cooperatively to repress herpesvirus infection.* J Virol, 2013. **87**(4): p. 2174-85.

71. Stanton, R., et al., *Analysis of the human herpesvirus-6 immediate-early 1 protein.* J Gen Virol, 2002. **83**(Pt 11): p. 2811-20.

72. Gravel, A., J. Gosselin, and L. Flamand, *Human Herpesvirus 6 immediate-early 1 protein is a sumoylated nuclear phosphoprotein colocalizing with promyelocytic leukemia protein-associated nuclear bodies.* J Biol Chem, 2002. **277**(22): p. 19679-87.

73. Kofod-Olsen, E., et al., *Human herpesvirus 6B U19 protein is a PML-regulated transcriptional activator that localizes to nuclear foci in a PML-independent manner.* J Gen Virol, 2008. **89**(Pt 1): p. 106-16.

74. Santoro, F., et al., *CD46 is a cellular receptor for human herpesvirus 6.* Cell, 1999. **99**(7): p. 817-27.

75. Maeki, T. and Y. Mori, *Features of Human Herpesvirus-6A and -6B Entry.* Adv Virol, 2012. **384069**(10): p. 23.

76. Tang, H., et al., *CD134 is a cellular receptor specific for human herpesvirus-6B entry.* Proc Natl Acad Sci U S A, 2013. **110**(22): p. 9096-9.

77. Boehmer, P.E. and A.V. Nimonkar, *Herpes virus replication.* IUBMB Life, 2003. **55**(1): p. 13-22.

78. Rutkowski, A.J., et al., *Widespread disruption of host transcription termination in HSV-1 infection.* Nat Commun, 2015. **6**(7126).

79. Krug, L.T. and P.E. Pellett, *Roseolovirus molecular biology: recent advances.* Curr Opin Virol, 2014. **9C**: p. 170-177.

80. Thomson, B.J., S. Dewhurst, and D. Gray, *Structure and heterogeneity of the a sequences of human herpesvirus 6 strain variants U1102 and Z29 and identification of human telomeric repeat sequences at the genomic termini.* J Virol, 1994. **68**(5): p. 3007-14.

81. Liu, X.F., et al., *Epigenetic control of cytomegalovirus latency and reactivation.* Viruses, 2013. **5**(5): p. 1325-45.

82. Pfeffer, S., et al., *Identification of virus-encoded microRNAs.* Science, 2004. **304**(5671): p. 734-6.

83. Cullen, B.R., *Herpesvirus microRNAs: phenotypes and functions.* Curr Opin Virol, 2011. **1**(3): p. 211-5.

84. Skalsky, R.L. and B.R. Cullen, *Viruses, microRNAs, and host interactions.* Annu Rev Microbiol, 2010. **64**: p. 123-41.

85. Murphy, E., et al., *Suppression of immediate-early viral gene expression by herpesvirus-coded microRNAs: implications for latency.* Proc Natl Acad Sci U S A, 2008. **105**(14): p. 5453-8.

86. Tuddenham, L., et al., *Small RNA deep sequencing identifies microRNAs and other small noncoding RNAs from human herpesvirus 6B.* J Virol, 2012. **86**(3): p. 1638-49.

87. Nukui, M., Y. Mori, and E.A. Murphy, *A human herpesvirus 6A-encoded microRNA: role in viral lytic replication.* J Virol, 2015. **89**(5): p. 2615-27.

88. Kondo, K., et al., *Latent human herpesvirus 6 infection of human monocytes/macrophages.* J Gen Virol, 1991. **72 ( Pt 6)**: p. 1401-8.

89. Luppi, M., et al., *Human herpesvirus 6 latently infects early bone marrow progenitors in vivo.* J Virol, 1999. **73**(1): p. 754-9.

90. Yasukawa, M., et al., *Latent infection and reactivation of human herpesvirus 6 in two novel myeloid cell lines.* Blood, 1999. **93**(3): p. 991-9.

91. Yoshikawa, T., et al., *Latent infection of human herpesvirus 6 in astrocytoma cell line and alteration of cytokine synthesis.* J Med Virol, 2002. **66**(4): p. 497-505.

92. Ahlqvist, J., et al., *Differential tropism of human herpesvirus 6 (HHV-6) variants and induction of latency by HHV-6A in oligodendrocytes.* J Neurovirol, 2005. **11**(4): p. 384-94.

93. Kondo, K. and K. Yamanishi, *HHV-6A, 6B, and 7: molecular basis of latency and reactivation*, in *Human Herpesviruses: Biology, Therapy, and Immunoprophylaxis*, A. Arvin, et al., Editors. 2007: Cambridge.

94. Kondo, K., et al., *Identification of human herpesvirus 6 latency-associated transcripts.* J Virol, 2002. **76**(8): p. 4145-51.

95. Kondo, K., et al., *Recognition of a novel stage of betaherpesvirus latency in human herpesvirus 6.* J Virol, 2003. **77**(3): p. 2258-64.

96. Rotola, A., et al., *U94 of human herpesvirus 6 is expressed in latently infected peripheral blood mononuclear cells and blocks viral gene expression in transformed lymphocytes in culture.* Proc Natl Acad Sci U S A, 1998. **95**(23): p. 13911-6.

97. Luppi, M., et al., *Three cases of human herpesvirus-6 latent infection: integration of viral genome in peripheral blood mononuclear cell DNA.* J Med Virol, 1993. **40**(1): p. 44-52.

98. Torelli, G., et al., *Targeted integration of human herpesvirus 6 in the p arm of chromosome 17 of human peripheral blood mononuclear cells in vivo.* J Med Virol, 1995. **46**(3): p. 178-88.

99. Daibata, M., et al., *Integration of human herpesvirus 6 in a Burkitt's lymphoma cell line.* Br J Haematol, 1998. **102**(5): p. 1307-13.

100. Nacheva, E.P., et al., *Human herpesvirus 6 integrates within telomeric regions as evidenced by five different chromosomal sites.* J Med Virol, 2008. **80**(11): p. 1952-8.

101. Arbuckle, J.H., et al., *The latent human herpesvirus-6A genome specifically integrates in telomeres of human chromosomes in vivo and in vitro.* Proc Natl Acad Sci U S A, 2010. **107**(12): p. 5563-8.

102. Osterrieder, N., N. Wallaschek, and B.B. Kaufer, *Herpesvirus Genome Integration into Telomeric Repeats of Host Cell Chromosomes.* Annual Review of Virology, 2014. **1**(1): p. 215-235.

103. Henderson, A., et al., *Chromosome site for Epstein-Barr virus DNA in a Burkitt tumor cell line and in lymphocytes growth-transformed in vitro.* Proc Natl Acad Sci U S A, 1983. **80**(7): p. 1987-91.

104. Matsuo, T., et al., *Persistence of the entire Epstein-Barr virus genome integrated into human lymphocyte DNA.* Science, 1984. **226**(4680): p. 1322-5.

105. Delecluse, H.J. and W. Hammerschmidt, *Status of Marek's disease virus in established lymphoma cell lines: herpesvirus integration is common.* J Virol, 1993. **67**(1): p. 82-92.

106. Delecluse, H.J., S. Schuller, and W. Hammerschmidt, *Latent Marek's disease virus can be activated from its chromosomally integrated state in herpesvirus-transformed lymphoma cells.* EMBO J, 1993. **12**(8): p. 3277-86.

107. Ohye, T., et al., *Dual roles for the telomeric repeats in chromosomally integrated human herpesvirus-6.* Sci Rep, 2014. **4**: p. 4559.

108. Prusty, B.K., G. Krohne, and T. Rudel, *Reactivation of chromosomally integrated human herpesvirus-6 by telomeric circle formation.* PLoS Genet, 2013. **9**(12): p. e1004033.

109. Huang, Y., et al., *Human telomeres that carry an integrated copy of human herpesvirus 6 are often short and unstable, facilitating release of the viral genome from the chromosome.* Nucleic Acids Res, 2014. **42**(1): p. 315-27.

110. Arbuckle, J.H. and P.G. Medveczky, *The molecular biology of human herpesvirus-6 latency and telomere integration.* Microbes Infect, 2011. **13**(8-9): p. 731-41.

111. Klobutcher, L.A., et al., *All gene-sized DNA molecules in four species of hypotrichs have the same terminal sequence and an unusual 3' terminus.* Proc Natl Acad Sci U S A, 1981. **78**(5): p. 3015-9.

112. Runge, K.W. and V.A. Zakian, *Introduction of extra telomeric DNA sequences into Saccharomyces cerevisiae results in telomere elongation.* Mol Cell Biol, 1989. **9**(4): p. 1488-97.

113. Delany, M.E., et al., *Telomeres in the chicken: genome stability and chromosome ends.* Poult Sci, 2003. **82**(6): p. 917-26.

114. Kipling, D. and H.J. Cooke, *Hypervariable ultra-long telomeres in mice.* Nature, 1990. **347**(6291): p. 400-2.

115. de Lange, T., et al., *Structure and variability of human chromosome ends.* Mol Cell Biol, 1990. **10**(2): p. 518-27.

116. Martinez, P. and M.A. Blasco, *Telomeric and extra-telomeric roles for telomerase and the telomere-binding proteins.* Nat Rev Cancer, 2011. **11**(3): p. 161-76.

117. Blasco, M.A., *Telomeres and human disease: ageing, cancer and beyond.* Nat Rev Genet, 2005. **6**(8): p. 611-22.

118. Samassekou, O., et al., *Sizing the ends: normal length of human telomeres.* Ann Anat, 2010. **192**(5): p. 284-91.

119. Greider, C.W., *Telomeres do D-loop-T-loop.* Cell, 1999. **97**(4): p. 419-22.

120. Gilson, E. and V. Geli, *How telomeres are replicated.* Nat Rev Mol Cell Biol, 2007. **8**(10): p. 825-38.

121. Hayflick, L. and P.S. Moorhead, *The serial cultivation of human diploid cell strains.* Exp Cell Res, 1961. **25**: p. 585-621.

122. Hayflick, L., *The Limited in Vitro Lifetime of Human Diploid Cell Strains.* Exp Cell Res, 1965. **37**: p. 614-36.

123. Capper, R., et al., *The nature of telomere fusion and a definition of the critical telomere length in human cells.* Genes Dev, 2007. **21**(19): p. 2495-508.

124. Hemann, M.T., et al., *The shortest telomere, not average telomere length, is critical for cell viability and chromosome stability.* Cell, 2001. **107**(1): p. 67-77.

125. der-Sarkissian, H., et al., *The shortest telomeres drive karyotype evolution in transformed cells.* Oncogene, 2004. **23**(6): p. 1221-8.

126. Draskovic, I. and A. Londono Vallejo, *Telomere recombination and alternative telomere lengthening mechanisms.* Front Biosci (Landmark Ed), 2013. **18**: p. 1-20.

127. Gocha, A.R., J. Harris, and J. Groden, *Alternative mechanisms of telomere lengthening: permissive mutations, DNA repair proteins and tumorigenic progression.* Mutat Res, 2013. **743-744**: p. 142-50.

128. Durant, S.T., *Telomerase-independent paths to immortality in predictable cancer subtypes.* J Cancer, 2012. **3**: p. 67-82.

129. Cesare, A.J. and R.R. Reddel, *Alternative lengthening of telomeres: models, mechanisms and implications.* Nat Rev Genet, 2010. **11**(5): p. 319-30.

130. Dunham, M.A., et al., *Telomere maintenance by recombination in human cells.* Nat Genet, 2000. **26**(4): p. 447-50.

131. Daibata, M., et al., *Chromosomal transmission of human herpesvirus 6 DNA in acute lymphoblastic leukaemia.* Lancet, 1998. **352**(9127): p. 543-4.

132. Arbuckle, J.H., et al., *Mapping the telomere integrated genome of human herpesvirus 6A and 6B.* Virology, 2013. **442**(1): p. 3-11.

133. Mori, T., et al., *Transmission of chromosomally integrated human herpesvirsus 6 (HHV-6) variant A from a parent to children leading to misdiagnosis of active HHV-6 infection.* Transpl Infect Dis, 2009. **11**(6): p. 503-6.

134. Tanaka-Taya, K., et al., *Human herpesvirus 6 (HHV-6) is transmitted from parent to child in an integrated form and characterization of cases with chromosomally integrated HHV-6 DNA.* J Med Virol, 2004. **73**(3): p. 465-73.

135. Kuhl, U., et al., *Chromosomally integrated human herpesvirus 6 in heart failure: prevalence and treatment.* Eur J Heart Fail, 2014.

136. Leong, H.N., et al., *The prevalence of chromosomally integrated human herpesvirus 6 genomes in the blood of UK blood donors.* J Med Virol, 2007. **79**(1): p. 45-51.

137. Ward, K.N., et al., *Human herpesvirus 6 DNA levels in cerebrospinal fluid due to primary infection differ from those due to chromosomal viral integration and have implications for diagnosis of encephalitis.* J Clin Microbiol, 2007. **45**(4): p. 1298-304.

138. Potenza, L., et al., *Prevalence of human herpesvirus-6 chromosomal integration (CIHHV-6) in Italian solid organ and allogeneic stem cell transplant patients.* Am J Transplant, 2009. **9**(7): p. 1690-7.

139. Hubacek, P., et al., *Prevalence of HHV-6 integrated chromosomally among children treated for acute lymphoblastic or myeloid leukemia in the Czech Republic.* J Med Virol, 2009. **81**(2): p. 258-63.

140. Lee, S.O., et al., *Chromosomally integrated human herpesvirus-6 in kidney transplant recipients.* Nephrol Dial Transplant, 2011. **26**(7): p. 2391-3.

141. Pellett, P.E., et al., *Chromosomally integrated human herpesvirus 6: questions and answers.* Rev Med Virol, 2012. **22**(3): p. 144-55.

142. Morris, C., et al., *Fine mapping of an apparently targeted latent human herpesvirus type 6 integration site in chromosome band 17p13.3.* J Med Virol, 1999. **58**(1): p. 69-75.

143. Clark, D.A., et al., *Transmission of integrated human herpesvirus 6 through stem cell transplantation: implications for laboratory diagnosis.* J Infect Dis, 2006. **193**(7): p. 912-6.

144. Watanabe, H., et al., *Chromosomal integration of human herpesvirus 6 DNA in anticonvulsant hypersensitivity syndrome.* Br J Dermatol, 2008. **158**(3): p. 640-2.

145. Daibata, M., et al., *Lymphoblastoid cell lines with integrated human herpesvirus type 6.* J Hum Virol, 1998. **1**(7): p. 475-81.

146. Ward, K.N., et al., *Human herpesvirus 6 chromosomal integration in immunocompetent patients results in high levels of viral DNA in blood, sera, and hair follicles.* J Clin Microbiol, 2006. **44**(4): p. 1571-4.

147. Hubacek, P., et al., *HHV-6 DNA throughout the tissues of two stem cell transplant patients with chromosomally integrated HHV-6 and fatal CMV pneumonitis.* Br J Haematol, 2009. **145**(3): p. 394-8.

148. Hall, C.B., et al., *Chromosomal integration of human herpesvirus 6 is the major mode of congenital human herpesvirus 6 infection.* Pediatrics, 2008. **122**(3): p. 513-20.

149. Hubacek, P., et al., *Failure of multiple antivirals to affect high HHV-6 DNAaemia resulting from viral chromosomal integration in case of severe aplastic anaemia.* Haematologica, 2007. **92**(10): p. e98-e100.

150. Sato, K., et al., *Chromosomally integrated human herpesvirus-6 requiring differential diagnosis of reactivation after allogeneic hematopoietic stem cell transplantation.* Rinsho Ketsueki, 2015. **56**(4): p. 406-11.

151. Sedlak, R.H., et al., *Identification of chromosomally integrated human herpesvirus 6 by droplet digital PCR.* Clin Chem, 2014. **60**(5): p. 765-72.

152. Pantry, S.N., et al., *Persistent human herpesvirus-6 infection in patients with an inherited form of the virus.* J Med Virol, 2013. **85**(11): p. 1940-6.

153. Gravel, A., et al., *Inherited chromosomally integrated human herpesvirus 6 as a predisposing risk factor for the development of angina pectoris.* Proc Natl Acad Sci U S A, 2015. **112**(26): p. 8058-63.

154. Lee, S.O., R.A. Brown, and R.R. Razonable, *Clinical significance of pretransplant chromosomally integrated human herpesvirus-6 in liver transplant recipients.* Transplantation, 2011. **92**(2): p. 224-9.

155. Montoya, J.G., et al., *Antiviral therapy of two patients with chromosomally-integrated human herpesvirus-6A presenting with cognitive dysfunction.* J Clin Virol, 2012. **55**(1): p. 40-5.

156. Strenger, V., et al., *Detection of HHV-6-specific mRNA and antigens in PBMCs of individuals with chromosomally integrated HHV-6 (ciHHV-6).* Clin Microbiol Infect, 2014. **20**(10): p. 1027-32.

157. Endo, A., et al., *Molecular and virological evidence of viral activation from chromosomally integrated human herpesvirus 6A in a patient with X-linked severe combined immunodeficiency.* Clin Infect Dis, 2014. **59**(4): p. 545-8.

158. Kobayashi, D., et al., *Quantitation of human herpesvirus-6 (HHV-6) DNA in a cord blood transplant recipient with chromosomal integration of HHV-6.* Transpl Infect Dis, 2011. **13**(6): p. 650-3.

159. Troy, S.B., et al., *Severe encephalomyelitis in an immunocompetent adult with chromosomally integrated human herpesvirus 6 and clinical response to treatment with foscarnet plus ganciclovir.* Clin Infect Dis, 2008. **47**(12): p. e93-6.

160. Wittekindt, B., et al., *Human herpes virus-6 DNA in cerebrospinal fluid of children undergoing therapy for acute leukaemia.* Br J Haematol, 2009. **145**(4): p. 542-5.

161. Gravel, A., C.B. Hall, and L. Flamand, *Sequence analysis of transplacentally acquired human herpesvirus 6 DNA is consistent with transmission of a chromosomally integrated reactivated virus.* J Infect Dis, 2013. **207**(10): p. 1585-9.

162. Hall, C.B., et al., *Transplacental congenital human herpesvirus 6 infection caused by maternal chromosomally integrated virus.* J Infect Dis, 2010. **201**(4): p. 505-7.

163. Gompels, U.A. and H.A. Macaulay, *Characterization of human telomeric repeat sequences from human herpesvirus 6 and relationship to replication.* J Gen Virol, 1995. **76 ( Pt 2)**: p. 451-8.

164. Achour, A., et al., *Length variability of telomeric repeat sequences of human herpesvirus 6 DNA.* J Virol Methods, 2009. **159**(1): p. 127-30.

165. Kishi, M., et al., *A repeat sequence, GGGTTA, is shared by DNA of human herpesvirus 6 and Marek's disease virus.* J Virol, 1988. **62**(12): p. 4824-7.

166. Kaufer, B.B., K.W. Jarosinski, and N. Osterrieder, *Herpesvirus telomeric repeats facilitate genomic integration into host telomeres and mobilization of viral DNA during reactivation.* J Exp Med, 2011. **208**(3): p. 605-15.

167. Greco, A., et al., *Role of the Short Telomeric Repeat Region in Marek's Disease Virus Replication, Genomic Integration, and Lymphomagenesis.* J Virol, 2014. **88**(24): p. 14138-47.

168. Okazaki, S., H. Ishikawa, and H. Fujiwara, *Structural analysis of TRAS1, a novel family of telomeric repeat-associated retrotransposons in the silkworm, Bombyx mori.* Mol Cell Biol, 1995. **15**(8): p. 4545-52.

169. Anzai, T., H. Takahashi, and H. Fujiwara, *Sequence-specific recognition and cleavage of telomeric repeat (TTAGG)(n) by endonuclease of non-long terminal repeat retrotransposon TRAS1.* Mol Cell Biol, 2001. **21**(1): p. 100-8.

170. Rapp, J.C., et al., *U94, the human herpesvirus 6 homolog of the parvovirus nonstructural gene, is highly conserved among isolates and is expressed at low mRNA levels as a spliced transcript.* Virology, 2000. **268**(2): p. 504-16.

171. Thomson, B.J., S. Efstathiou, and R.W. Honess, *Acquisition of the human adeno-associated virus type-2 rep gene by human herpesvirus type-6.* Nature, 1991. **351**(6321): p. 78-80.

172. Im, D.S. and N. Muzyczka, *The AAV origin binding protein Rep68 is an ATP-dependent site-specific endonuclease with DNA helicase activity.* Cell, 1990. **61**(3): p. 447-57.

173. Im, D.S. and N. Muzyczka, *Factors that bind to adeno-associated virus terminal repeats.* J Virol, 1989. **63**(7): p. 3095-104.

174. Hickman, A.B., et al., *The nuclease domain of adeno-associated virus rep coordinates replication initiation using two distinct DNA recognition interfaces.* Mol Cell, 2004. **13**(3): p. 403-14.

175. Surosky, R.T., et al., *Adeno-associated virus Rep proteins target DNA sequences to a unique locus in the human genome.* J Virol, 1997. **71**(10): p. 7951-9.

176. Tratschin, J.D., J. Tal, and B.J. Carter, *Negative and positive regulation in trans of gene expression from adeno-associated virus vectors in mammalian cells by a viral rep gene product.* Mol Cell Biol, 1986. **6**(8): p. 2884-94.

177. Linden, R.M., E. Winocour, and K.I. Berns, *The recombination signals for adeno-associated virus site-specific integration.* Proc Natl Acad Sci U S A, 1996. **93**(15): p. 7966-72.

178. Im, D.S. and N. Muzyczka, *Partial purification of adeno-associated virus Rep78, Rep52, and Rep40 and their biochemical characterization.* J Virol, 1992. **66**(2): p. 1119-28.

179. Thomson, B.J., et al., *Human herpesvirus 6 (HHV-6) is a helper virus for adeno-associated virus type 2 (AAV-2) and the AAV-2 rep gene homologue in HHV-6 can mediate AAV-2 DNA replication and regulate gene expression.* Virology, 1994. **204**(1): p. 304-11.

180. Walker, S.L., R.S. Wonderling, and R.A. Owens, *Mutational analysis of the adeno-associated virus Rep68 protein: identification of critical residues necessary for site-specific endonuclease activity.* J Virol, 1997. **71**(4): p. 2722-30.

181. Walker, S.L., R.S. Wonderling, and R.A. Owens, *Mutational analysis of the adeno-associated virus type 2 Rep68 protein helicase motifs.* J Virol, 1997. **71**(9): p. 6996-7004.

182. Dhepakson, P., et al., *Human herpesvirus-6 rep/U94 gene product has single-stranded DNA-binding activity.* J Gen Virol, 2002. **83**(Pt 4): p. 847-54.

183. Trempe, F., et al., *Characterization of human herpesvirus 6A/B U94 as ATPase, helicase, exonuclease and DNA-binding proteins.* Nucleic Acids Res, 2015. **43**(12): p. 6084-98.

184. Turner, S., D. DiLuca, and U. Gompels, *Characterisation of a human herpesvirus 6 variant A 'amplicon' and replication modulation by U94-Rep 'latency gene'.* J Virol Methods, 2002. **105**(2): p. 331-41.

185. Mori, Y., et al., *Expression of human herpesvirus 6B rep within infected cells and binding of its gene product to the TATA-binding protein in vitro and in vivo.* J Virol, 2000. **74**(13): p. 6096-104.

186. Araujo, J.C., et al., *Human herpesvirus 6A ts suppresses both transformation by H-ras and transcription by the H-ras and human immunodeficiency virus type 1 promoters.* J Virol, 1995. **69**(8): p. 4933-40.

187. Araujo, J.C., et al., *Cell lines containing and expressing the human herpesvirus 6A ts gene are protected from both H-ras and BPV-1 transformation.* Oncogene, 1997. **14**(8): p. 937-43.

188. Caselli, E., et al., *Human herpesvirus 6 (HHV-6) U94/REP protein inhibits betaherpesvirus replication.* Virology, 2006. **346**(2): p. 402-14.

189. Borenstein, R. and N. Frenkel, *Cloning human herpes virus 6A genome into bacterial artificial chromosomes and study of DNA replication intermediates.* Proc Natl Acad Sci U S A, 2009. **106**(45): p. 19138-43.

190. Borenstein, R., H. Zeigerman, and N. Frenkel, *The DR1 and DR6 first exons of human herpesvirus 6A are not required for virus replication in culture and are deleted in virus stocks that replicate well in T-cell lines.* J Virol, 2010. **84**(6): p. 2648-56.

191. Tang, H., et al., *Human herpesvirus 6 encoded glycoprotein Q1 gene is essential for virus growth.* Virology, 2010. **407**(2): p. 360-7.

192. Tischer, B.K., G.A. Smith, and N. Osterrieder, *En passant mutagenesis: a two step markerless red recombination system.* Methods Mol Biol, 2010. **634**: p. 421-30.

193. Tischer, B.K., et al., *Two-step red-mediated recombination for versatile high-efficiency markerless DNA manipulation in Escherichia coli.* Biotechniques, 2006. **40**(2): p. 191-7.

194. Shizuya, H., et al., *Cloning and stable maintenance of 300-kilobase-pair fragments of human DNA in Escherichia coli using an F-factor-based vector.* Proc Natl Acad Sci U S A, 1992. **89**(18): p. 8794-7.

195. Messerle, M., et al., *Cloning and mutagenesis of a herpesvirus genome as an infectious bacterial artificial chromosome.* Proc Natl Acad Sci U S A, 1997. **94**(26): p. 14759-63.

196. Murphy, K.C., *Use of bacteriophage lambda recombination functions to promote gene replacement in Escherichia coli.* J Bacteriol, 1998. **180**(8): p. 2063-71.

197. Zagursky, R.J. and J.B. Hays, *Expression of the phage lambda recombination genes exo and bet under lacPO control on a multi-copy plasmid.* Gene, 1983. **23**(3): p. 277-92.

198. Yu, D., et al., *An efficient recombination system for chromosome engineering in Escherichia coli.* Proc Natl Acad Sci U S A, 2000. **97**(11): p. 5978-83.

199. Sakaki, Y., et al., *Purification and properties of the gamma-protein specified by bacteriophage lambda: an inhibitor of the host RecBC recombination enzyme.* Proc Natl Acad Sci U S A, 1973. **70**(8): p. 2215-9.

200. Little, J.W., *An exonuclease induced by bacteriophage lambda. II. Nature of the enzymatic reaction.* J Biol Chem, 1967. **242**(4): p. 679-86.

201. Wu, Z., et al., *Domain structure and DNA binding regions of beta protein from bacteriophage lambda.* J Biol Chem, 2006. **281**(35): p. 25205-14.

202. Kmiec, E. and W.K. Holloman, *Beta protein of bacteriophage lambda promotes renaturation of DNA.* J Biol Chem, 1981. **256**(24): p. 12636-9.

203. Lee, E.C., et al., *A highly efficient Escherichia coli-based chromosome engineering system adapted for recombinogenic targeting and subcloning of BAC DNA.* Genomics, 2001. **73**(1): p. 56-65.

204. Colleaux, L., et al., *Universal code equivalent of a yeast mitochondrial intron reading frame is expressed into E. coli as a specific double strand endonuclease.* Cell, 1986. **44**(4): p. 521-33.

205. Yeo, W.M., Y. Isegawa, and V.T. Chow, *The U95 protein of human herpesvirus 6B interacts with human GRIM-19: silencing of U95 expression reduces viral load and abrogates loss of mitochondrial membrane potential.* J Virol, 2008. **82**(2): p. 1011-20.

206. Takemoto, M., et al., *The R3 region, one of three major repetitive regions of human herpesvirus 6, is a strong enhancer of immediate-early gene U95.* J Virol, 2001. **75**(21): p. 10149-60.

207. San Filippo, J., P. Sung, and H. Klein, *Mechanism of eukaryotic homologous recombination.* Annu Rev Biochem, 2008. **77**: p. 229-57.

208. Budke, B., et al., *RI-1: a chemical inhibitor of RAD51 that disrupts homologous recombination in human cells.* Nucleic Acids Res, 2012. **40**(15): p. 7347-57.

209. Kaufer, B.B. and L. Flamand, *Chromosomally integrated HHV-6: impact on virus, cell and organismal biology.* Curr Opin Virol, 2014. **9C**: p. 111-118.

210. Osterrieder, N., et al., *Marek's disease virus: from miasma to model.* Nat Rev Microbiol, 2006. **4**(4): p. 283-94.

211. Frenkel, N., et al., *Isolation of a new herpesvirus from human CD4+ T cells.* Proc Natl Acad Sci U S A, 1990. **87**(2): p. 748-52.

212. Black, J.B. and P.E. Pellett, *Human herpesvirus 7.* Rev Med Virol, 1999. **9**(4): p. 245-62.

213. Megaw, A.G., et al., *The DNA sequence of the RK strain of human herpesvirus 7.* Virology, 1998. **244**(1): p. 119-32.

214. Secchiero, P., et al., *Identification of human telomeric repeat motifs at the genome termini of human herpesvirus 7: structural analysis and heterogeneity.* J Virol, 1995. **69**(12): p. 8041-5.

215. Nicholas, J., *Determination and analysis of the complete nucleotide sequence of human herpesvirus.* J Virol, 1996. **70**(9): p. 5975-89.

216. Lusso, P., et al., *CD4 is a critical component of the receptor for human herpesvirus 7: interference with human immunodeficiency virus.* Proc Natl Acad Sci U S A, 1994. **91**(9): p. 3872-6.

217. van Cleef, K.W., et al., *The rat cytomegalovirus homologue of parvoviral rep genes, r127, encodes a nuclear protein with single- and double-stranded DNA-binding activity that is dispensable for virus replication.* J Gen Virol, 2004. **85**(Pt 7): p. 2001-13.

218. Zhang, H., et al., *A novel bat herpesvirus encodes homologues of major histocompatibility complex classes I and II, C-type lectin, and a unique family of immune-related genes.* J Virol, 2012. **86**(15): p. 8014-30.

219. Potts, P.R. and H. Yu, *The SMC5/6 complex maintains telomere length in ALT cancer cells through SUMOylation of telomere-binding proteins.* Nat Struct Mol Biol, 2007. **14**(7): p. 581-90.

220. Zhong, Z.H., et al., *Disruption of telomere maintenance by depletion of the MRE11/RAD50/NBS1 complex in cells that use alternative lengthening of telomeres.* J Biol Chem, 2007. **282**(40): p. 29314-22.

221. Jiang, W.Q., et al., *Suppression of alternative lengthening of telomeres by Sp100-mediated sequestration of the MRE11/RAD50/NBS1 complex.* Mol Cell Biol, 2005. **25**(7): p. 2708-21.

222. Schumacher, A.J., et al., *The HSV-1 exonuclease, UL12, stimulates recombination by a single strand annealing mechanism.* PLoS Pathog, 2012. **8**(8): p. e1002862.

223. Balasubramanian, N., et al., *Physical interaction between the herpes simplex virus type 1 exonuclease, UL12, and the DNA double-strand break-sensing MRN complex.* J Virol, 2010. **84**(24): p. 12504-14.

224. Reuven, N.B., et al., *The herpes simplex virus type 1 alkaline nuclease and single-stranded DNA binding protein mediate strand exchange in vitro.* J Virol, 2003. **77**(13): p. 7425-33.

225. Reuven, N.B., et al., *Catalysis of strand exchange by the HSV-1 UL12 and ICP8 proteins: potent ICP8 recombinase activity is revealed upon resection of dsDNA substrate by nuclease.* J Mol Biol, 2004. **342**(1): p. 57-71.

226. Lamarche, B.J., N.I. Orazio, and M.D. Weitzman, *The MRN complex in double-strand break repair and telomere maintenance.* FEBS Lett, 2010. **584**(17): p. 3682-95.

227. Deng, Z., et al., *HSV-1 remodels host telomeres to facilitate viral replication.* Cell Rep, 2014. **9**(6): p. 2263-78.

228. Alex, M., et al., *DNA-binding activity of adeno-associated virus Rep is required for inverted terminal repeat-dependent complex formation with herpes simplex virus ICP8.* J Virol, 2012. **86**(5): p. 2859-63.

229. Deng, Z., et al., *Telomeric proteins regulate episomal maintenance of Epstein-Barr virus origin of plasmid replication.* Mol Cell, 2002. **9**(3): p. 493-503.

230. Klein, H.L., *The consequences of Rad51 overexpression for normal and tumor cells.* DNA Repair, 2008. **7**(5): p. 686-93.

231. Lord, C.J. and A. Ashworth, *RAD51, BRCA2 and DNA repair: a partial resolution*: Nat Struct Mol Biol. 2007 Jun;14(6):461-2.

232. Li, W. and H. Ma, *Double-stranded DNA breaks and gene functions in recombination and meiosis.* Cell Res, 2006. **16**(5): p. 402-12.

233. Wang, C., L. Zhao, and S. Lu, *Role of TERRA in the regulation of telomere length.* Int J Biol Sci, 2015. **11**(3): p. 316-23.

234. Azzalin, C.M., et al., *Telomeric repeat containing RNA and RNA surveillance factors at mammalian chromosome ends.* Science, 2007. **318**(5851): p. 798-801.

235. Gottschling, D.E., et al., *Position effect at S. cerevisiae telomeres: reversible repression of Pol II transcription.* Cell, 1990. **63**(4): p. 751-62.

236. Baur, J.A., et al., *Telomere position effect in human cells.* Science, 2001. **292**(5524): p. 2075-7.

237. Ottaviani, A., E. Gilson, and F. Magdinier, *Telomeric position effect: from the yeast paradigm to human pathologies?* Biochimie, 2008. **90**(1): p. 93-107.

238. Kaspersen, M.D., et al., *Human herpesvirus-6A/B binds to spermatozoa acrosome and is the most prevalent herpesvirus in semen from sperm donors.* PLoS One, 2012. **7**(11): p. 7.

239. Liszewski, M.K., et al., *Emerging roles and new functions of CD46.* Springer Semin Immunopathol, 2005. **27**(3): p. 345-58.

240. Kong, C.M., X.W. Lee, and X. Wang, *Telomere shortening in human diseases.* Febs J, 2013. **280**(14): p. 3180-93.

241. De Vries, B.B., et al., *Telomeres: a diagnosis at the end of the chromosomes.* J Med Genet, 2003. **40**(6): p. 385-98.

242. Biesecker, L.G., *The end of the beginning of chromosome ends*: Am J Med Genet. 2002 Feb 1;107(4):263-6.

243. Walter, S., et al., *Subtelomere FISH in 50 children with mental retardation and minor anomalies, identified by a checklist, detects 10 rearrangements including a de novo balanced translocation of chromosomes 17p13.3 and 20q13.33.* Am J Med Genet A, 2004. **1**(4): p. 364-73.

244. Baralle, D., *Chromosomal aberrations, subtelomeric defects, and mental retardation.* Lancet, 2001. **358**(9275): p. 7-8.

245. Lee, S.O., R.A. Brown, and R.R. Razonable, *Chromosomally integrated human herpesvirus-6 in transplant recipients.* Transpl Infect Dis, 2012. **14**(4): p. 346-54.

246. Shalem, O., et al., *Genome-scale CRISPR-Cas9 knockout screening in human cells.* Science, 2014. **343**(6166): p. 84-7.

247. Peng, J., et al., *High-throughput screens in mammalian cells using the CRISPR-Cas9 system.* Febs J, 2015. **282**(11): p. 2089-96.

248. Wade, M., *High-Throughput Silencing Using the CRISPR-Cas9 System: A Review of the Benefits and Challenges.* J Biomol Screen, 2015. **20**(8): p. 1027-39.

249. Hsu, P.D., E.S. Lander, and F. Zhang, *Development and applications of CRISPR-Cas9 for genome engineering.* Cell, 2014. **157**(6): p. 1262-78.

250. Doudna, J.A. and E. Charpentier, *Genome editing. The new frontier of genome engineering with CRISPR-Cas9.* Science, 2014. **346**(6213): p. 1258096.

251. Hu, W., et al., *RNA-directed gene editing specifically eradicates latent and prevents new HIV-1 infection.* Proc Natl Acad Sci U S A, 2014. **111**(31): p. 11461-6.

252. Ebina, H., et al., *Harnessing the CRISPR/Cas9 system to disrupt latent HIV-1 provirus.* Sci Rep, 2013. **3**(2510).

253. Wang, J. and S.R. Quake, *RNA-guided endonuclease provides a therapeutic strategy to cure latent herpesviridae infection.* Proc Natl Acad Sci U S A, 2014. **111**(36): p. 13157-62.

# 12 Acknowledgments

After all those years, there are so many people I would like to thank. I want to start with thanking Prof. Klaus Osterrieder, for giving me the opportunity to work in his institute and for his helpful input during my FLMs. Then of course my direct supervisor Prof. Benedikt B. Kaufer for his guidance, help and support as well as the fruitful 'trouble-shooting' during my entire PhD. A special thank also goes to my mentor from the BCP-department Prof. Petra Knaus, who agreed to supervise and evaluate my thesis. Thanks also to our collaborators from the Laval University (Quebec, Canada) Prof. Louis Flamand and Dr. Annie Gravel. As funding is a necessity, thanks as well to the ZIBI graduate school (IMPRS and GRK) and to all the ZIBI coordinators, past and present, especially Juliane and Susanne.

Additionally, I want to thank all present and former members of the Institut für Virologie of the FU Berlin, who supported me throughout the years and spent countless hours with me in (and outside) the lab. A special thank goes to our wonderful TAs Ann, Netti and Michi for constant help and answers to also the dumbest of questions. Moreover, the entire Kaufer lab made the work in the lab really pleasant. I will definitely miss the 'lunch group' with alternating cast, which always helped to take a break from science and talk about the really important stuff in life ☺. I want to thank Annachiara, Timo, Tereza, Kathrin, Renato, Darren, Sina, Nadine, Luca, Anirban, Tobi, Bart, Inês, Maren, Pratik, Jakob, Dusan and everyone that I might have forgotten for many great memories.

Last but not least I want to thank my friends and especially my boyfriend and my family, who always stood by my side and had the patience to keep up with my mood swings over the past years. Without you I would not be who and where I am today!

# 13 Curriculum vitae

**For reasons of data protection,**

**the curriculum vitae is not included in the online version**

**For reasons of data protection,**

**the curriculum vitae is not included in the online version**

# 14 Publications

1) Gaertner B, Johnston J, Chen K, **Wallaschek N**, Paulson A, Garruss AS, Gaudenz K, De Kumar B, Krumlauf R, Zeitlinger J. *Cell reports*, 2012

   Poised RNA polymerase II changes over developmental time and prepares genes for future expression.

2) Osterrieder N, **Wallaschek N**, Kaufer BB. *Annual Reviews Virology*, 2014

   Herpesvirus genome integration into telomeric repeats of host cell chromosomes.

3) Kühl U, Lassner D, **Wallaschek N**, Gross UM, Krueger GR, Seeberg B, Kaufer BB, Escher F, Poller W, Schultheiss HP. *European Journal of Heart Failure*, 2015

   Chromosomally Integrated Human Herpesvirus 6 in Heart Failure- Prevalence and Treatment.

4) Trempe F, Gravel A, Dubuc I, **Wallaschek N**, Collin V, Gilbert-Girard S, Morissette G, Kaufer BB, Flamand L. *Nucleic Acids Research*, 2015

   Characterization of human herpesvirus 6A/B U94 as ATPase, helicase, exonuclease and DNA-binding proteins.

5) **Wallaschek N**, Gravel A, Mori Y, Flamand L, Kaufer BB.

   Role of the herpesvirus telomeric repeats in human herpesvirus 6 integration. *In preparation*

*6)* Gravel A, Dubuc I, **Wallaschek N**, Gilbert-Girard S, Collin V, Kaufer BB, Flamand L.

   Development of a cellular model to study HHV-6 chromosomal integration. *In preparation*

7) **Wallaschek N**, Gravel A, Flamand L, Kaufer BB.

   Role of the putative U94 recombinase in human herpesvirus 6 integration. *In preparation*